

## V AND R-BAND GALAXY LUMINOSITY FUNCTIONS AND LOW SURFACE BRIGHTNESS GALAXIES IN THE CENTURY SURVEY

WARREN R. BROWN<sup>1</sup>, MARGARET J. GELLER, DANIEL G. FABRICANT, AND MICHAEL J. KURTZ

Harvard-Smithsonian Center for Astrophysics, 60 Garden St., Cambridge, MA 02138

*Accepted by the Astronomical Journal*

### ABSTRACT

We use 64 deg<sup>2</sup> of deep *V* and *R* CCD images to measure the local *V* and *R* band luminosity function of galaxies. The  $V_0 < 16.7$  and  $R_0 < 16.2$  redshift samples contain 1255 and 1251 galaxies and are 98.1% and 98.2% complete, respectively. We apply *k* corrections before the magnitude selection so that the completeness is to the same depth for all spectral types. The *V* and *R* faint end slopes are surprisingly identical:  $\alpha = -1.07 \pm 0.09$ . Representative Schechter function parameters for  $H_0 = 100$  are:  $M_R^* = -20.88 \pm 0.09$ ,  $\phi_R^* = 0.016 \pm 0.003 \text{ Mpc}^{-3}$  and  $M_V^* = -20.23 \pm 0.09$ ,  $\phi_V^* = 0.020 \pm 0.003 \text{ Mpc}^{-3}$ . The *V* and *R* local luminosity densities,  $j_R = (1.9 \pm 0.6) \times 10^8 L_\odot$  and  $j_V = (2.2 \pm 0.7) \times 10^8 L_\odot$ , are in essential agreement with the recent 2dF and SDSS determinations.

All low surface brightness (LSB) galaxies fall in the large scale structure delineated by high surface brightness galaxies. The properties and surface number density of our LSB galaxies are consistent with the LSB galaxy catalog of O'Neil, Bothun & Cornell, suggesting that our samples are complete for LSB galaxies to the magnitude limits. We measure colors, surface brightnesses, and luminosities for our samples, and find strong correlations among these galaxy properties. The color-surface brightness relation is  $(V-R)_0 = (-0.11 \pm 0.05)\mu_{R,0} + (2.6 \pm 0.9)$ .

*Subject headings:* cosmology: observations — galaxies: fundamental parameters — galaxies: luminosity function — galaxies: photometry — large scale structure of universe

### 1. INTRODUCTION

The galaxy luminosity function (LF), the number of galaxies per unit luminosity per unit volume, is a fundamental quantity in observational cosmology. The galaxy LF figures prominently in the study of galaxy evolution, interpretation of faint galaxy counts, and measurement of the luminosity density of the Universe. Deep but narrow “pencil-beam” redshift surveys, including the Canada France Redshift Survey (Lilly et al. 1995), the Autofib Redshift Survey (Ellis et al. 1996), and the Canadian Network for Observational Cosmology Redshift Survey (Lin et al. 1999), probe evolution of the galaxy LF for  $z < 1$ . The local galaxy LF is the benchmark for these studies.

The local galaxy LF is measured from large angular scale redshift surveys; Table 1 summarizes all of these surveys with  $> 1000$  galaxies. The LF parameters are given in the Schechter (1976) parameterization, where  $\phi^*$  is the normalization (galaxies per  $\text{Mpc}^{-3}$ ),  $\alpha$  is the faint end slope, and  $M^*$  is the characteristic absolute magnitude at the “break” between the exponential bright end and power-law faint end of the LF. The Center for Astrophysics Redshift Survey (CfA2, Marzke et al. 1994) and the complementary Southern Sky Redshift Survey (SSRS2, Marzke et al. 1998) are complete but relatively shallow surveys. The Stromlo-APM Redshift Survey (APM, Loveday et al. 1992) and Durham/UKST Galaxy Redshift Survey (D/UKST, Ratcliffe et al. 1998) are sparsely-sampled surveys of modest depth. The ESO Slice Project Redshift Survey (ESP, Zucca et al. 1997) and the on-going 2 Degree Field Galaxy Redshift Survey (2dF, Cross et al. 2001) are both deeper surveys with mean redshift  $\bar{z} = 0.10$ . Only the Las Cam-

panas Redshift Survey (LCRS, Lin et al. 1996) and the Sloan Digital Sky Survey (SDSS, Blanton et al. 2001) are CCD-based, and together with the Century Survey (CS, Geller et al. 1997) are the only *R*-selected surveys. Multiple passband photometry has not been available for these complete, large galaxy surveys except for the SDSS.

We have deep *V*- and *R*-band CCD images for 64 deg<sup>2</sup> of the Century Survey (CS, Geller et al. 1997). The original CS is a 102 square degree redshift survey containing 1762 galaxies to a limiting magnitude  $R = 16.13$ . The original CS is complete and requires no sampling corrections; selection at *R* minimizes galactic extinction and *k* corrections. The original CS LF parameters, based on CCD-calibrated photographic photometry, are comparable to those derived from surveys of similar depth (Table 1).

Here we determine the local galaxy LF by extending the original CS *R* sample to  $R_0 < 16.2$  mag and present a new *V* sample to  $V_0 < 16.7$  mag. The redshift samples are 98% complete and contain  $\sim 1250$  galaxies. We give attention to details of the construction of clean redshift catalogs, and offer the following subtle, but important, modifications to previous approaches to local LF determinations.

We have *V* and *R* photometry for the same region of sky. The SDSS (Blanton et al. 2001) is the only other large, local redshift survey with multi-passband photometry. Accurate colors allow us to constrain the *k* correction for each galaxy. We apply *k* corrections *before* the magnitude selection to ensure that we sample different spectral types to the same depth.

The CCD photometry has average errors  $\pm 0.049$  mag, much lower than the  $\pm 0.25$  mag errors in the original photographic photometry. The CCD images have ap-

<sup>1</sup>Visiting Astronomer, Kitt Peak National Observatory, National Optical Astronomy Observatory, which is operated by the Association of Universities for Research in Astronomy, Inc. under cooperative agreement with the National Science Foundation.

proximately twice the resolution of scanned photographic plates, allowing us to better separate close pairs of galaxies. Our redshifts, measured from long-slit spectra, are complete even in high density regions and have no surface brightness constraints.

One of the major concerns in measuring the galaxy LF is the proper inclusion of low surface brightness galaxies. Sprayberry et al. (1997), for example, estimate that the CfA redshift survey may miss 1/3 of the local galaxy population because of the limiting surface brightness of the photographic photometry. Our CCD photometry extends to a limiting sky brightness of  $26 R$  mag arcsec $^{-2}$ , allowing a test of the photographic CS completeness for low surface brightness galaxies. Our data also allow an examination of the relative distribution of low surface brightness galaxies and the large scale structure defined by high surface brightness galaxies.

In section 2 we describe the data and errors, and in section 3 we define the photometric samples. In section 4 we study the characteristics of the galaxies, emphasizing the properties and distribution of low surface brightness galaxies. In section 5 we discuss the LF determination. We conclude in section 6. Appendix A contains a detailed comparison of the photographic and CCD-based CS photometry. Appendix B presents the the  $V$  and  $R$  CCD photometry.

## 2. DATA

We obtained Johnson  $V$  and Kron-Cousins  $R$  broadband images with the MOSAIC camera (Muller et al. 1998) on the Kitt Peak National Observatory 0.9m telescope in 1998 December and 1999 February. MOSAIC is an 8 CCD array with pixel scale 0.424 arcsec pixel $^{-1}$  and field of view 59' x 59' on the 0.9m. We obtained three offset 200 sec  $R$  and 333 sec  $V$  images at each position along the western 64 deg $^2$  of the CS slice (Geller et al. 1997):  $8^{\text{h}}5 < \alpha_{\text{B1950}} < 13^{\text{h}}5$ ,  $29^{\circ} < \delta_{\text{B1950}} < 30^{\circ}$ .

To complete the sample to  $V_0 = 16.70$  and  $R_0 = 16.20$  mag, we measured 242 new redshifts with the FAST spectrograph (Fabricant et al. 1998) on the Fred Lawrence Whipple Observatory 1.5m telescope in 2000 April and 2000 November (to be published in Wegner et al. 2001). We used the 300 line grating to obtain 6 Å FWHM resolution and spectral coverage from 3650 Å to 7500 Å. We obtained velocities with the cross-correlation package RVSAO (Kurtz & Mink 1998). The mean uncertainty of the velocities is  $\pm 40$  km s $^{-1}$ . The new redshifts make our  $V$  and  $R$  samples 98.1% and 98.2% complete, respectively.

### 2.1. Processing

We obtained bias and flat field calibration images in the standard fashion, and processed them with the *IRAF* MSCRED package. The MOSAIC images contain variable row-to-row bias fluctuations of  $\pm 3$  counts as well as large scale moiré patterns of amplitude  $\lesssim 3$  counts. Drifts in the various clocks in the CCD controllers produce the variable bias levels; they are not reproducible or completely removable (Valdes 1999, private communication). To reduce the row-to-row bias fluctuations, we fit and subtract the over-scan region on a row-to-row basis. This procedure leaves large-scale bias features near chip edges. To remove these, we smooth the median-combined bias images with a 20

pixel box and subtract them from the data. This approach avoids introducing additional noise from the non-repeating moiré patterns.

The moiré patterns modulate the dome flats by only 1 part in 5000; thus we use these flats in the standard fashion. This procedure leaves center-to-edge background changes of  $\sim 10\%$ , resulting from the different colors of the dome flat lamp and the night sky. "Night sky flats" are a median combination of a night's worth of data images (scaled to a common background level) for each filter. We smooth the night sky flats with a 20 pixel box to increase their S/N. This approach minimizes the introduction of additional noise at small scales; bad pixel masks eliminate hot pixels and bad columns from the smoothing. Division by the night sky flats flattens the background to 2% at large scales. Dark images have means of  $\leq 0.1$  counts, and we make no correction for dark current.

### 2.2. Astrometry

Good astrometry is critical for working with multi-chip data. The MOSAIC optical system causes a 2.0% pixel area change over the field of view of the KPNO 0.9m (Davis 1998). We re-bin the processed images with *IRAF* using the astrometric solutions provided to correct the scale changes. We then use WCSTools (Mink 1999) to refine the zero-point and rotation of the coordinate system for each chip. We refine the coordinate system with the Hubble Space Telescope Guide Star Catalog (Lasker et al. 1990), excluding the 5 brightest stars per field to cull the objects with the worst proper-motion. Depending on seeing conditions and star density, typical coordinate system fits use  $\sim 20$  stars per chip and provide coordinates good to 0''.3 – 0''.5.

### 2.3. Photometric calibration

We use Landolt fields (Landolt 1992) and the M67 cluster (Montgomery et al. 1993) for flux calibration. The M67 photometry, although less precise than the Landolt photometry, extends over a half degree and is available for 1000+ stars. The flux calibration is typically based on 1000  $R$  band and 7500  $V$  band standard star measurements per night.

We performed a series of tests on the flux calibration images. First, to test for linearity in the CCDs we imaged M67 at low airmass with back-to-back 10 and 100 second exposures. The difference in stellar magnitudes between the two exposure times is  $\delta m = -0.004 \pm 0.005$  mag. We conclude there is no significant non-linearity over the count rates appropriate for the galaxies.

We compare magnitude zero points for the Landolt (1992) 14'' circular aperture magnitudes and the adaptive-aperture "total" magnitudes that we use for galaxies. The zero-point solutions for both aperture magnitudes are within  $1\sigma$  on the nights of best and worst seeing. Thus we adopt adaptive-aperture total magnitudes throughout. Finally, we compare the photometric solution based on the Landolt fields alone to the full photometric solution including the M67 fields. The photometric solutions agree to  $\leq 1\sigma$ , giving us confidence in the M67 photometric calibrations.

We compute the photometric solution as follows. We do not fit the zero points, extinction coefficients, and color

terms simultaneously because of degeneracy in the photometric solution. The color term is small and easily washed out by errors in the zero point and extinction coefficient; thus we first solve for the color term. Using standards taken at identical airmass on the same night (so that the extinction coefficient is constant), the color term is the slope of the  $(m_{\text{instrumental}} - m_{\text{true}})$  vs. color line. Only the Landolt field in chip 2 allows an accurate color term determination (see Figure 1); the small range of  $(V - R)$  colors in M67 provide little leverage on the color term. We used the chip 2 color term for all 8 chips because all 8 chips look through the same filter, and because the color term is primarily affected by filter transmission. The color term values for the other 7 chips agree within their errors with the chip 2 value. The color terms are constant from night to night; thus we use the average color term for all 7 nights of observations:  $\text{CT}_R = -0.013 \pm 0.005$  mag and  $\text{CT}_V = 0.072 \pm 0.005$  mag.

Once we subtract the color term from the standard star observations, we determine the extinction coefficient from a linear fit of the magnitude vs. airmass line. The extinction coefficient is atmospheric and we assume it is identical for all 8 chips. The nightly fluctuations in the extinction coefficient were of order the error; we use the average extinction coefficient of all nights in an observing run. Finally, subtracting the color term and extinction term from the standard star observations, we determine the zero-point for each individual chip, for each night. Depending on the nightly sky conditions, the residual RMS error in the standard star calibration is  $\pm 0.02 - 0.04$  mag.

#### 2.4. Galaxy photometry

We use SExtractor (Bertin & Arnouts 1996) to make  $10^4$  photometric galaxy measurements in our 300 Gb of images. SExtractor performs background subtraction, convolves the images with a detection filter, and measures circular aperture, isophotal, and adaptive-aperture magnitudes. The adaptive-aperture magnitudes are elliptical apertures that include  $\simeq 90\%$  of the flux and are corrected to total magnitudes assuming Gaussian convolved profiles. We use these total magnitudes throughout.

We set a detection threshold of  $25 R$  mag  $\text{arcsec}^{-2}$ . Our limiting sky brightness is 26 mag  $\text{arcsec}^{-2}$  in both passbands. We apply  $R$  apertures to aligned  $V$  images. This process assures that the light in each bandpass comes from the *same physical region* of a galaxy. With  $\sim 7000$  objects per image, we can align  $V$ -band images to within  $\pm 0.05$  pixels of their companion  $R$ -band images.

We use a gaussian convolution filter with FWHM greater than the seeing to optimally detect extended galaxies. SExtractor detects the low surface brightness galaxies found by visual inspection, including an extreme object with an exponential scale length of  $30''$  and central surface brightness 23.4 mag  $\text{arcsec}^{-2}$  in  $V$  (at  $12^{\text{h}}31^{\text{m}}58^{\text{s}}42, 29^{\circ}42'33.2''$  J2000).

We follow Sprayberry et al. (1997) and define low surface brightness (hereafter LSB) galaxies as extended objects with  $\mu(0)_B > 22$  mag  $\text{arcsec}^{-2}$ , where  $\mu(0)$  is the central surface brightness for an exponential profile,

$$\mu(r) = \mu(0) + 1.086r/\alpha_l. \quad (1)$$

$\mu(r)$  is the surface brightness as a function of radius  $r$  and  $\alpha_l$  is the scale length in arcseconds. We take the aver-

age  $(B - V) = 0.79$  mag LSB galaxy color from O’Neil et al. (1997b) and the average  $(V - R) = 0.40$  mag from our own sample of LSB galaxies to define LSB galaxies in the  $V$  and  $R$ -bands as objects with  $\mu(0)_V > 21.2$  and  $\mu(0)_R > 20.8$  mag  $\text{arcsec}^{-2}$ .

We select galaxies from each  $V$  and  $R$  catalog with a combination of FWHM, isophotal area, and central surface brightness criteria. We make a magnitude cut at  $R = 16.5 + A_{R\text{max}}$ , and then visually examine every selected object. Our photometry recovers all original CS galaxies. The CCD imaging resolves 2% of the original CS objects into multiple objects (Appendix A).

Approximately 20% of the  $10^4$  galaxy measurements are either cut off by CCD boundaries, fall on cosmic rays or bad columns, or are poorly fit by SExtractor. The poorly fit galaxies are commonly irregular LSB galaxies, galaxies near a bright star, or unusually large galaxies. We obtain photometry of poorly fit galaxies by hand with a modified version of GALPHOT (Freudling 1993), a front end for the *IRAF ELLIPSE* package. This procedure allows us to mask unwanted artifacts and to center apertures on difficult objects properly.

SExtractor and GALPHOT total magnitudes appear equally robust. We fit surface brightness profiles, using GALPHOT, to 101 randomly selected CS galaxies. Comparison of the total integrated magnitudes to the SExtractor total magnitudes yields a  $1\sigma$  scatter of  $\pm 0.05$  mag and a  $-0.01$  mag offset. On average, integrating the GALPHOT profile yields only 1% more flux than SExtractor total magnitudes.

We imaged each square degree at least 3 times. We compute final magnitudes and positions from the weighted averages of individual measurements. This approach avoids the need to stack the offset images and takes advantage of the good S/N of the CS galaxies. Using multiple measurements allows us to measure our errors: Figure 2 shows the distribution of the RMS scatter of identical galaxies measured on different nights. The median RMS error is  $\pm 0.025$  mag; this value includes both measurement and zero point errors. When we plot the average magnitude offset between fields observed on different nights, non-photometric conditions, including 0.05 mag extinction from cirrus bands, are strikingly obvious. We add a corrective offset to catalogs with cirrus extinction less than 0.2 mag, and assign larger errors to those catalogs. We see no structure in the cirrus extinction at the 1 degree scale during our exposures.

The final photometric error (Appendix B) is a sum in quadrature of the zero-point error and the RMS photometric scatter determined for multiple measurements of each galaxy. The average final photometric error is  $\pm 0.049$  mag in both passbands.

Figure 3 compares our CCD photometry with the photographic CS photometry. The zero-point offset  $\Delta R_{\text{CCD-photographic}} = 0.014 \pm 0.22$  mag is small and well within our average zero-point error  $\pm 0.034$  mag. The  $\pm 0.22$  mag RMS scatter between the CCD and photographic photometry is consistent with the  $\pm 0.25$  mag photographic error estimate of Geller et al. (1997). Appendix A compares the CCD and photographic catalogs in detail.

##### 2.4.1. Corrections

We take galactic extinction corrections from Schlegel et al. (1998), who combine *COBE*/DIRBE and *IRAS*/ISSA data to map dust emission in the Milky Way. The CS strip is at high galactic latitude, thus the average extinction is  $A_R = 0.053$  and  $A_V = 0.065$  mag (Figure 4a). Schlegel et al. (1998) estimate that the errors in the extinction correction are  $\sim 16\%$  of the extinction.

The final photometry also includes  $k$  corrections to correct observed magnitudes to restframe magnitudes. Because we know the  $(V - R)$  color and the redshift of each galaxy, we can better constrain the  $k$  correction for each galaxy. We interpolate tables provided by Poggianti (1997) for types E, Sa, and Sc, and Frei & Gunn (1994) for type Im. The  $k$  corrections range  $0 < k_R < 0.20$  and  $-0.05 < k_V < 0.30$  mag. The average values are  $k_R = 0.061$  and  $k_V = 0.089$  mag (see Figure 4b). Figure 5 demonstrates the efficacy of the  $k$  corrections: after correction the apparent cosmological reddening is almost entirely removed.

The errors in the  $k$  correction are difficult to quantify. There is significant spectral variation within morphological classes of galaxies, but we bypass the usual difficulty of determining morphologies by using colors. Broadband colors more tightly fit a given *spectral* type; colors are effectively very low resolution spectra. We obtain one estimate of the  $k$  correction error by propagating the  $(V - R)$  error. The errors are of order of the  $k$  correction itself. Thus we make the conservative assumption that the  $k$  correction error is the value of the  $k$  correction. If we were to ignore the  $k$  correction error in the LF calculation, the faint end slope would be  $-0.04$  steeper and the characteristic absolute magnitude  $M^* = -0.04$  to  $-0.09$  mag brighter (see Equation 5 below).

### 3. SAMPLE DEFINITION

Our data cover the CS strip  $8^{\text{h}}32^{\text{m}}45^{\text{s}} < \alpha_{\text{B1950}} < 13^{\text{h}}27^{\text{m}}31^{\text{s}}$ ,  $29^{\circ}0'0'' < \delta_{\text{B1950}} < 30^{\circ}0'0''$  for a total of  $64.13 \text{ deg}^2$ . We find that  $0.13 \text{ deg}^2$ , or  $0.2\%$ , of the CS strip is masked by  $R < 12$  mag bright stars. Thus the total area used for the LF calculation is  $64.0 \text{ deg}^2$ .

#### 3.1. Magnitude Limits

Our samples are magnitude limited to  $V_0 < 16.70$  and  $R_0 < 16.20$  mag. The median rest-frame color of the  $V$  and  $R$  samples is  $(V - R)_0 = 0.53 \pm 0.07$  mag. Thus the two samples are of comparable depth.

We apply galactic extinction and  $k$  corrections *before* performing the magnitude selection. This procedure ensures that we sample different spectral types to the same depth in each sample. If we do not apply  $k$  corrections before the magnitude selection, the limiting absolute magnitude at a particular redshift is a function of spectral type. In a purely apparent-magnitude limited redshift survey, late type galaxies are sampled to fainter absolute magnitudes than early type galaxies.

Early redshift surveys, including the APM (Loveday et al. 1992), CfA (Marzke et al. 1994), and SSRS2 (Marzke et al. 1998), sample mean redshifts  $\bar{z} < 0.05$  and have poor photometric precision:  $\pm 0.3 - 0.4$  mag.  $K$  corrections for some of these early surveys are approximated as a single value for all galaxy types. Although formally incorrect, the  $k$  corrections used for these surveys are much smaller

than the photometric error. More recent surveys, including the LCRS (Lin et al. 1996), ESP (Zucca et al. 1997), and the current 2dF (Cross et al. 2001) and SDSS (Blanton et al. 2001), access deeper redshifts ( $\bar{z} \simeq 0.1$ ) and reach photometric accuracies of  $\pm 0.1 - 0.2$  mag, yet continue to apply uncorrected apparent magnitude cuts. At the 2dF limiting redshift  $z = 0.12$  (Cross et al. 2001) there is a  $k_B \simeq 0.47$  mag spread between ellipticals and irregulars (Frei & Gunn 1994). As a result, the survey samples irregulars to a 0.47 fainter absolute magnitude than it does ellipticals.

Applying  $k$  corrections before the magnitude selection makes very little difference for our low redshift ( $\bar{z} = 0.064$ )  $V$  and  $R$  samples. Although it is impossible to create directly comparable samples, we calculate LFs for galactic extinction-corrected magnitude limits  $m_V = 16.70 + (\text{median } k_V)$  and  $m_R = 16.20 + (\text{median } k_R)$ . These samples contain  $< 2\%$  fewer galaxies than their pre- $k$  corrected counterparts, and thus are of similar depth. The characteristic absolute magnitudes  $M^*$  are  $+0.01$  to  $+0.06$  fainter, and the faint end slopes change by  $\pm 0.01$  (see Equation 5 below). For deeper samples and bluer passbands the effects are, of course, larger.

#### 3.1.1. Completeness

Completeness, as normally quoted, is the fraction of galaxies with redshifts in an apparent magnitude-limited sample. Application of the  $k$  correction may bring fainter galaxies without redshifts into the sample. To minimize this problem, we measured redshifts for galaxies to  $R_{\text{lim}} + k_{R\text{max}}$  and  $V_{\text{lim}} + k_{V\text{max}}$ . We have 77% (303 of 392) complete redshifts in the interval  $(V_{\text{lim}}, V_{\text{lim}} + k_{V\text{max}})$ , and a similar fraction in  $R$ . To estimate our true completeness, we assume that the faint galaxies without redshifts have approximately the same distribution of  $k$  corrections as the sample with redshifts (Figure 4b). Thus

$$\text{completeness} = \frac{N_{\text{tot}} + \int_{m_{\text{lim}}}^{m_{\text{lim}} + k_{\text{max}}} n(m) f_k(m) dm}{N_{\text{tot}} + N_{k_{\text{max}}}}, \quad (2)$$

where  $N_{\text{tot}}$  is the total number of galaxies within our  $k$ -corrected magnitude limit  $m < m_{\text{lim}}$ ,  $n(m)$  is the number of galaxies per  $dm$  fainter than the magnitude limit,  $f_k(m)$  is the fraction of galaxies with  $k$  corrections equal to  $m$ , and  $N_{k_{\text{max}}}$  is the total number of galaxies in the interval  $(m_{\text{lim}} \leq m \leq m_{\text{lim}} + k_{\text{max}})$ .

Equation 2 yields 98.1% completeness in  $V$  and 98.2% completeness in  $R$ . The completeness is to the *same depth* for all spectral types. Furthermore, our long slit spectra have *no* sampling bias in high density regions (e.g. because of fiber positioning constraints) nor is there any bias in surface brightness (as encountered by some fiber surveys). The fraction of galaxies without redshifts that may, given the observed distribution of  $k$  corrections, be shifted into our samples limits our completeness.

#### 3.2. Redshift Limits

We construct LFs for  $1,000 \leq cz \leq 45,000 \text{ km s}^{-1}$ , where  $cz$  is the recession velocity in the Local Group frame,  $cz = cz_{\odot} + 300 \sin l \cos b$ , corrected for Virgo-centric infall. The lower velocity limit eliminates regions where peculiar velocities may be a large fraction of the Hubble flow; the upper limit is where the survey becomes sparse.

Because we calculate recession velocities from the Local Group frame, we include the effect of Virgo infall. We apply the Virgo-centric infall model of Kraan-Korteweg (1986) with the Sandage infall value  $v_{vc} = 220 \text{ km s}^{-1}$ . The Virgo infall model only affects the  $\sim 50$  galaxies in our samples with  $cz < 6,000 \text{ km s}^{-1}$ . Beyond  $6,000 \text{ km s}^{-1}$ , the Virgo infall correction is equivalent to an additive dipole velocity of  $\simeq 200 \text{ km s}^{-1}$  that makes galaxies appear slightly brighter. The Virgo infall correction changes our LFs by making the  $V$  and  $R$  faint end slopes  $+0.03$  flatter; the characteristic absolute magnitudes  $M^*$  brighten by just -.01 mag (see Equation 5 below).

### 3.3. Luminosities

We calculate absolute magnitudes from

$$M = m - k - A - 5 \log D_L(z) - 25, \quad (3)$$

where  $m$  is the observed magnitude,  $k$  is the  $k$  correction,  $A$  is the galactic extinction correction, and  $D_L$  is the luminosity distance. We use the distance measure formulae described by Hogg (1999) and compute the luminosity distance for three cosmologies. To allow comparisons with earlier work, we use  $H_0=100 \text{ km s}^{-1} \text{ Mpc}^{-1}$ ,  $\Omega_m = 1.0$ , and  $\Omega_\Lambda = 0.0$  (CDM). We also use the flat cosmology  $H_0=75$ ,  $\Omega_m = 0.3$ , and  $\Omega_\Lambda = 0.7$  ( $\Lambda$ CDM), consistent with recent measurements. To compare with the original CS open cosmology, we use the open cosmology  $H_0=100$ ,  $\Omega_m = 0.3$ , and  $\Omega_\Lambda = 0.0$  (OCDM). Choosing alternative values for  $H_0 = 100h \text{ km s}^{-1} \text{ Mpc}^{-1}$  shifts all absolute magnitudes by  $5\log_{10}h$  and changes number densities by  $h^3$ .

## 4. SAMPLE PROPERTIES

Here we examine the luminosities, colors, and surface brightnesses of the galaxies in our  $V$  and  $R$  magnitude limited samples. The data show strong correlations between luminosity, color, and surface brightness.

We examine the population of LSB galaxies in detail. When we select LSB galaxies in the same way as O'Neil et al. (1997a), we find a similar surface number density of galaxies and distribution of scale lengths and central surface brightnesses. This agreement suggests we are complete for LSB galaxies to our magnitude limit. When we do not impose a minimum angular diameter limit (that will select against dwarfs), we find more blue LSB galaxies than O'Neil et al. (1997a). LSB galaxies fall in the large scale structure marked by high surface brightness galaxies.

### 4.1. Color-Surface Brightness Relation

Figure 6 shows the color-surface brightness relation for the  $R$ -selected sample,  $(V-R)_0 = (-0.11 \pm 0.05)\mu_{R,0} + (2.6 \pm 0.9)$ . The error is the formal error of the least squares fit. The rest frame color,  $(V-R)_0$ , includes galactic extinction and  $k$  corrections. The rest frame central surface brightness,  $\mu_{R,0}$ , is

$$\mu_{R,0} = \mu_R - 10 \log_{10}(1+z) - k_R, \quad (4)$$

where  $z$  is the redshift and  $k_R$  is the  $k$  correction. This relation is based on the sub-sample with SExtractor peak surface brightnesses,  $\mu_R$ , avoiding assumptions about fitting light profile shapes. We make no corrections for inclination or internal extinction. The color-surface brightness

relation is valid in the range  $0.35 < (V-R)_0 < 0.60 \text{ mag}$  and  $17 < \mu_{R,0} < 21 \text{ mag arcsec}^{-2}$ .

The color-surface brightness relation is not tight. However, it disagrees with the complete lack of correlation between color and central surface brightness claimed by McGaugh & Bothun (1994) and O'Neil et al. (1997a). They measure a continuous range of colors, from very blue to very red, at low surface brightnesses. In contrast, Figure 6 shows that the lowest surface brightness galaxies in our sample are among the bluest galaxies in our sample. Our deep  $R$  images allow a sensitive search for red LSB galaxies, yet we find very few.

The disagreement with McGaugh & Bothun (1994) and O'Neil et al. (1997a) may be a consequence of their minimum angular diameter. Angular diameter-limited surveys are biased toward finding intrinsically large galaxies; only very nearby dwarfs are included in such surveys. From deep CCD images of the Cancer and Pegasus clusters and fields in the Great Wall region, O'Neil et al. (1997a) cataloged 127 LSB galaxies with  $\theta > 26''$ . We do not impose a minimum angular diameter. We thus include more low surface brightness blue dwarfs.

### 4.2. Color-Luminosity Relation

Figure 7 shows the color-absolute magnitude relation for the  $R$ -selected galaxies,  $(V-R)_0 = (-0.08 \pm 0.03)M_R - (1.13 \pm 0.5)$ . The error is the formal error of the least squares fit.  $M_R$  is the  $R$  band absolute magnitude. The scatter about the color-absolute magnitude relation is large in part because we make no corrections for inclination or internal extinction.

Visvanathan (1981) measures color-absolute magnitude relations for 55 Virgo and field spirals in the  $V$ ,  $r$ , and  $IV$  filters. His passbands allow a rough comparison with our data, though we cannot convert the narrow (300Å at 6738 Å)  $r$  filter to Kron-Cousins  $R$  to obtain a proper zero-point. There are numerous measurements of the elliptical galaxy color-magnitude relation, but these are not comparable with our field galaxy sample. Visvanathan (1981) finds a  $(V-r)$  slope of  $-0.06 \pm 0.04$ , similar to our result.

### 4.3. Luminosity-Surface Brightness Relation

Figure 8 shows the luminosity-surface brightness relation for the  $R$ -selected galaxies,  $M_R = (2.1 \pm 0.7)\mu_{R,0} - (60.3 \pm 2)$ .

For comparison, the 2dF survey finds an identically strong luminosity-surface brightness relation in the  $b_J$  band, with slope  $2.4^{+1.5}_{-0.5}$  (Cross et al. 2001). Driver (1999) uses a volume-limited sample of 47 galaxies from the Hubble Deep Field and finds  $M_{F450W} = (1.5 \pm 0.2)\mu_e - (50 \pm 2)$ . Here  $\mu_e$  is the rest frame, mean surface brightness within the half light ("effective") radius of the 25  $I$ (F814W) mag  $\text{arcsec}^{-2}$  isophote. Figure 8 shows the Driver (1999) luminosity-surface brightness relation assuming  $(B-R) = 1.2$  (Fukugita et al. 1995). The Driver (1999) luminosity-surface brightness slope is shallower than ours, but we are unable to discriminate between the two relations. Cross et al. (2001) do not publish a zero-point, preventing a comparison here.

#### 4.4. Low Surface Brightness Galaxies

We explore the surface brightness completeness of our sample by comparing it with the O'Neil et al. (1997a) 26'' angular diameter-limited LSB galaxy catalog. O'Neil et al. (1997b) publish  $B$  photometry and  $(B-V)$  colors. We thus use the  $V$  catalog for the comparison.

We follow O'Neil et al. (1997a) and determine the central surface brightness  $\mu(0)_V$  and scale length  $\alpha_V$  of LSB galaxies by fitting exponential functions to the  $V$  surface brightness profiles. To compare with O'Neil et al. (1997a) we assume  $\alpha_B = \alpha_V$ . Our experience shows this assumption is acceptable;  $V$  scale lengths are  $\sim 5\%$  larger than our  $R$  scale lengths. We note that if  $\alpha_B > \alpha_V$ , the 26'' diameter limit will include fewer galaxies in the  $V$  sample than in the  $B$  sample. We use the exponential profile to find the radius of the LSB galaxies at the limiting sky brightness  $\mu_{sky} = 26$  mag arcsec $^{-2}$  with  $r = \alpha_V / 1.086 (\mu_{sky} - \mu(0)_V)$ . The comparison with O'Neil et al. (1997a) also assumes  $\mu(0)_V = \mu(0)_B - (B-V)$ . This is a rough approximation because we assume the average  $(B-V) = 0.79$  mag for the 40% of the O'Neil et al. (1997b) sample without  $(B-V)$  colors.

Figure 9 shows  $\mu(0)_V$  vs.  $\alpha_V$  for LSB galaxies which satisfy  $V < 16.70$  mag,  $\mu(0)_V > 21.2$  mag arcsec $^{-2}$ , and  $\theta > 26''$  in the O'Neil et al. (1997a) catalog and in the  $V$  sample. The solid and dashed lines show the limiting magnitude  $V_{lim} = 16.70$  for a face-on, pure exponential disk galaxy for limiting sky brightnesses 26 and 28 mag arcsec $^{-2}$ . Galaxies satisfying the magnitude limit should fall above the lines; galaxies which fall below are LSB galaxies with central peaks or extended wings poorly fit by an exponential profile. O'Neil et al. (1997a) lack redshifts. Their central surface brightnesses and magnitudes, although galactic extinction corrected, are not rest-frame corrected. The effect should be small because the redshifts should be small.

Figure 9 shows that our LSB galaxies cover the same range of scale length and central surface brightness as the O'Neil et al. (1997a) galaxies. A Kolmogorov-Smirnov test gives a 50% probability of the surface brightnesses being drawn from the same sample, and a 11% probability of the scale lengths being drawn from the same sample. A significant fraction of the scale lengths in our sample are smaller than those in O'Neil et al. (1997a). Applying the 26'' diameter limit at the sky limit may not be a good comparison. If we instead apply the 26'' diameter limit at  $\mu_{sky} = 25$  mag arcsec $^{-2}$ , our smallest scale length is approximately equal to the smallest O'Neil et al. (1997a) scale length and a K-S test gives a 67% probability that the scale lengths are drawn from the same sample.

Figure 9 indicates that bright magnitude-limited surveys using CCD photometry are unlikely to miss LSB galaxies. LSB galaxies with central surface brightness near the limiting sky brightness must also have extreme scale lengths in order to be bright enough for inclusion in bright magnitude-limited samples. Such galaxies are rare in Figure 9. The mean scale length of LSB galaxies in the O'Neil et al. (1997a) sample is 8''. A galaxy with an 8'' exponential scale length has the same  $V = 16.7$  isophotal magnitude with a central surface brightness only 0.20 mag arcsec $^{-2}$  fainter for limiting sky brightnesses of 26 and 28 mag arcsec $^{-2}$  (see Figure 9). This inclusion of essentially

all appropriate LSB galaxies in our sample is in agreement with the de Jong & Lacey (2000) local Sb-Sdm galaxy bivariate distribution functions.

Although we cannot compare the space density of LSB galaxies with O'Neil et al. (1997a), we can compare the surface number density to a given limiting magnitude. For  $V < 16.70$ ,  $\mu(0)_V > 21.2$ , and  $\theta > 26''$ , the O'Neil et al. (1997a) catalog contains 44 LSB galaxies over 27 deg $^2$  or 1.6 deg $^{-2}$ ; we have 40 LSB galaxies over 64 deg $^2$  or 0.63 deg $^{-2}$ . O'Neil et al. (1997a) find a factor of 2.6 more LSB galaxies per deg $^2$  than we do.

Clustering in the galaxy distribution probably explains the apparent deficiency of LSB galaxies in the CS. O'Neil et al. (1997a) search for LSB galaxies in the Pegasus and Cancer clusters and around known galaxies in the Great Wall region. The average galaxy density in our sample is much lower than in these regions. If LSB galaxies are clustered like high surface brightness galaxies, as Mo et al. (1994) claim for the CfA and *IRAS* surveys, we can account for the difference. We contrast counts of galaxies in 0.56 deg $^2$  fields (the typical field size used by O'Neil et al. 1997a) centered on known CS galaxies with counts in fields positioned at random. The count around known galaxies in the CS catalog is 2.3 times the count in the random fields. Thus accounting for clustering brings the surface number density of LSB galaxies in our sample in agreement to  $\sim 15\%$  with the O'Neil et al. (1997a) measurements.

Figure 10 shows the  $V$ -limited redshift survey to 12000 km s $^{-1}$ ; all LSB galaxies fall in the large-scale structure marked by the high surface brightness galaxies. O'Neil et al. (2000) draw a similar conclusion for galaxies in the Pegasus and Cancer clusters.

The LSB galaxies in the CS are mostly at low redshift and thus are intrinsically faint. Figure 11 shows the absolute magnitudes of the  $R$  sample as a function of redshift; circles mark the LSB galaxies. The intrinsic faintness of the LSB galaxies is consistent with the absolute magnitude-surface brightness relation. The 1000 km/s velocity limit eliminates a third of the LSB galaxies (Figure 10) from the LF calculation.

#### 5. LUMINOSITY FUNCTIONS

We compute the LF using two related methods unbiased by density inhomogeneities in the galaxy distribution: the parametric maximum-likelihood method of Sandage et al. (1979, hereafter STY) and the nonparametric stepwise maximum-likelihood method of Efstathiou et al. (1988, hereafter EEP). Others have described the details of the calculations (e.g. Lin et al. 1996). We do not reproduce them here. We assume that the LF is independent of position, and determine its shape and amplitude separately.

We assume a Schechter (1976) parameterization of the LF,

$$\phi(M) = 0.4 \ln(10) \phi^* [10^{0.4(M^* - M)}]^{(1+\alpha)} \exp(-10^{0.4(M^* - M)}), \quad (5)$$

where  $\phi^*$  is the normalization (galaxies per unit volume),  $\alpha$  is the faint end slope, and  $M^*$  is the characteristic absolute magnitude. However, the observed LF is a convolution of the true LF and the photometric error. In the STY calculations, we make the approximation that our errors are Gaussian distributed and use the Schechter LF convolved with the total photometric error. The error is a sum in

quadrature of the zero-point, measurement, galactic extinction, and  $k$  correction errors.

### 5.1. Results

Figure 12 shows the full  $R$  magnitude-limited redshift slice. Figures 13 and 14 show the STY (curve) and EEP (symbols with error bars) estimates of the LF for the  $R$  and  $V$  magnitude limited samples in the OCDM cosmology. The inset boxes shows the  $2\sigma$   $\chi^2$  error ellipses for  $M^*$  and  $\alpha$ . Table 2 summarizes the results. Schechter function parameters for the OCDM cosmology are:  $M_R^* = -20.88 \pm 0.09$ ,  $\alpha_R = -1.07 \pm 0.09$ , and  $\phi_R^* = 0.016 \pm 0.003 \text{ Mpc}^{-3}$  and  $M_V^* = -20.23 \pm 0.09$ ,  $\alpha_V = -1.07 \pm 0.09$ , and  $\phi_V^* = 0.020 \pm 0.003 \text{ Mpc}^{-3}$ .

Surprisingly, the  $V$  and  $R$  local galaxy LF faint end slopes are identical. These LFs apply to  $V$  and  $R$  magnitude-limited samples to comparable depth of the same region of sky. From the color-magnitude relation (Figure 7), we expect that the  $V$  sample would lose red, intrinsically bright galaxies and gain blue, intrinsically faint galaxies, thus producing a steeper faint end slope.

To examine the behavior of these samples, Figures 15 and 16 show the LFs of the bluest 1/3 and reddest 1/3 of the  $R$  and  $V$ -selected samples. We divide the sample in thirds to separate the blue and red colors cleanly, given the typical  $\pm 0.07$  mag  $(V-R)$  error. Figure 17 plots the distribution of rest frame  $(V-R)_0$  colors, with lines marking the  $R$   $(V-R)_0 < 0.499$  and  $(V-R)_0 > 0.555$  mag and  $V$   $(V-R)_0 < 0.494$  and  $(V-R)_0 > 0.551$  mag color cuts. The reddest third generally includes galaxy types Sab and earlier; the bluest third generally includes galaxy types Sc and later.

The bright end of the LF is primarily composed of red, luminous, early-type galaxies and the faint end is composed of blue, intrinsically faint, late-type galaxies. The reddest third LFs show an excess of extremely luminous  $M_V < -22$  cD galaxies and contain no galaxies less luminous than  $M_V > -18$ . The bluest third of the  $V$  and  $R$ -selected samples show no excess of luminous galaxies, but instead determine the entire faint end slope. For  $M_V > -17.5$ , 50% of the galaxies in the magnitude-limited samples are LSB galaxies.

Our  $R$  LF agrees with the original CS LF to within the  $1\sigma$  error of the original CS. The appropriate comparison, however, is with the CS-West LF (Geller et al. 1997); our  $64 \text{ deg}^2$  covers the west half of the CS and does not include the Corona Borealis region. Compared to the CS-West LF, the new  $R$  faint end slope  $\alpha_R$  is  $+0.10$  shallower, the new  $M_R^*$  is  $-0.15$  mag brighter, and the new amplitude  $\phi_R^*$  is 35% lower. The differences, although not formally significant, are attributable to the cleaner sample and refinements of the analysis.

### 5.2. Discussion

#### 5.2.1. The $V$ and $R$ faint end slopes

Here we attempt to determine why the  $V$  and  $R$  faint end slopes appear to be independent of passband. We examine the galaxies unique to the  $V$  and  $R$  samples and study their effect on the LF determinations.

44 of 1255  $V$ -selected galaxies are unique to the  $V$  sample (triangles in Figures 6 and 7), and 40 of 1251  $R$ -selected galaxies are unique to the  $R$  sample (squares in Figures 6

and 7). The 44  $V$  galaxies have lower peak surface brightness and luminosity than the 40  $R$  galaxies. The mean luminosity of the 44  $V$  galaxies is  $\overline{M}_V = -18.9 \pm 1.4$ ; the mean luminosity of the 40  $R$  galaxies is  $\overline{M}_R = -20.8 \pm 0.8$ . Consistent with the color-magnitude relation, the 44  $V$  galaxies are significantly bluer than the 40  $R$  galaxies. Mean rest-frame colors are  $(V-R)_0 = 0.39 \pm 0.06$  mag for the 44  $V$  galaxies and  $(V-R)_0 = 0.59 \pm 0.04$  mag for the 40  $R$  galaxies. Figures 15 and 16 show that the faint end slope of the  $V$  bluest third is  $-0.14$  steeper than the  $R$  bluest third. Similarly, the  $V$  reddest third faint end slope is shallower than the  $R$  reddest third.

The  $V$  and  $R$  faint end slopes probably appear identical because the weight of the LF fit comes from the knee of the LF around  $M^*$ , and  $M^*$  and  $\alpha$  are strongly correlated.  $\alpha$  and  $M^*$  have a correlation coefficient of  $\rho_{\alpha,M^*} \simeq 0.9$  (Schechter 1976). Figure 18 illustrates that the  $V$ - and  $R$ -only galaxies contribute to the LF largely around  $M^*$ , but represent only 3% of the galaxies within 1 magnitude of  $M^*$ . We conclude that identical  $V$  and  $R$  faint end slopes result from fitting the 97%  $M^*$  galaxies common to both samples.

This result suggests that a magnitude-limited LF is a rather blunt tool for characterizing the faint end of the local galaxy population. Furthermore, the faint end comes from a necessarily small volume in a magnitude-limited survey. The population of low luminosity galaxies in the sample is sensitive to local large scale structure. A volume-limited sample of galaxies, complete to low luminosities, would provide a much better determination of the faint end slope of the galaxy LF.

Surveys of clusters, including Virgo (Sandage et al. 1985) and Coma (Bernstein et al. 1995), probe the galaxy LF to faint luminosities. Although it has become clear in recent years that dwarfs contribute to steep faint end slopes, there is little consensus on the slope. Published values of the faint end slope in clusters and groups range from  $-1.2$  to less than  $-2.0$ , and various authors (e.g. Driver & Phillipps 1996; Trentham 1998) make a convincing case for a flat bright end slope and an upturn around  $-18 < M_B < -16$  mag. In these studies, cluster membership is based primarily on statistical background subtraction for lack of redshifts. A faint end slope as steep as  $-2$  was recently supported by Kambas et al. (2000) who assume every LSB galaxy in their images is a member of the Fornax cluster. The numerical simulations of Valotto et al. (2001) show there is a strong tendency for projection effects to cause an apparent rising faint end slope in clusters. Although our samples are limited to  $M_V < -17$  mag, we note that our results are consistent with a faint end slope as steep as  $\alpha \simeq -1.2$ .

#### 5.2.2. Luminosity density

A fundamental quantity provided by the galaxy LF is the local luminosity density of the Universe,

$$j = \phi^* L^* \Gamma(\alpha + 2). \quad (6)$$

We use  $M_{V\odot} = +4.82$  and  $M_{R\odot} = +4.28$  mag (Cox 2000). Table 2 summarizes the local luminosity densities. For the OCDM cosmology,  $j_R = 1.9 \pm 0.6 \times 10^8 h L_\odot \text{ Mpc}^{-3}$  and  $j_V = 2.2 \pm 0.7 \times 10^8 h L_\odot \text{ Mpc}^{-3}$ .

In the luminosity range  $-23 < M_V < -17$  mag, LSB galaxies appear to contribute little to the total luminosity density of the local universe. The magnitude-surface brightness relation shows that the bulk of LSB galaxies are of intrinsic low luminosity, and our shallow faint end slope limits the number of LSB galaxies that might contribute to the luminosity density. Our samples provide no constraints on whether LSB galaxies make a larger contribution to the local luminosity density at fainter absolute magnitudes.

Figure 19 compares the luminosity densities and limiting magnitudes of various surveys (Table 1). The surveys use a common CDM cosmology; choosing alternative values for  $H_0 = 100h \text{ km s}^{-1} \text{ Mpc}^{-1}$  shifts  $j$  by the factor  $h$ . We compare luminosity densities in the  $b_J$  band. We convert our  $V$  sample to  $b_J$  using the typical Sab color  $(b_J - R) = 1.2$  of Fukugita et al. (1995), plus our mean  $(V - R)_0 = 0.53$ . We convert the LCRS with  $(b_J - R) = 1.1$  (Lin et al. 1996). The CfA2 Zwicky magnitudes are adjusted by  $(b_J - m_Z) = -0.35$  (Gaztañaga & Dalton 2000). We note that no correction to the CfA amplitude is needed. Both Bothun & Cornell (1990) and Grogan & Geller (1999) find no significant photometric scale error in samples of 107 and 230 northern Zwicky galaxies.

Figure 19 shows the effect of large scale structure on measurements of the local luminosity density. The northern surveys, which sample the adjacent Virgo cluster and Great Wall region, measure a systematically higher luminosity density than southern surveys of comparable depth. This discrepancy is a result of the absence of nearby rich clusters in the south (i.e. Marzke et al. 1998). The ESP and 2dF appear to go deep enough to sample beyond this southern under-dense region.

The CS luminosity density is comparable to the luminosity density measured by the northern redshift surveys and by the deepest southern redshift surveys. The CS luminosity density is identical with the northern CfA and SDSS surveys when variation in luminosity density over large scale is accounted for. The rich Corona Borealis region in the eastern half of the original CS contains 75% more luminosity density than the western half plotted in Figure 19. When averaged together, the  $b_J$  luminosity density of the full CS is  $\simeq 3.0 \pm 0.7 \times 10^8 h L_\odot \text{ Mpc}^{-3}$ , nearly identical to the CfA and SDSS results.

### 5.2.3. Comparison with other luminosity functions

In Figure 20 we compare the CS  $R$ -band local galaxy LF with other CCD based surveys and with the 2dF survey. The LCRS has Gunn  $r$  photometry calibrated in Cousins  $R$ ; we offset  $M^*$  by  $(R - r) = -0.1$  mag (Shectman et al. 1996). To compare the SDSS  $r^*$ -band LF, we shift  $M^*$  by  $(R - r^*) = -0.22$  (Fukugita et al. 1996). The 2dF is a  $b_J$  photographic-based survey; we shift  $M^*$  by  $(b_J - R) = 1.2$  mag. 1.2 mag is the typical  $(b_J - R)$  of an Sab galaxy (Fukugita et al. 1995) and is consistent with the mean color of the SSRS2 (Marzke & da Costa 1997). We plot the 2dF with its  $b_J$  normalization, though this is probably too large for the  $R$  band. We find a 30% increase in normalization  $\phi^*$  from our  $R$  to  $V$  samples, similar to the 30% increase in normalization from  $r^*$  to  $g^*$  in the SDSS (Blanton et al. 2001). All four LFs in Figure 20 share a common CDM cosmology.

The CS LF parameters  $M^*$ ,  $\alpha$ , and  $\phi^*$  agree at the  $1\sigma$  level with the 2dF and SDSS LF parameters. On the other hand, the CS disagrees with the LCRS  $M^*$  at the  $5\sigma$  level and  $\alpha$  at the  $4\sigma$  level. The probable cause of this disagreement is the surface-brightness limit the LCRS impose on their survey. The LCRS probably samples only the bright end of the luminosity-surface brightness relation, leading to a deficiency of galaxies in the faint end. Furthermore, the LCRS uses isophotal photometry which may lead to an underestimate of the normalization (Blanton et al. 2001). The CS, 2dF, and SDSS make corrections to total magnitudes and have statistically common results. We note that the 2dF and SDSS have systematically steeper faint end slopes and larger normalizations than the CS which may result from the greater depth of these surveys, or from the  $k$ -correction bias (see section 3.1) which tends to add galaxies to the faint end of the LF.

The faint end slopes of our color selected sub-samples are consistent with those found by Marzke & da Costa (1997). Marzke & da Costa (1997) measure plate-based  $(B - R)$  colors for a complete,  $B_{26} < 14.5$  sub-sample of the SSRS2. Making a cut at  $(B_{26} - R_{B26}) = 1.3$ , approximately the color of an Sbc galaxy, they find faint end slopes of  $-1.46 \pm 0.18$  and  $-0.72 \pm 0.24$  for the blue and red halves of their sample. We find  $-1.29$  to  $-1.43 \pm 0.15$  faint end slopes for the bluest third of our samples, and  $-0.21$  to  $-0.13 \pm 0.25$  faint end slopes for the reddest thirds. The reddest thirds are closer to the  $-0.26$  faint end slope of reddest quartile of Marzke & da Costa (1997). The LFs for the red and blue sub-samples are consistent with the overall picture laid out by Binggeli et al. (1988), who describe the galaxy populations which contribute the total galaxy LF.

## 6. CONCLUSIONS

We construct clean 1255 and 1251 member  $V_0 < 16.7$  and  $R_0 < 16.2$  magnitude-limited samples of galaxies from  $64 \text{ deg}^2$  of photometry of the Century Survey (Geller et al. 1997). CCD photometry allows improvements in resolution, linearity, and sensitivity to LSB galaxies; average photometric errors are  $\pm 0.049$  mag. Colors allow more accurate  $k$  corrections. We apply  $k$  corrections before the magnitude selection is performed to ensure all spectral types are sampled to the same depth. The redshifts, obtained from long-slit spectra, are complete even in high density regions and have no surface brightness constraints (as encountered by some fiber surveys). The samples cover  $8^\circ.5 < \alpha_{\text{B1950}} < 13^\circ.5$ ,  $29^\circ < \delta_{\text{B1950}} < 30^\circ$  in the northern sky, and are 98% complete.

We examine the properties of the galaxies in our  $V$  and  $R$  samples, emphasizing the characteristics of the LSB population. We observe strong correlations between color, surface brightness, and luminosity, and construct the following relations for the  $R$  sample:  $(V - R)_0 = (-0.11 \pm 0.05)\mu_{R,0} + (2.6 \pm 0.9)$ ,  $(V - R)_0 = (-0.08 \pm 0.03)M_R - (1.13 \pm 0.5)$ , and  $M_R = (2.1 \pm 0.7)\mu_{R,0} - (60.3 \pm 2)$ .

The LSB galaxy surface number density and distribution of scale lengths and central surface brightnesses are consistent with the angular diameter-limited LSB catalog of O’Neil et al. (1997a), suggesting we are complete for LSB galaxies to our magnitude limit. The LSB galaxies all fall in large scale structure marked by high surface brightness galaxies.

The faint end slopes of the  $V$  and  $R$  local galaxy LFs are surprisingly identical ( $\alpha = -1.07$ , OCDM), probably because of the 97%  $M^*$  galaxies common to the  $V$  and  $R$  samples and because of the strong correlation between  $\alpha$  and  $M^*$  that dominates the LF determination. The OCDM local luminosity densities are:  $j_R = 1.9 \pm 0.6 \times 10^8 hL_\odot$  and  $j_V = 2.2 \pm 0.7 \times 10^8 hL_\odot$ . The luminosity densities are dependent on large scale structure, and are consistent with the northern (CfA and SDSS) redshift surveys and the deepest southern (2dF and ESP) redshift surveys. In the luminosity range  $-23 < M_V < -17$

mag, LSB galaxies appear to contribute little to the total luminosity density of the local universe.

We thank Scott Kenyon, Ken Rines, Perry Berlind, and Mike Calkins for their assistance with the observations, and Susan Tokarz for processing the FAST spectra. We also thank Gary Wegner, John Thorstensen, and Ronald Marzke for their careful work creating the Century Survey. This research was supported by the Smithsonian Institution.

## REFERENCES

- Bernstein, G. M., Nichol, R. C., Tyson, J. A., Ulmer, M. P., & Wittman, D. 1995, AJ, 110, 1507  
 Bertin, E. & Arnouts, S. 1996, A&AS, 117, 393  
 Binggeli, B., Sandage, A., & Tammann, G. A. 1988, ARA&A, 26, 509  
 Blanton, M. R. et al. 2001, AJ, 121, 2358  
 Bothun, G. D. & Cornell, M. E. 1990, AJ, 99, 1004  
 Cox, A. N. 2000, Allen's astrophysical quantities (Allen's astrophysical quantities, 4th ed. Publisher: New York: AIP Press; Springer, 2000. Edited by Arthur N. Cox. ISBN: 0387987460)  
 Cross, N. et al. 2001, MNRAS, in press  
 Davis, L. E. 1998, in ASP Conf. Ser. 145: Astronomical Data Analysis Software and Systems VII, ed. R. Albrecht, R. N. Hook, & H. A. Bushouse, Vol. 7 (San Francisco: ASP), 184  
 de Jong, R. S. & Lacey, C. 2000, ApJ, 545, 781  
 Driver, S. P. 1999, ApJ, 526, L69  
 Driver, S. P. & Phillipps, S. 1996, ApJ, 469, 529  
 Efstathiou, G., Ellis, R. S., & Peterson, B. A. 1988, MNRAS, 232, 431  
 Ellis, R. S., Colless, M., Broadhurst, T., Heyl, J., & Glazebrook, K. 1996, MNRAS, 280, 235  
 Fabricant, D., Cheimets, P., Caldwell, N., & Geary, J. 1998, PASP, 110, 79  
 Frei, Z. & Gunn, J. E. 1994, AJ, 108, 1476  
 Freudling, W. 1993, in 5th ESO/ST-ECF Data Analysis Workshop, ed. P. J. Grosbol & R. C. E. de Ruijsscher (Garching bei München: ESO), 27  
 Fukugita, M., Ichikawa, T., Gunn, J. E., Doi, M., Shimasaku, K., & Schneider, D. P. 1996, AJ, 111, 1748  
 Fukugita, M., Shimasaku, K., & Ichikawa, T. 1995, PASP, 107, 945  
 Gaztañaga, E. & Dalton, G. B. 2000, MNRAS, 312, 417  
 Geller, M. J., Kurtz, M. J., Wegner, G., Thorstensen, J. R., Fabricant, D. G., Marzke, R. O., Huchra, J. P., Schild, R. E., & Falco, E. E. 1997, AJ, 114, 2205  
 Grogin, N. A. & Geller, M. J. 1999, AJ, 118, 2561  
 Hogg, D. W. 1999, preprint (astro-ph/9905116)  
 Kambas, A., Davies, J. I., Smith, R. M., Bianchi, S., & Haynes, J. A. 2000, AJ, 120, 1316  
 Kent, S. M., Ramella, M., & Nonino, M. 1993, AJ, 105, 393  
 Kraan-Korteweg, R. C. 1986, A&AS, 66, 255  
 Kurtz, M. J. & Mink, D. J. 1998, PASP, 110, 934  
 Landolt, A. U. 1992, AJ, 104, 340  
 Lasker, B. M., Sturch, C. R., McLean, B. J., Russell, J. L., Jenkner, H., & Shara, M. M. 1990, AJ, 99, 2019  
 Lilly, S. J., Tresse, L., Hammer, F., Crampton, D., & Le Fevre, O. 1995, ApJ, 455, 108  
 Lin, H., Kirshner, R. P., Schechter, P. L., Shectman, S. A., Landy, S. D., Oemler, A., Tucker, D. L., & Schechter, P. L. 1996, ApJ, 464, 60  
 Lin, H., Yee, H. K. C., Carlberg, R. G., Morris, S. L., Sawicki, M., Patton, D. R., Wirth, G., & Shepherd, C. W. 1999, ApJ, 518, 533  
 Loveday, J., Peterson, B. A., Efstathiou, G., & Maddox, S. J. 1992, ApJ, 390, 338  
 Marzke, R. O. & da Costa, L. N. 1997, AJ, 113, 185  
 Marzke, R. O., da Costa, L. N., Pellegrini, P. S., Willmer, C. N. A., & Geller, M. J. 1998, ApJ, 503, 617  
 Marzke, R. O., Huchra, J. P., & Geller, M. J. 1994, ApJ, 428, 43  
 McGaugh, S. S. & Bothun, G. D. 1994, AJ, 107, 530  
 Mink, D. J. 1999, in ASP Conf. Ser. 172: Astronomical Data Analysis Software and Systems VIII, ed. D. M. Mehringer, R. L. Plante, & D. A. Roberts, Vol. 8 (San Francisco: ASP), 498  
 Mo, H. J., McGaugh, S. S., & Bothun, G. D. 1994, MNRAS, 267, 129  
 Montgomery, K. A., Marschall, L. A., & Janes, K. A. 1993, AJ, 106, 181  
 Muller, G. P., Reed, R., Armandroff, T., Boroson, T. A., & Jacoby, G. H. 1998, Proc. SPIE, 3355, 577  
 O'Neil, K., Bothun, G. D., & Cornell, M. E. 1997a, AJ, 113, 1212  
 O'Neil, K., Bothun, G. D., & Schombert, J. 2000, AJ, 119, 136  
 O'Neil, K., Bothun, G. D., Schombert, J., Cornell, M. E., & Impey, C. D. 1997b, AJ, 114, 2448  
 Poggianti, B. M. 1997, A&AS, 122, 399  
 Ramella, M., Nonino, M., Geller, M., & Kent, S. 1995, Memorie della Societa Astronomica Italiana, 66, 113  
 Ratcliffe, A., Shanks, T., Parker, Q. A., & Fong, R. 1998, MNRAS, 293, 197  
 Sandage, A., Binggeli, B., & Tammann, G. A. 1985, AJ, 90, 1759  
 Sandage, A., Tammann, G. A., & Yahil, A. 1979, ApJ, 232, 352  
 Schechter, P. 1976, ApJ, 203, 297  
 Schlegel, D. J., Finkbeiner, D. P., & Davis, M. 1998, ApJ, 500, 525  
 Shectman, S. A., Landy, S. D., Oemler, A., Tucker, D. L., Lin, H., Kirshner, R. P., & Schechter, P. L. 1996, ApJ, 470, 172  
 Sprayberry, D., Impey, C. D., Irwin, M. J., & Bothun, G. D. 1997, ApJ, 482, 104  
 Trentham, N. 1998, MNRAS, 294, 193  
 Valotto, C. A., Moore, B., & Lambas, D. G. 2001, ApJ, 546, 157  
 Visvanathan, N. 1981, A&A, 100, L20  
 Wegner, G. et al. 2001, AJ, submitted  
 Zucca, E. et al. 1997, A&A, 326, 477

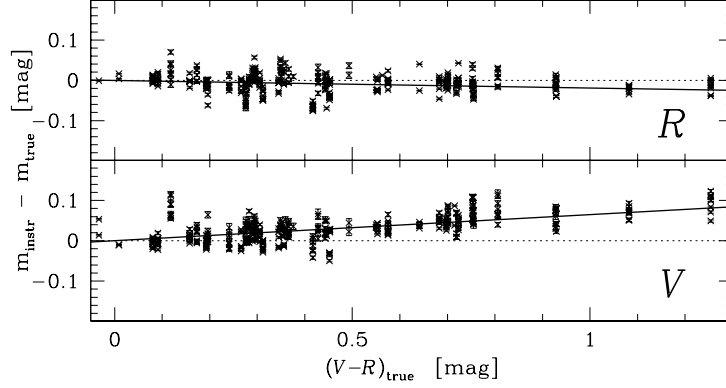


FIG. 1.— MOSAIC chip 2  $R$  and  $V$  color terms, including data from all nights.

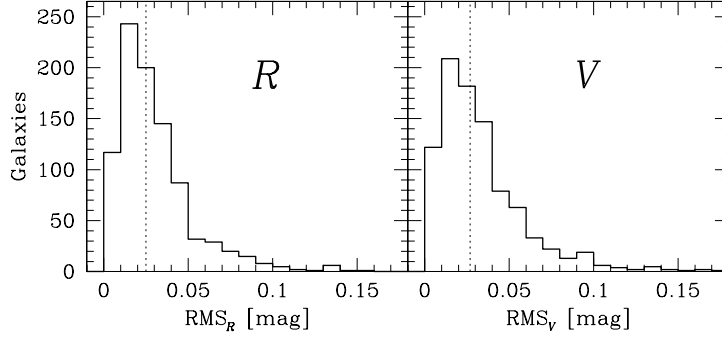


FIG. 2.— Distribution of RMS photometric errors, for galaxies with  $\geq 3$  observations. Dotted lines show the median values  $\text{RMS}_R = \pm 0.025$  and  $\text{RMS}_V = \pm 0.027$  mag.

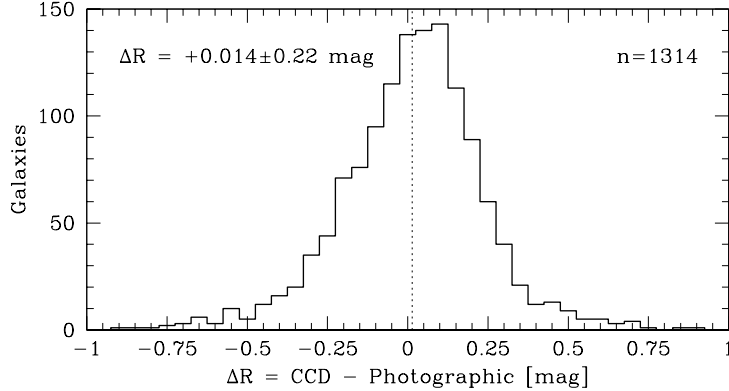


FIG. 3.— Comparison of Century Survey CCD and photographic photometry.

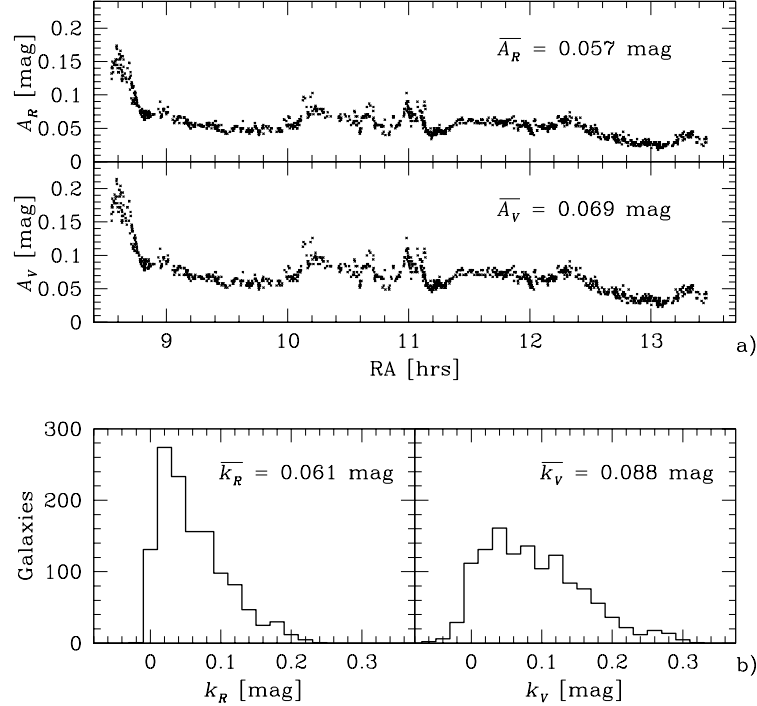


FIG. 4.— a) Galactic extinction and b)  $k$  corrections.

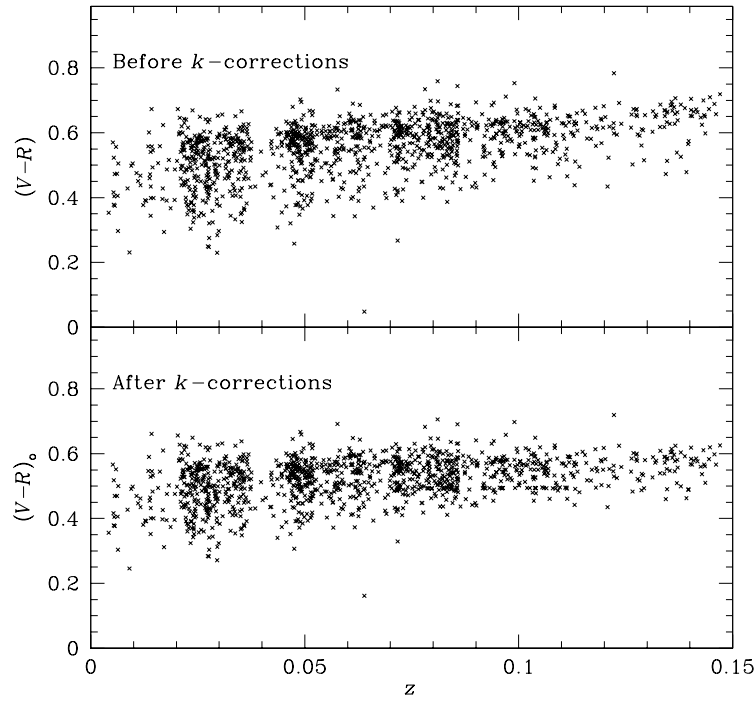


FIG. 5.— Distribution of  $(V-R)$  colors before and after  $k$  corrections for the  $R$ -selected sample.

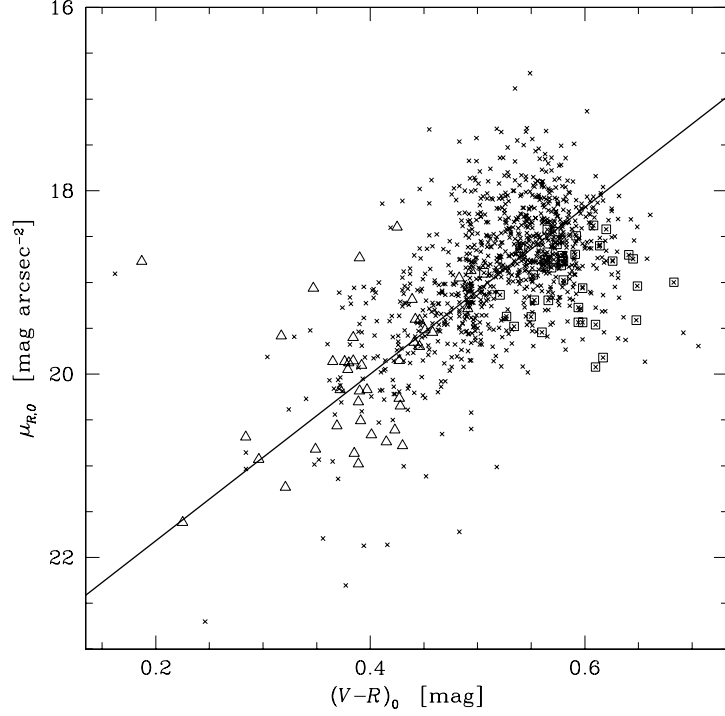


FIG. 6.— Rest frame color-peak surface brightness relation for the  $R$ -selected sample:  $(V-R)_0 = (-0.11 \pm 0.05)\mu_{R,0} + (2.6 \pm 0.9)$ . Open squares mark the 40 galaxies unique to the  $R$  sample, open triangle mark the 44 galaxies unique to the  $V$  sample.

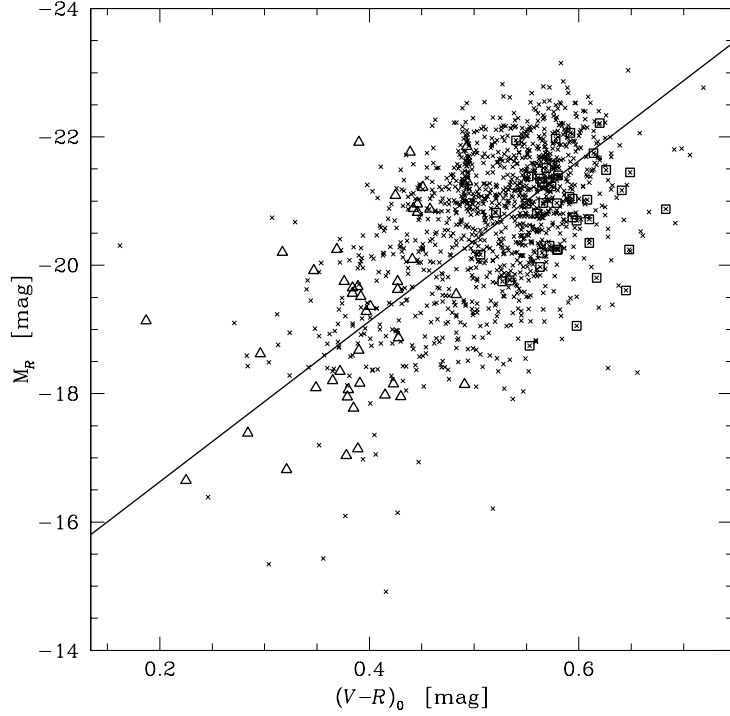


FIG. 7.— Rest frame color-absolute magnitude relation for the  $R$ -selected sample:  $(V-R)_0 = (-0.08 \pm 0.03)M_R - (1.13 \pm 0.5)$ . Open squares mark the 40 galaxies unique to the  $R$  sample, open triangle mark the 44 galaxies unique to the  $V$  sample.

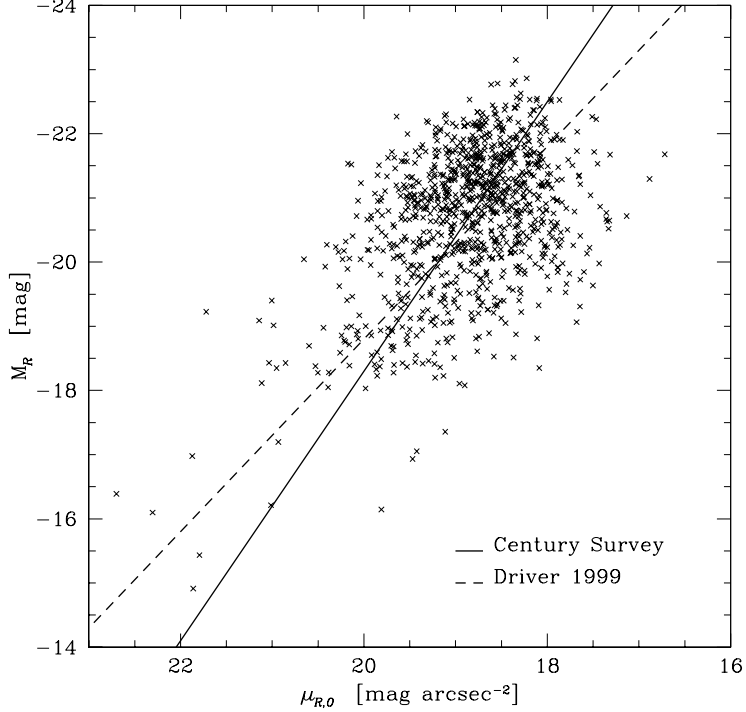


FIG. 8.— Absolute magnitude-surface brightness relation for the  $R$ -selected sample:  $M_R = (2.5 \pm 0.7)\mu_{R,0} - (68 \pm 2)$ .

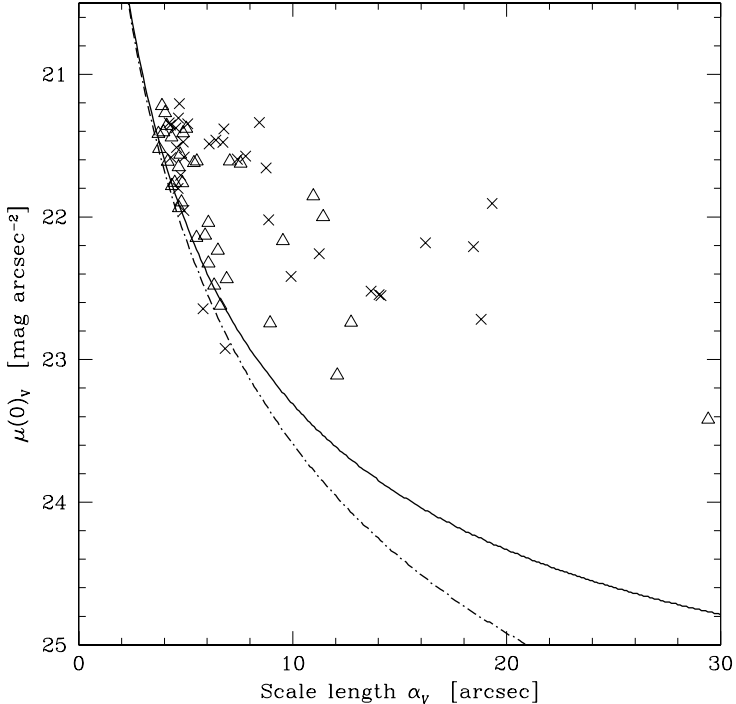


FIG. 9.— Surface brightness vs. scale length comparison of galaxies satisfying  $V < 16.70$  mag,  $\mu(0)_V > 21.2$  mag arcsec $^{-2}$ , and  $\theta > 26''$  for the O'Neil et al. (1997b) LSB catalog ('x's) and our  $V$ -selected sample (triangles). The lines show the  $V = 16.70$  limiting magnitude for a face-on, pure exponential disk profile with limiting sky surface brightnesses of 26 (solid) and 28 (dash-dot) mag arcsec $^{-2}$ .

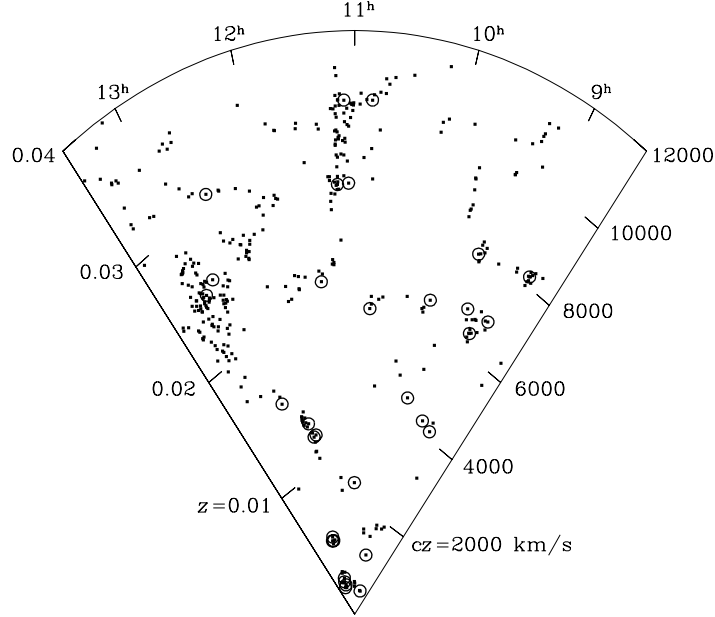


FIG. 10.— Cone diagram for the  $V_0 < 16.70$  Century Survey sample to  $z = 0.04$ . All low surface brightness galaxies  $\mu_V(0)_0 > 21.2$ , marked with circles, fall in large scale structure marked by high surface brightness galaxies.

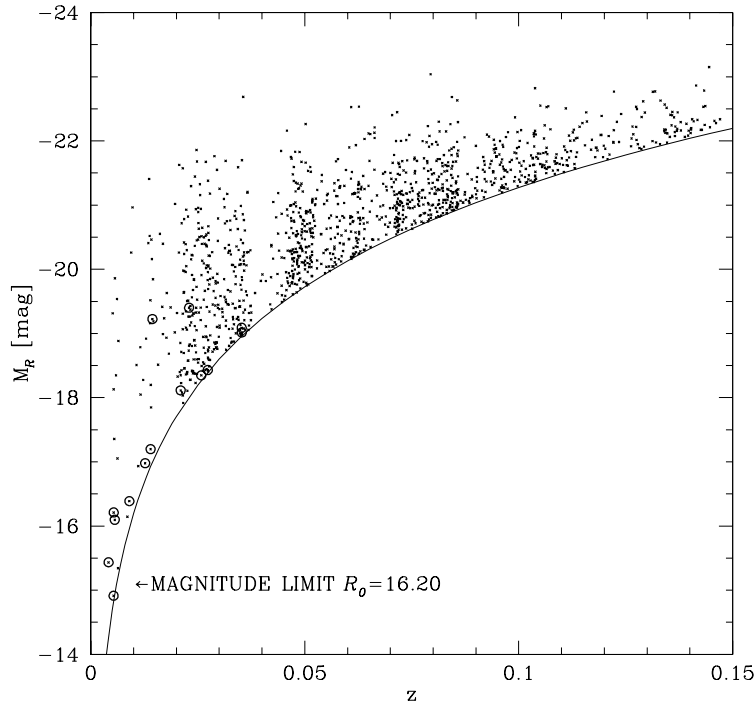


FIG. 11.— Distribution of absolute magnitude with redshift. Low surface brightness galaxies  $\mu_{R,0} > 20.8$ , marked with circles, are clearly low luminosity systems. The line shows the limiting  $R$  absolute magnitude vs. redshift.

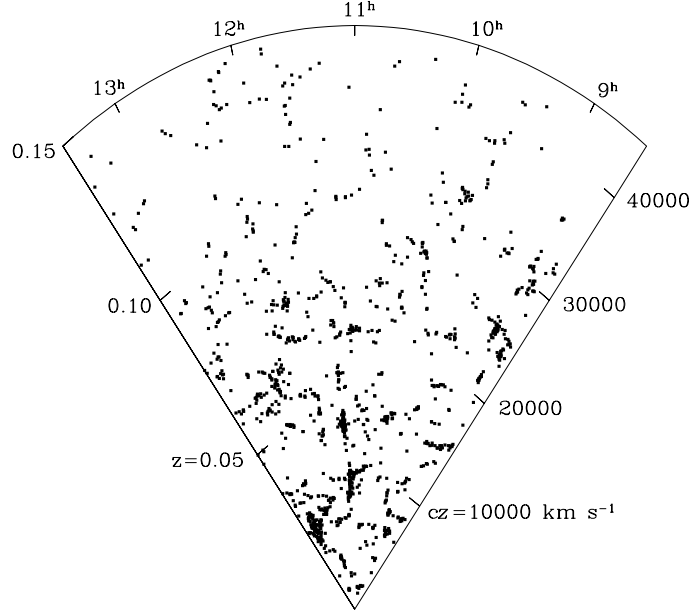


FIG. 12.— Cone diagram for the full  $R_0 < 16.20$  Century Survey sample.

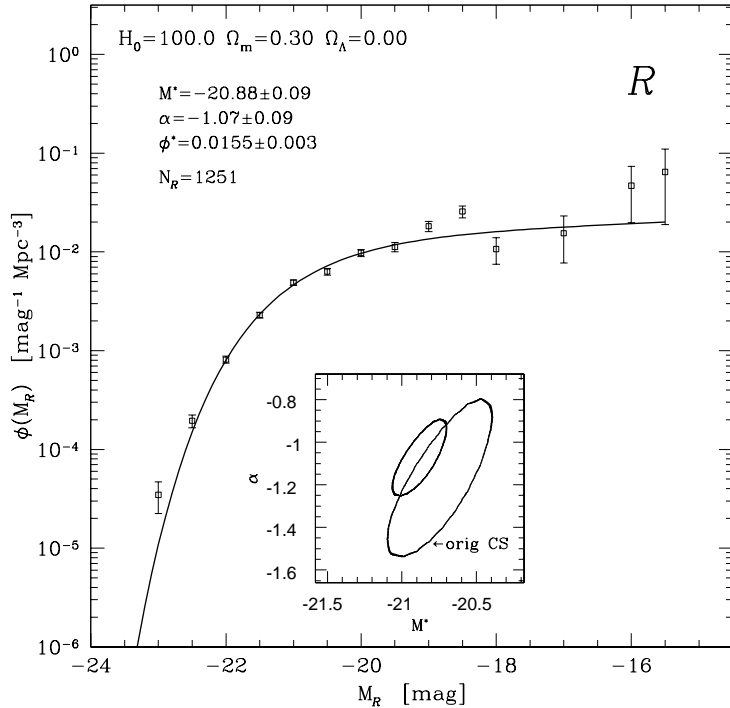


FIG. 13.—  $R_0 < 16.20$  galaxy luminosity function (OCDM). Inset shows the  $2\sigma \chi^2$  error ellipse for  $M^*$  and  $\alpha$ .

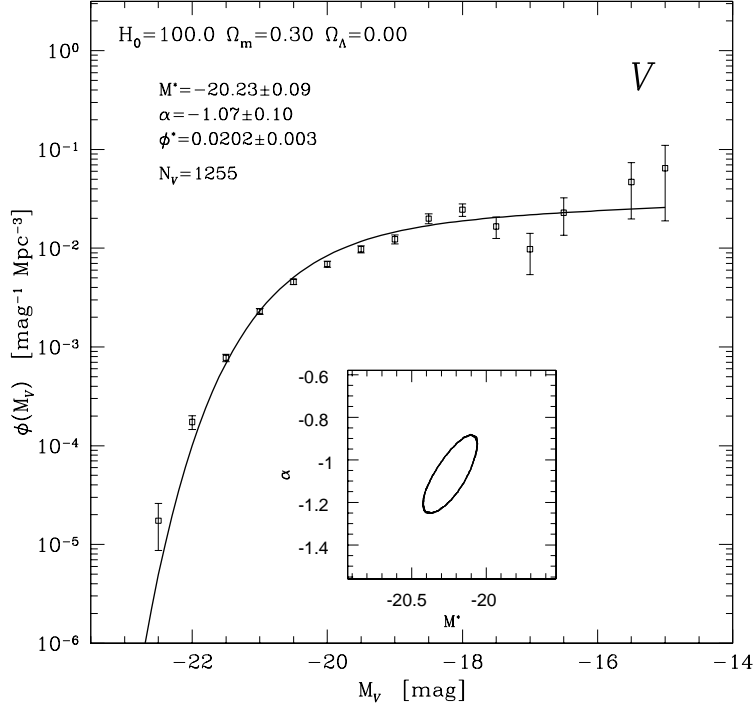


FIG. 14.—  $V_0 < 16.70$  galaxy luminosity function (OCDM). Inset shows the  $2\sigma \chi^2$  error ellipse for  $M^*$  and  $\alpha$ .

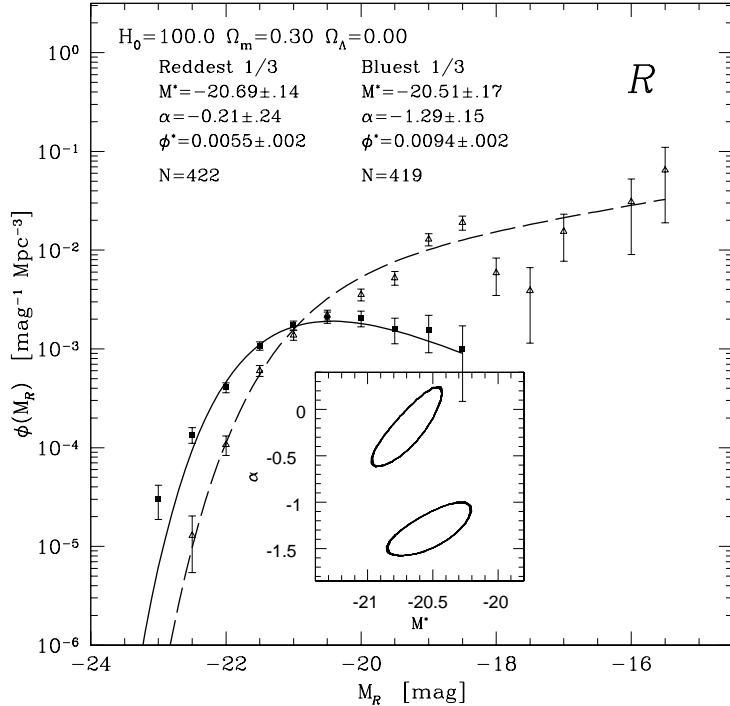


FIG. 15.— Luminosity functions of the reddest 1/3 (solid line) and bluest 1/3 (dashed line) of the  $R$ -selected sample (OCDM). Inset shows the  $2\sigma \chi^2$  error ellipses for  $M^*$  and  $\alpha$ .

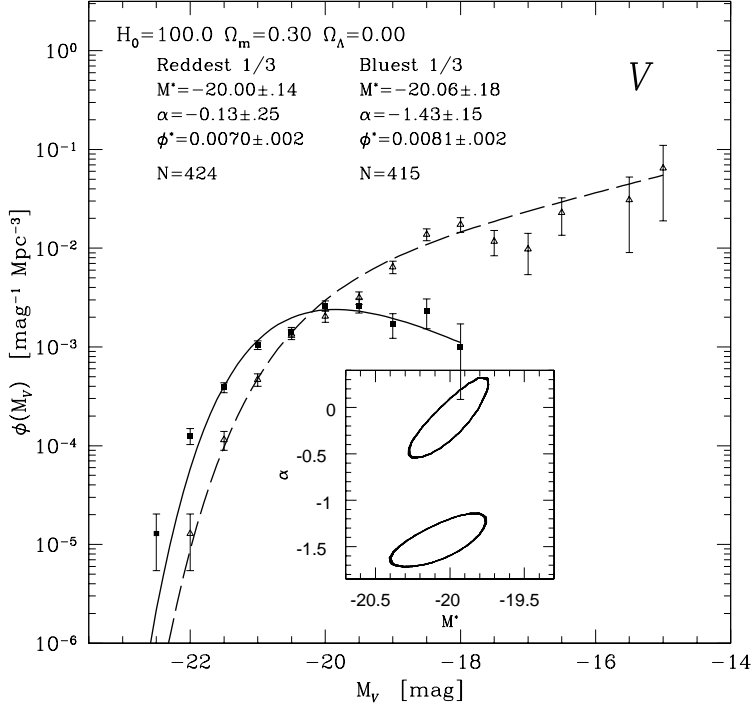


FIG. 16.— Luminosity functions of the reddest 1/3 (solid line) and bluest 1/3 (dashed line) of the  $V$ -selected sample (OCDM). Inset shows the  $2\sigma \chi^2$  error ellipses for  $M^*$  and  $\alpha$ .

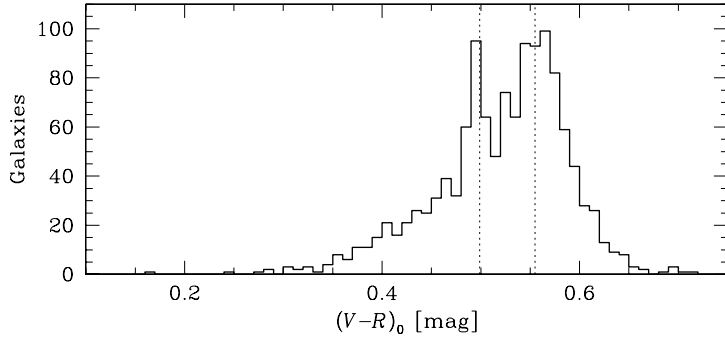


FIG. 17.— Histogram of the rest-frame  $(V-R)_0$  colors. Dotted lines mark the bluest and reddest thirds of the  $R$ -selected sample.

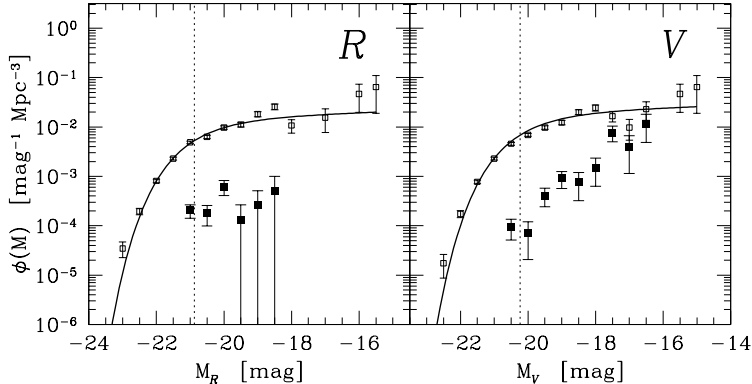


FIG. 18.— Luminosity distribution of the galaxies unique to the  $V$  and  $R$  samples (solid squares) compared with the full samples. The dotted line marks  $M^*$  (OCDM).

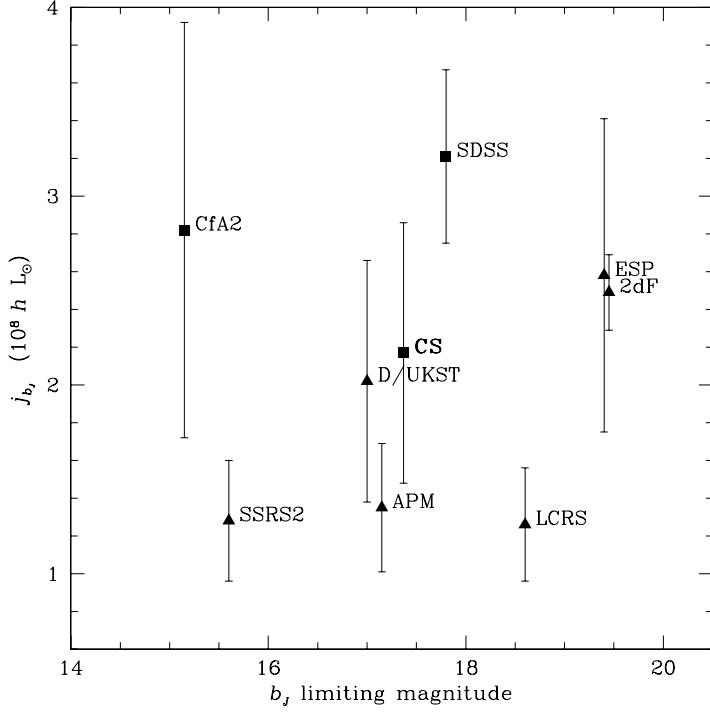


FIG. 19.— Luminosity density  $j_b$  and the  $b_J$ -limiting magnitude of various redshift surveys (Table 1). Squares mark the northern surveys, triangles mark the southern surveys. The CS luminosity density is for the western  $64 \text{ deg}^2$  studied in this paper; averaging in the eastern half of the CS would raise the luminosity density to  $3.0 \pm 0.7 \times 10^8 h L_\odot \text{ Mpc}^{-3}$ .

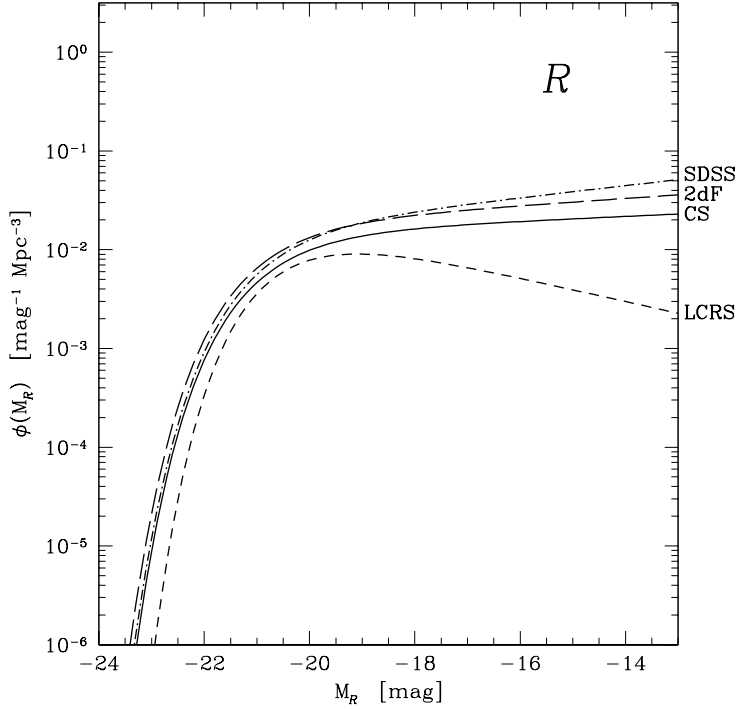


FIG. 20.— Comparison of CCD-based local galaxy luminosity function determinations, including the current 2dF. We assume  $(R - r^*) = -0.22$  for the SDSS (Fukugita et al. 1996),  $(B - R) = 1.2$  for the 2dF (Fukugita et al. 1995), and  $(R - r) = -0.10$  for the LCRS (Shectman et al. 1996).

## APPENDIX

## COMPARISON OF CCD AND PHOTOGRAPHIC PHOTOMETRY

Our data allows comparison between the photographic and CCD photometry of 1374 CS galaxies. The photographic photometry is accurate and remarkably complete. CCD photometry offers improvements in precision, linearity, and resolution over the photographic photometry.

The CCD photometry reveals a residual non-linearity in the photographic photometry. The brightest  $R < 11$  mag CS galaxies are typically 0.5 mag brighter than their photographic magnitudes; this CCD–photographic offset decreases with increasing magnitude. The original photometry was calibrated by fixing a preliminary zero point on each plate by comparison to the drift scans of Ramella et al. (1995) and Kent et al. (1993) at  $R = 16.0$ . Data from all plates was then combined and a preliminary global slope for the scale error was obtained. The zero point was then redetermined (at  $R = 16.0$ ) for each plate, using the preliminary relation, and a new global slope was determined. This process converged after two iterations. Our CCD photometry indicates a residual slope of  $-0.06$  mag / mag — an error of 10% in the original zero-point slope. This error is consistent with the variation in non-linearity between photographic plates, and underscores the improvement possible with CCD photometry.

Our CCD data, with 0.424 arcsec pixels and  $\text{FWHM} < 1.5$  arcsec seeing, has roughly twice the resolution of the scanned photographic images, with 1.3 arcsec pixels and  $\text{FWHM} \sim 2$  arcsec seeing. We discover 2% of the 1374 CS galaxies have previously unresolved companions. 70% of the resolved objects are companion galaxies. The CCD photometry typically places the brightest companion  $\sim 0.5$  mag fainter than the original CS “galaxy.” 30% of the close companions are stars superimposed on faint galaxies; for these objects CCD photometry of the galaxy typically reveals a  $\sim 1$  mag offset from the original photographic catalog.

Ignoring problematic cases (bright galaxies  $R < 12$  and galaxies with previously unresolved companions) the zero-point offset between the uncorrected CCD and photographic catalogs is  $\Delta R_{\text{CCD-photographic}} = 0.014 \pm 0.22$  mag. Figure 3 plots the distribution of  $\Delta R_{\text{CCD-photographic}}$  for 1314 CS galaxies. The accuracy of the CCD and photographic photometry is identical to within the average CCD zero-point error  $\pm 0.034$  mag. The  $\pm 0.22$  mag scatter, a sum in quadrature of the CCD and photographic photometric error, shows that the  $\pm 0.25$  mag error of Geller et al. (1997) is slightly overestimated.

To investigate the CS completeness we apply the original CS (uncorrected) magnitude limit  $R < 16.13$  mag and velocity limits  $1,000 < cz < 45,000$  km s $^{-1}$  to the CCD and photographic photometric catalogs. The photographic sample contains  $n_{\text{photo}} = 959$  galaxies, and the CCD sample contains  $n_{\text{CCD}} = 971$  galaxies. Thus the photographic sample is  $n_{\text{photo}}/n_{\text{CCD}} = 98.8\%$  complete compared to the CCD sample.

We now explore the properties of the galaxies specific to the photographic and CCD samples. The CCD sample excludes 121 galaxies from the original photographic sample, and includes 133 new galaxies. 60% of the 133 galaxies lie within  $1\sigma = 0.22$  mag of  $R = 16.13$ . Thus the major difference between the CCD and photographic samples is galaxies scattering above/below the limiting magnitude. The next most numerous addition/subtraction of galaxies comes from the 27 previously unresolved companions. Of the remaining objects specific to the CCD catalog, only 3 are LSB galaxies. Using the  $\mu(0)_R > 20.8$  mag arcsec $^{-2}$  definition of a LSB galaxy, the photographic catalog contains 12 LSB galaxies to  $R < 16.13$  mag and the CCD catalog 15. Thus the photographic catalog is 80% complete compared to the CCD catalog in LSB galaxies. We conclude that, despite non-linearity and resolution problems, the CS photographic catalog is nearly as complete as the CCD catalog.

## CENTURY SURVEY CCD PHOTOMETRY

Table 3 contains the CCD photometry for the CS  $V$  and  $R$  samples. There are a total of 1295 galaxies. Column 1 is the galaxy identification; IDs under 3000 are galaxies listed in the original Century Survey photographic catalog. Column 2 is the J2000 right ascension in hours, minutes, and seconds. Column 3 is the J2000 declination in degrees, arcminutes, and arcseconds. Columns 4 and 5 are the measured  $R$  and  $V$  magnitudes; the magnitude errors are a sum in quadrature of the zero-point error and the measurement error. Column 6 is the  $E(B-V)$  extinction value from Schlegel et al. (1998) for that RA and Dec; we derive galactic extinctions from  $A = E(B-V) \cdot A/E(B-V)$  using  $A/E(B-V)$  values from Table 6 of Schlegel et al. (1998). Columns 7 and 8 are  $k$  corrections interpolated from Poggianti (1997) types E, Sa, and Sc and Frei & Gunn (1994) type Im for the Kron Cousins  $R$  and Johnson  $V$  filters. The  $V$  and  $R$  samples are defined by  $V - A_V - k_V < 16.70$  and  $R - A_R - k_R < 16.20$  mag.

TABLE 1  
LOCAL GALAXY LUMINOSITY FUNCTIONS

Survey	$\bar{z}$	Area (deg $^2$ )	Galaxies	Mag Limit	$M^* + 5 \log h$ (mag)	$\alpha$	$\phi^*$ ( $h^3$ Mpc $^{-3}$ )	Ref.
CS	.06	102	1762	$R = 16.13$	$-20.73 \pm 0.18$	$-1.17 \pm 0.19$	$0.025 \pm 0.006$	1
SDSS	.10	140	11275	$r^* = 17.6$	$-20.67 \pm 0.03$	$-1.15 \pm 0.03$	$0.019 \pm 0.002$	2
LCRS	.10	700	18678	$r \sim 17.5$	$-20.29 \pm 0.02$	$-0.70 \pm 0.05$	$0.019 \pm 0.001$	3
2dF	.10	257	20765	$b_J = 19.45$	$-19.75 \pm 0.05$	$-1.09 \pm 0.03$	$0.0202 \pm 0.0002$	4
D/UKST	.05	$\sim 1500$	$\sim 2500$	$b_J \sim 17$	$-19.68 \pm 0.10$	$-1.04 \pm 0.08$	$0.017 \pm 0.003$	5
ESP	.10	23	3342	$b_J = 19.4$	$-19.61^{+0.06}_{-0.08}$	$-1.22^{+0.06}_{-0.07}$	$0.020 \pm 0.004$	6
SSRS2	.025	5550	5036	$m_{B(0)} = 15.5$	$-19.43 \pm 0.06$	$-1.12 \pm 0.05$	$0.013 \pm 0.002$	7
CfA2	.025	6900	9063	$m_Z = 15.5$	$-18.8 \pm 0.03$	$-1.0 \pm 0.2$	$0.04 \pm 0.01$	8
APM	.05	4300	1658	$b_J = 17.15$	$-19.15 \pm 0.13$	$-0.97 \pm 0.15$	$0.014 \pm 0.002$	9

Note. — Local redshift surveys with  $> 1000$  galaxies and  $\bar{z} > 0.01$ . Luminosity function parameters use a  $H_0 = 100$  CDM cosmology.

References. — (1) Geller et al. (1997); (2) Blanton et al. (2001); (3) Lin et al. (1996); (4) Cross et al. (2001); (5) Ratcliffe et al. (1998); (6) Zucca et al. (1997); (7) Marzke et al. (1998); (8) Marzke et al. (1994); (9) Loveday et al. (1992)

TABLE 2  
CENTURY SURVEY LF

$H_0, \Omega_m, \Omega_\Lambda$	Band	Galaxies	$M^*$ (mag)	$\alpha$	$\phi^*$ (Mpc $^{-3}$ )	$j$ ( $10^8 L_\odot$ )
100, 1.0, 0.0	$R$	1251	$-20.84 \pm 0.09$	$-1.06 \pm 0.09$	$0.016 \pm 0.003$	$1.88 \pm 0.59$
	$V$	1255	$-20.20 \pm 0.09$	$-1.06 \pm 0.09$	$0.021 \pm 0.004$	$2.21 \pm 0.69$
75, 0.3, 0.7	$R$	1251	$-21.57 \pm 0.09$	$-1.09 \pm 0.09$	$0.0060 \pm 0.0006$	$1.39 \pm 0.34$
	$V$	1255	$-20.92 \pm 0.09$	$-1.09 \pm 0.09$	$0.0079 \pm 0.0009$	$1.65 \pm 0.43$
100, 0.3, 0.0	$R$	1251	$-20.88 \pm 0.09$	$-1.07 \pm 0.09$	$0.016 \pm 0.003$	$1.88 \pm 0.58$
	$V$	1255	$-20.23 \pm 0.09$	$-1.07 \pm 0.10$	$0.020 \pm 0.003$	$2.21 \pm 0.70$
$R_{\text{blue } 1/3}$	419		$-20.51 \pm 0.17$	$-1.29 \pm 0.15$	$0.009 \pm 0.002$	$0.97 \pm 0.51$
	$R_{\text{red } 1/3}$	422	$-20.69 \pm 0.14$	$-0.21 \pm 0.24$	$0.006 \pm 0.001$	$0.50 \pm 0.11$
	$V_{\text{blue } 1/3}$	415	$-20.06 \pm 0.18$	$-1.43 \pm 0.15$	$0.008 \pm 0.002$	$1.05 \pm 0.59$
$V_{\text{red } 1/3}$	424		$-20.00 \pm 0.14$	$-0.13 \pm 0.25$	$0.007 \pm 0.001$	$0.56 \pm 0.12$

TABLE 3  
CENTURY SURVEY CCD PHOTOMETRY<sup>a</sup>

ID	RA <sub>J2000</sub>	Dec <sub>J2000</sub>	$R$	$V$	$E(B-V)^b$	$k_R^c$	$k_V^c$
cs2	8 35 49.11	28 53 13.5	$15.11 \pm 0.11$	$15.63 \pm 0.12$	0.050	0.02	0.04
cs3	8 35 54.33	29 25 37.9	$15.93 \pm 0.04$	$16.60 \pm 0.06$	0.047	0.10	0.15
cs4	8 35 54.60	29 41 32.7	$16.00 \pm 0.06$	$16.67 \pm 0.06$	0.053	0.14	0.20
cs6	8 36 03.35	28 57 46.9	$15.53 \pm 0.04$	$16.07 \pm 0.05$	0.054	0.03	0.06
cs8	8 36 14.38	29 03 16.2	$15.70 \pm 0.05$	$16.36 \pm 0.07$	0.057	0.10	0.15

<sup>a</sup>[The complete version of this table is in the electronic edition of the Journal. The printed edition contains only a sample.]

<sup>b</sup>Values from Schlegel et al. (1998).

<sup>c</sup>Values interpolated from Poggianti (1997) types E, Sa, and Sc and Frei & Gunn (1994) type Im for the Kron Cousins  $R$  and Johnson  $V$  filters.

Table 1. Century Survey CCD Photometry

ID	RA <sub>J2000</sub>	Dec <sub>J2000</sub>	<i>R</i>	<i>V</i>	<i>E(B-V)</i> <sup>a</sup>	<i>k<sub>R</sub></i> <sup>b</sup>	<i>k<sub>V</sub></i> <sup>b</sup>
cs2	8 35 49.11	28 53 13.5	15.11 ± 0.11	15.63 ± 0.12	0.050	0.02	0.04
cs3	8 35 54.33	29 25 37.9	15.93 ± 0.04	16.60 ± 0.06	0.047	0.10	0.15
cs4	8 35 54.60	29 41 32.7	16.00 ± 0.06	16.67 ± 0.06	0.053	0.14	0.20
cs6	8 36 03.35	28 57 46.9	15.53 ± 0.04	16.07 ± 0.05	0.054	0.03	0.06
cs8	8 36 14.38	29 03 16.2	15.70 ± 0.05	16.36 ± 0.07	0.057	0.10	0.15
cs3002	8 36 20.77	29 16 37.6	16.24 ± 0.07	16.80 ± 0.07	0.053	0.05	0.09
cs9	8 36 38.16	29 34 00.5	15.39 ± 0.04	16.00 ± 0.08	0.051	0.05	0.09
cs3003	8 36 56.09	29 48 06.4	16.34 ± 0.06	16.91 ± 0.05	0.056	0.04	0.07
cs11	8 36 59.35	29 45 23.0	15.80 ± 0.05	16.40 ± 0.05	0.056	0.04	0.08
cs3004	8 37 12.46	29 43 44.7	16.35 ± 0.05	17.04 ± 0.06	0.055	0.15	0.21
cs12	8 37 32.14	29 04 37.6	15.18 ± 0.05	15.77 ± 0.06	0.055	0.05	0.09
cs13	8 37 48.66	29 46 56.4	15.63 ± 0.05	16.27 ± 0.06	0.057	0.06	0.10
cs14	8 37 54.17	29 47 42.4	16.34 ± 0.05	16.91 ± 0.05	0.058	0.06	0.10
cs3006	8 38 14.95	29 45 20.6	16.15 ± 0.08	16.75 ± 0.10	0.065	0.10	0.16
cs15	8 38 23.27	29 45 21.3	15.77 ± 0.06	16.45 ± 0.05	0.066	0.14	0.20
cs16	8 38 33.06	29 28 54.7	16.16 ± 0.04	16.75 ± 0.05	0.064	0.07	0.12
cs17	8 38 39.56	29 11 27.7	15.95 ± 0.04	16.48 ± 0.03	0.055	0.01	0.02
cs18	8 38 48.08	29 22 11.9	15.18 ± 0.05	15.78 ± 0.05	0.058	0.07	0.12
cs19	8 38 50.04	28 55 17.2	15.45 ± 0.08	16.09 ± 0.05	0.053	0.11	0.16
cs3010	8 39 14.69	28 50 11.3	16.35 ± 0.05	16.95 ± 0.10	0.051	0.08	0.13
cs20	8 39 15.85	28 50 39.4	14.17 ± 0.05	14.90 ± 0.03	0.051	0.12	0.18
cs21	8 39 31.44	29 09 13.8	15.50 ± 0.05	16.15 ± 0.05	0.061	0.09	0.14
cs22	8 39 46.17	29 16 54.6	15.76 ± 0.04	16.45 ± 0.03	0.061	0.11	0.16
cs23	8 39 56.79	28 59 15.2	16.30 ± 0.06	17.02 ± 0.08	0.053	0.13	0.18
cs24	8 40 02.36	29 49 02.7	14.60 ± 0.03	15.18 ± 0.05	0.058	0.05	0.10
cs25	8 40 10.71	29 07 24.6	15.86 ± 0.05	16.53 ± 0.05	0.053	0.10	0.15
cs26	8 40 15.09	29 25 17.1	16.01 ± 0.07	16.65 ± 0.09	0.059	0.09	0.14
cs27	8 40 15.67	28 50 43.9	14.97 ± 0.11	15.62 ± 0.19	0.063	0.10	0.14
cs28	8 40 21.41	29 12 53.2	16.13 ± 0.05	16.70 ± 0.05	0.055	0.05	0.09
cs3005	8 40 24.16	29 25 02.5	16.43 ± 0.05	16.83 ± 0.06	0.059	0.01	0.00
cs29	8 40 29.20	29 26 40.4	14.59 ± 0.04	15.17 ± 0.08	0.060	0.04	0.08
cs30	8 40 50.62	29 12 00.2	16.17 ± 0.10	16.78 ± 0.11	0.047	0.08	0.13
cs31	8 40 54.44	29 19 44.7	15.21 ± 0.03	15.77 ± 0.10	0.052	0.06	0.10
cs32	8 40 59.22	29 13 22.0	15.64 ± 0.06	16.34 ± 0.08	0.047	0.12	0.17
cs33	8 41 02.36	29 03 39.3	15.29 ± 0.05	15.95 ± 0.04	0.049	0.13	0.19
cs34	8 41 03.88	29 13 43.2	15.08 ± 0.05	15.70 ± 0.08	0.046	0.09	0.13

Table 1—Continued

ID	RA <sub>J2000</sub>	Dec <sub>J2000</sub>	<i>R</i>	<i>V</i>	<i>E(B-V)</i> <sup>a</sup>	<i>k<sub>R</sub></i> <sup>b</sup>	<i>k<sub>V</sub></i> <sup>b</sup>
cs35	8 41 07.74	29 19 30.4	16.20 ± 0.04	16.79 ± 0.13	0.051	0.07	0.12
cs36	8 41 17.74	29 15 17.3	15.99 ± 0.05	16.65 ± 0.06	0.047	0.10	0.15
cs3012	8 41 19.75	29 29 14.4	16.40 ± 0.04	16.98 ± 0.08	0.060	0.07	0.11
cs3014	8 41 36.93	29 08 11.1	16.32 ± 0.06	16.97 ± 0.05	0.049	0.09	0.14
cs37	8 41 43.56	29 30 44.9	16.04 ± 0.03	16.66 ± 0.03	0.058	0.08	0.13
cs38	8 41 45.83	29 47 55.5	15.35 ± 0.04	16.00 ± 0.04	0.054	0.12	0.17
cs3016	8 42 21.84	29 06 11.1	16.22 ± 0.04	16.79 ± 0.04	0.050	0.07	0.11
cs39	8 42 45.47	29 23 59.2	14.94 ± 0.05	15.51 ± 0.07	0.048	0.02	0.05
cs3017	8 42 57.40	29 39 40.5	16.33 ± 0.06	17.00 ± 0.10	0.047	0.13	0.18
cs42	8 43 21.21	28 49 51.9	15.03 ± 0.04	15.64 ± 0.03	0.045	0.09	0.14
cs44	8 43 44.86	29 19 21.0	16.16 ± 0.06	16.71 ± 0.03	0.053	0.05	0.08
cs45 <sup>c</sup>	8 44 21.37	29 06 09.6	16.32 ± 0.05	16.83 ± 0.05	0.047	0.02	0.04
cs3022	8 44 35.15	29 17 14.3	16.40 ± 0.07	17.01 ± 0.09	0.056	0.10	0.15
cs46	8 44 36.55	29 21 12.8	15.58 ± 0.05	16.20 ± 0.10	0.056	0.11	0.17
cs47	8 44 53.42	29 39 21.9	16.27 ± 0.04	16.87 ± 0.05	0.041	0.10	0.15
cs3023	8 44 53.56	28 49 52.4	16.37 ± 0.04	16.97 ± 0.03	0.048	0.05	0.08
cs48	8 45 12.47	29 18 22.8	16.06 ± 0.03	16.68 ± 0.04	0.051	0.11	0.16
cs49	8 45 20.84	29 18 01.1	16.27 ± 0.11	16.91 ± 0.09	0.049	0.12	0.17
cs50	8 45 37.76	29 40 17.3	16.10 ± 0.04	16.68 ± 0.04	0.036	0.06	0.11
cs51	8 45 47.12	29 16 18.2	16.06 ± 0.09	16.71 ± 0.11	0.045	0.12	0.18
cs52	8 45 48.21	29 20 54.8	15.79 ± 0.04	16.34 ± 0.04	0.044	0.04	0.08
cs53	8 45 55.88	29 46 26.1	16.26 ± 0.05	16.94 ± 0.06	0.033	0.07	0.10
cs54	8 45 56.69	29 15 25.0	15.93 ± 0.15	16.71 ± 0.27	0.044	0.19	0.24
cs55	8 45 58.60	29 18 48.6	15.50 ± 0.04	16.11 ± 0.05	0.043	0.10	0.16
cs3025	8 46 00.03	29 05 48.8	16.11 ± 0.04	16.76 ± 0.05	0.042	0.10	0.15
cs56	8 46 08.03	29 22 47.4	15.22 ± 0.05	15.87 ± 0.05	0.043	0.08	0.13
cs57	8 46 20.60	29 23 03.9	15.94 ± 0.04	16.54 ± 0.04	0.042	0.10	0.15
cs58	8 46 26.11	29 45 38.8	16.32 ± 0.07	16.89 ± 0.07	0.034	0.06	0.10
cs59	8 46 26.73	29 34 21.0	16.14 ± 0.04	16.72 ± 0.04	0.035	0.06	0.11
cs60	8 46 28.91	29 40 54.4	15.88 ± 0.05	16.54 ± 0.05	0.035	0.09	0.14
cs61	8 46 32.49	29 35 55.4	14.48 ± 0.09	15.16 ± 0.10	0.035	0.10	0.14
cs62	8 46 35.12	29 36 15.3	15.88 ± 0.05	16.50 ± 0.07	0.035	0.08	0.12
cs63	8 46 37.83	29 39 02.4	16.16 ± 0.06	16.78 ± 0.07	0.035	0.08	0.12
cs64	8 46 39.25	29 48 42.0	15.34 ± 0.04	16.02 ± 0.04	0.034	0.10	0.15
cs43	8 46 39.56	29 08 20.2	16.54 ± 0.03	16.83 ± 0.04	0.053	0.00	-0.02
cs65	8 46 42.38	29 38 48.9	16.19 ± 0.04	16.77 ± 0.04	0.035	0.06	0.11

Table 1—Continued

ID	RA <sub>J2000</sub>	Dec <sub>J2000</sub>	<i>R</i>	<i>V</i>	<i>E(B-V)</i> <sup>a</sup>	<i>k<sub>R</sub></i> <sup>b</sup>	<i>k<sub>V</sub></i> <sup>b</sup>
cs3027	8 46 43.38	28 54 31.6	16.34 ± 0.03	17.03 ± 0.06	0.043	0.12	0.17
cs66	8 46 57.19	29 28 11.7	15.52 ± 0.05	16.13 ± 0.06	0.039	0.07	0.12
cs67	8 47 09.01	29 46 55.9	15.64 ± 0.04	16.19 ± 0.05	0.033	0.03	0.07
cs68	8 47 12.95	29 36 14.4	15.54 ± 0.05	16.10 ± 0.07	0.036	0.05	0.08
cs69	8 47 24.71	29 05 15.4	16.24 ± 0.08	16.94 ± 0.05	0.038	0.18	0.24
cs70	8 47 27.23	28 50 41.6	15.65 ± 0.04	16.09 ± 0.04	0.040	0.01	0.01
cs71	8 47 34.02	29 44 21.3	15.69 ± 0.04	16.22 ± 0.04	0.033	0.03	0.05
cs72	8 47 42.35	29 01 22.4	15.74 ± 0.04	16.41 ± 0.06	0.039	0.16	0.22
cs73	8 47 55.02	29 25 32.2	16.09 ± 0.08	16.74 ± 0.08	0.037	0.12	0.18
cs74	8 48 10.29	29 31 44.7	16.15 ± 0.05	16.63 ± 0.06	0.036	0.01	0.02
cs75	8 48 10.47	29 29 28.9	14.15 ± 0.05	14.75 ± 0.05	0.035	0.03	0.05
cs76	8 48 18.62	29 23 45.6	16.03 ± 0.08	16.69 ± 0.09	0.035	0.16	0.22
cs77	8 48 20.70	29 04 27.1	15.98 ± 0.05	16.54 ± 0.05	0.032	0.04	0.07
cs3032	8 48 25.63	29 44 09.0	16.37 ± 0.07	17.00 ± 0.06	0.034	0.14	0.21
cs78	8 48 31.42	29 21 18.1	16.01 ± 0.05	16.61 ± 0.08	0.033	0.11	0.17
cs79	8 49 11.76	29 15 23.8	16.29 ± 0.09	16.85 ± 0.15	0.032	0.06	0.10
cs80	8 49 27.23	29 31 11.6	14.49 ± 0.04	14.94 ± 0.04	0.031	0.01	0.01
cs3033	8 49 32.54	29 26 19.3	16.31 ± 0.03	16.86 ± 0.04	0.031	0.06	0.09
cs81	8 49 56.77	29 38 54.5	16.02 ± 0.05	16.63 ± 0.04	0.029	0.12	0.17
cs82	8 50 03.57	29 36 24.0	16.05 ± 0.05	16.67 ± 0.07	0.029	0.12	0.18
cs83	8 50 07.09	29 32 52.2	14.92 ± 0.03	15.52 ± 0.04	0.028	0.11	0.17
cs84	8 50 07.66	29 32 56.8	15.29 ± 0.03	15.92 ± 0.03	0.028	0.13	0.19
cs3040	8 50 14.20	29 40 50.1	16.23 ± 0.05	16.89 ± 0.06	0.028	0.15	0.20
cs85	8 50 23.84	29 31 41.8	16.21 ± 0.03	16.68 ± 0.03	0.027	0.01	0.02
cs86	8 50 24.97	29 40 51.5	15.93 ± 0.05	16.34 ± 0.04	0.028	0.01	0.00
cs87	8 50 27.66	29 06 03.2	15.29 ± 0.09	15.89 ± 0.08	0.029	0.05	0.09
cs88	8 50 32.45	29 07 35.8	15.95 ± 0.06	16.59 ± 0.05	0.029	0.12	0.17
cs90	8 50 49.88	29 35 58.0	16.31 ± 0.05	16.93 ± 0.04	0.026	0.12	0.18
cs3043 <sup>c</sup>	8 50 54.79	29 17 15.2	16.24 ± 0.04	16.51 ± 0.04	0.030	0.00	-0.04
cs91	8 50 56.82	29 12 00.4	14.96 ± 0.05	15.42 ± 0.05	0.028	0.01	0.01
cs92	8 51 00.09	29 10 53.6	14.62 ± 0.05	15.03 ± 0.06	0.028	0.01	0.00
cs93	8 51 07.35	29 37 08.8	16.36 ± 0.04	17.02 ± 0.06	0.026	0.10	0.15
cs95	8 51 48.64	29 16 46.4	14.86 ± 0.05	15.46 ± 0.04	0.027	0.03	0.05
cs97	8 51 54.11	28 50 55.9	16.28 ± 0.05	16.94 ± 0.07	0.029	0.13	0.18
cs98	8 51 54.41	29 25 36.3	16.03 ± 0.05	16.67 ± 0.05	0.024	0.10	0.15
cs3045	8 51 56.98	29 28 48.9	16.05 ± 0.04	16.66 ± 0.05	0.025	0.09	0.14

Table 1—Continued

ID	RA <sub>J2000</sub>	Dec <sub>J2000</sub>	<i>R</i>	<i>V</i>	<i>E(B-V)</i> <sup>a</sup>	<i>k<sub>R</sub></i> <sup>b</sup>	<i>k<sub>V</sub></i> <sup>b</sup>
cs99	8 52 03.10	29 43 15.9	15.62 ± 0.06	16.18 ± 0.05	0.026	0.09	0.14
cs100	8 52 07.11	28 50 12.1	15.58 ± 0.05	16.31 ± 0.04	0.028	0.16	0.22
cs101	8 52 08.26	29 41 37.4	15.54 ± 0.05	15.90 ± 0.04	0.026	0.01	-0.02
cs102	8 52 09.87	29 25 21.5	16.26 ± 0.04	16.91 ± 0.04	0.025	0.11	0.16
cs103	8 52 11.49	29 29 06.1	16.13 ± 0.04	16.73 ± 0.05	0.024	0.09	0.14
cs104	8 52 12.85	29 24 39.0	14.64 ± 0.16	15.24 ± 0.07	0.025	0.09	0.14
cs105	8 52 14.34	29 20 18.8	15.35 ± 0.03	15.96 ± 0.03	0.024	0.09	0.14
cs106	8 52 15.12	29 40 20.5	16.23 ± 0.04	16.77 ± 0.03	0.025	0.07	0.10
cs107	8 52 15.73	29 25 47.1	15.85 ± 0.06	16.41 ± 0.06	0.025	0.07	0.12
cs3046	8 52 15.89	29 42 51.1	15.63 ± 0.06	16.25 ± 0.04	0.026	0.12	0.18
cs108	8 52 16.49	29 42 47.8	15.58 ± 0.05	16.18 ± 0.06	0.026	0.11	0.17
cs109	8 52 23.88	28 54 47.1	15.76 ± 0.10	16.39 ± 0.10	0.028	0.11	0.16
cs110	8 52 27.07	28 55 40.1	16.07 ± 0.08	16.72 ± 0.08	0.028	0.10	0.15
cs111	8 52 27.51	29 40 07.1	15.77 ± 0.05	16.32 ± 0.05	0.025	0.04	0.07
cs113	8 52 45.15	29 09 04.4	16.30 ± 0.04	16.91 ± 0.04	0.027	0.11	0.16
cs114	8 52 46.76	28 55 28.8	15.53 ± 0.05	16.12 ± 0.06	0.029	0.08	0.13
cs3039	8 53 10.00	29 21 40.0	16.36 ± 0.03	16.93 ± 0.03	0.028	0.09	0.14
cs3047	8 53 12.06	29 14 53.6	16.30 ± 0.06	16.82 ± 0.05	0.028	0.04	0.06
cs3048	8 53 27.98	29 04 56.8	16.31 ± 0.11	16.97 ± 0.13	0.027	0.12	0.17
cs116	8 53 47.77	29 12 33.7	16.32 ± 0.06	16.95 ± 0.06	0.026	0.10	0.15
cs117	8 53 50.30	29 04 23.9	15.58 ± 0.09	16.24 ± 0.19	0.025	0.11	0.16
cs118	8 53 50.61	29 06 41.0	15.65 ± 0.10	16.22 ± 0.10	0.025	0.07	0.12
cs119	8 53 53.63	29 00 18.6	15.69 ± 0.04	16.31 ± 0.04	0.025	0.09	0.14
cs120	8 54 01.62	29 07 31.1	16.23 ± 0.05	16.83 ± 0.05	0.025	0.08	0.14
cs3050	8 54 03.63	29 03 05.8	15.54 ± 0.05	16.30 ± 0.04	0.025	0.15	0.21
cs121	8 54 04.55	29 03 12.7	14.57 ± 0.05	15.19 ± 0.03	0.025	0.09	0.14
cs122	8 54 08.56	29 21 26.6	15.63 ± 0.03	16.03 ± 0.03	0.029	0.02	0.00
cs3052	8 54 14.86	28 54 09.3	16.09 ± 0.03	16.67 ± 0.03	0.028	0.08	0.13
cs123	8 54 21.13	29 02 45.2	16.07 ± 0.04	16.39 ± 0.03	0.026	0.00	-0.03
cs124	8 54 23.07	28 56 59.6	15.43 ± 0.04	15.97 ± 0.05	0.027	0.05	0.08
cs94	8 54 31.97	29 09 14.1	16.34 ± 0.05	16.72 ± 0.05	0.026	0.01	0.00
cs125	8 54 35.79	29 01 39.5	15.39 ± 0.06	16.03 ± 0.04	0.027	0.10	0.15
cs126	8 54 38.29	29 11 24.5	15.48 ± 0.07	16.16 ± 0.06	0.027	0.11	0.16
cs127	8 54 41.83	29 00 13.5	15.86 ± 0.05	16.53 ± 0.04	0.027	0.12	0.17
cs128	8 54 43.67	29 19 06.2	16.30 ± 0.04	16.95 ± 0.05	0.028	0.10	0.16
cs129	8 54 51.09	28 51 05.9	16.14 ± 0.04	16.80 ± 0.03	0.026	0.11	0.16

Table 1—Continued

ID	RA <sub>J2000</sub>	Dec <sub>J2000</sub>	<i>R</i>	<i>V</i>	<i>E(B-V)</i> <sup>a</sup>	<i>k<sub>R</sub></i> <sup>b</sup>	<i>k<sub>V</sub></i> <sup>b</sup>
cs130	8 54 54.38	29 01 23.7	15.91 ± 0.04	16.53 ± 0.03	0.027	0.09	0.14
cs131	8 54 57.92	29 03 22.6	15.99 ± 0.12	16.61 ± 0.11	0.027	0.09	0.14
cs132	8 55 12.42	29 30 06.3	16.07 ± 0.03	16.61 ± 0.06	0.026	0.05	0.08
cs115	8 56 11.12	28 46 54.1	16.33 ± 0.05	16.79 ± 0.14	0.028	0.04	0.03
cs133	8 56 20.00	28 58 51.8	15.80 ± 0.05	16.37 ± 0.05	0.027	0.04	0.07
cs134	8 56 29.25	29 40 03.9	14.68 ± 0.03	15.21 ± 0.03	0.027	0.03	0.06
cs135	8 56 30.19	29 02 38.5	16.20 ± 0.17	16.68 ± 0.09	0.027	0.04	0.04
cs136	8 57 00.56	29 39 42.4	15.83 ± 0.05	16.42 ± 0.06	0.027	0.08	0.13
cs137	8 58 57.81	28 54 06.0	14.61 ± 0.03	15.03 ± 0.03	0.030	0.01	0.00
cs3055	8 59 16.89	28 48 28.9	16.37 ± 0.04	16.78 ± 0.03	0.027	0.01	0.00
cs138	8 59 49.50	29 25 32.1	16.02 ± 0.03	16.58 ± 0.06	0.028	0.05	0.09
cs139	8 59 52.36	29 04 19.5	16.11 ± 0.04	16.81 ± 0.05	0.034	0.13	0.18
cs140	9 00 07.37	29 37 57.8	14.59 ± 0.02	15.07 ± 0.04	0.025	0.01	0.02
cs142	9 00 25.86	29 47 45.3	15.06 ± 0.02	15.49 ± 0.02	0.026	0.01	0.01
cs143	9 00 40.86	29 35 40.3	16.05 ± 0.03	16.53 ± 0.03	0.027	0.01	0.02
cs144	9 00 44.93	29 40 55.9	15.35 ± 0.05	15.82 ± 0.03	0.026	0.02	0.02
cs3057	9 01 24.10	29 03 35.9	16.29 ± 0.09	16.86 ± 0.10	0.030	0.04	0.07
cs145	9 01 32.73	29 32 33.8	15.17 ± 0.04	15.70 ± 0.05	0.029	0.03	0.05
cs146	9 01 46.98	29 04 15.3	15.26 ± 0.04	15.72 ± 0.03	0.030	0.01	0.02
cs147	9 01 50.75	29 00 32.5	15.27 ± 0.03	15.82 ± 0.03	0.030	0.06	0.09
cs148	9 02 50.59	28 59 22.2	16.23 ± 0.05	16.75 ± 0.04	0.028	0.04	0.06
cs149	9 02 56.01	28 56 29.2	15.37 ± 0.04	16.01 ± 0.03	0.027	0.06	0.09
cs150	9 03 19.84	29 07 46.2	14.20 ± 0.06	14.80 ± 0.05	0.028	0.03	0.04
cs151	9 03 42.55	29 17 46.0	14.11 ± 0.04	14.61 ± 0.04	0.031	0.01	0.01
cs152	9 03 43.51	29 42 38.6	16.00 ± 0.04	16.63 ± 0.04	0.028	0.06	0.10
cs155	9 06 00.30	29 20 41.1	15.53 ± 0.07	15.91 ± 0.05	0.024	0.00	0.00
cs157	9 06 37.87	29 04 09.3	16.02 ± 0.17	16.56 ± 0.08	0.026	0.03	0.06
cs153 <sup>c</sup>	9 06 47.23	28 57 31.5	16.31 ± 0.10	16.74 ± 0.11	0.029	0.01	0.01
cs158	9 06 47.64	29 13 10.0	15.54 ± 0.06	16.13 ± 0.05	0.022	0.05	0.08
cs160	9 07 08.88	29 28 34.1	16.07 ± 0.04	16.52 ± 0.06	0.023	0.02	0.02
cs161	9 07 17.12	29 21 50.2	15.63 ± 0.03	16.24 ± 0.04	0.023	0.08	0.13
cs162	9 08 01.62	29 32 41.5	16.16 ± 0.06	16.86 ± 0.11	0.024	0.16	0.21
cs163	9 08 28.47	28 54 39.9	14.23 ± 0.07	14.87 ± 0.03	0.025	0.03	0.05
cs164	9 08 29.31	28 49 22.5	16.10 ± 0.16	16.69 ± 0.12	0.024	0.11	0.16
cs165	9 08 39.31	29 35 24.5	16.18 ± 0.14	16.74 ± 0.04	0.025	0.04	0.07
cs166	9 08 56.81	29 05 30.8	15.61 ± 0.05	16.21 ± 0.14	0.026	0.10	0.16

Table 1—Continued

ID	RA <sub>J2000</sub>	Dec <sub>J2000</sub>	<i>R</i>	<i>V</i>	<i>E(B-V)</i> <sup>a</sup>	<i>k<sub>R</sub></i> <sup>b</sup>	<i>k<sub>V</sub></i> <sup>b</sup>
cs3063	9 09 21.76	29 23 47.5	15.62 ± 0.06	16.13 ± 0.05	0.022	0.02	0.04
cs168	9 09 42.38	29 09 53.6	15.91 ± 0.04	16.47 ± 0.04	0.026	0.04	0.07
cs169	9 09 59.98	29 04 25.2	16.01 ± 0.05	16.66 ± 0.04	0.025	0.13	0.19
cs3062	9 10 07.80	29 16 34.9	16.36 ± 0.05	16.63 ± 0.04	0.024	0.00	-0.06
cs173	9 11 29.85	29 18 39.8	14.97 ± 0.05	15.61 ± 0.05	0.022	0.06	0.10
cs174	9 11 30.91	28 49 35.8	13.61 ± 0.03	14.21 ± 0.06	0.025	0.04	0.06
cs175	9 11 48.56	29 30 08.2	16.18 ± 0.03	16.74 ± 0.04	0.025	0.03	0.06
cs176	9 11 54.28	29 34 09.3	14.89 ± 0.09	15.40 ± 0.09	0.025	0.01	0.03
cs177	9 12 23.41	28 59 31.5	16.34 ± 0.03	17.06 ± 0.03	0.022	0.17	0.23
cs178	9 12 24.45	29 00 11.9	15.69 ± 0.06	16.36 ± 0.04	0.022	0.15	0.20
cs179	9 12 26.57	28 58 43.9	15.84 ± 0.06	16.50 ± 0.03	0.022	0.14	0.20
cs180	9 12 45.31	29 25 17.9	14.18 ± 0.03	14.77 ± 0.03	0.024	0.02	0.04
cs183	9 12 58.91	29 30 17.9	16.17 ± 0.03	16.74 ± 0.06	0.023	0.10	0.15
cs184	9 13 01.00	29 32 17.3	15.24 ± 0.03	15.86 ± 0.04	0.023	0.03	0.04
cs185	9 13 03.04	29 00 35.0	16.16 ± 0.03	16.84 ± 0.06	0.023	0.15	0.21
cs186	9 13 17.10	29 06 59.9	15.84 ± 0.05	16.20 ± 0.03	0.023	0.00	0.00
cs187	9 13 31.42	28 57 05.8	12.98 ± 0.03	13.64 ± 0.04	0.024	0.04	0.06
cs188	9 13 48.68	29 10 21.4	14.10 ± 0.04	14.51 ± 0.03	0.022	0.00	0.00
cs3067	9 13 53.17	29 04 40.8	15.63 ± 0.03	16.19 ± 0.03	0.021	0.04	0.08
cs3068	9 13 54.21	29 04 50.7	16.08 ± 0.03	16.55 ± 0.04	0.021	0.02	0.03
cs189 <sup>c</sup>	9 13 54.32	29 10 42.3	15.99 ± 0.08	16.34 ± 0.04	0.022	0.00	0.00
cs190	9 14 14.77	29 41 43.6	16.13 ± 0.02	16.67 ± 0.03	0.020	0.02	0.03
cs193	9 14 51.43	29 39 27.8	16.36 ± 0.03	17.02 ± 0.05	0.019	0.18	0.25
cs194	9 14 52.10	29 01 48.2	16.29 ± 0.03	16.92 ± 0.04	0.022	0.07	0.12
cs195	9 14 59.72	29 43 48.9	12.55 ± 0.06	13.06 ± 0.05	0.019	0.01	0.03
cs196	9 15 03.56	29 16 11.4	13.75 ± 0.04	14.31 ± 0.03	0.022	0.02	0.04
cs197	9 15 11.23	29 15 09.1	15.67 ± 0.04	16.12 ± 0.03	0.022	0.01	0.01
cs198	9 15 50.85	28 54 01.6	16.16 ± 0.03	16.60 ± 0.03	0.021	0.03	0.02
cs182	9 15 53.58	28 47 32.2	16.31 ± 0.03	16.77 ± 0.06	0.023	0.02	0.02
cs199	9 16 18.78	28 53 20.1	15.16 ± 0.09	15.55 ± 0.10	0.020	0.01	0.00
cs200	9 16 41.11	29 20 22.0	14.13 ± 0.07	14.74 ± 0.07	0.020	0.04	0.07
cs201	9 16 47.54	29 21 12.4	15.93 ± 0.04	16.46 ± 0.07	0.020	0.03	0.05
cs202	9 17 00.15	29 21 03.0	15.22 ± 0.04	15.62 ± 0.03	0.021	0.01	0.00
cs203	9 17 04.21	29 31 17.7	16.23 ± 0.04	16.82 ± 0.02	0.021	0.09	0.14
cs3069 <sup>c</sup>	9 17 07.15	29 31 57.6	16.35 ± 0.03	16.74 ± 0.03	0.021	0.01	0.00
cs204	9 17 08.26	29 22 15.7	14.67 ± 0.03	15.20 ± 0.04	0.020	0.02	0.04

Table 1—Continued

ID	RA <sub>J2000</sub>	Dec <sub>J2000</sub>	<i>R</i>	<i>V</i>	<i>E(B-V)</i> <sup>a</sup>	<i>k<sub>R</sub></i> <sup>b</sup>	<i>k<sub>V</sub></i> <sup>b</sup>
cs205	9 17 16.50	29 01 03.9	14.54 ± 0.05	15.08 ± 0.03	0.022	0.04	0.07
cs206	9 18 50.41	29 02 23.3	14.87 ± 0.04	15.55 ± 0.03	0.021	0.10	0.15
cs207	9 19 01.52	29 19 42.0	15.84 ± 0.04	16.37 ± 0.04	0.021	0.04	0.07
cs208	9 19 26.90	29 11 36.1	16.27 ± 0.04	16.90 ± 0.03	0.021	0.10	0.15
cs209	9 19 44.55	28 56 15.6	14.89 ± 0.11	15.50 ± 0.06	0.021	0.06	0.10
cs210	9 20 08.34	29 31 30.1	16.34 ± 0.07	17.00 ± 0.08	0.021	0.18	0.27
cs211	9 20 13.47	28 59 19.9	15.13 ± 0.04	15.76 ± 0.03	0.020	0.07	0.12
cs212	9 20 25.13	29 04 18.1	16.18 ± 0.04	16.63 ± 0.05	0.021	0.03	0.03
cs213	9 20 56.56	28 52 55.6	14.85 ± 0.04	15.25 ± 0.04	0.020	0.01	0.00
cs215	9 21 07.75	28 55 47.8	14.40 ± 0.06	15.02 ± 0.06	0.020	0.04	0.07
cs3072	9 21 29.56	29 41 39.1	16.24 ± 0.05	16.75 ± 0.05	0.020	0.03	0.05
cs217	9 22 51.14	28 55 52.5	15.63 ± 0.04	16.24 ± 0.03	0.019	0.08	0.13
cs218	9 22 51.30	28 55 31.0	15.82 ± 0.04	16.41 ± 0.04	0.019	0.07	0.12
cs219 <sup>c</sup>	9 22 53.78	29 19 44.4	14.88 ± 0.07	15.32 ± 0.09	0.022	0.01	0.01
cs220	9 22 53.96	29 28 28.4	15.46 ± 0.05	16.06 ± 0.05	0.021	0.06	0.11
cs221	9 23 19.76	29 46 08.9	15.79 ± 0.04	16.39 ± 0.04	0.021	0.06	0.10
cs223	9 23 48.07	29 33 38.4	15.95 ± 0.04	16.55 ± 0.04	0.021	0.08	0.12
cs224	9 23 48.60	29 20 27.0	15.62 ± 0.04	16.07 ± 0.04	0.020	0.01	0.02
cs225	9 23 54.28	29 07 34.3	16.21 ± 0.09	16.70 ± 0.12	0.022	0.01	0.03
cs226	9 24 01.44	29 07 25.0	15.03 ± 0.03	15.63 ± 0.03	0.022	0.03	0.06
cs227	9 24 02.23	29 08 31.7	15.76 ± 0.03	16.22 ± 0.04	0.022	0.03	0.03
cs228	9 24 46.33	28 48 58.3	14.62 ± 0.03	15.11 ± 0.05	0.021	0.01	0.02
cs229	9 25 17.41	29 29 30.8	14.28 ± 0.05	14.87 ± 0.08	0.019	0.03	0.05
cs230	9 25 55.97	29 39 28.4	15.64 ± 0.05	16.21 ± 0.04	0.022	0.05	0.10
cs231	9 26 00.71	29 28 41.0	15.39 ± 0.04	15.94 ± 0.03	0.021	0.06	0.10
cs232	9 26 56.64	29 04 42.0	15.18 ± 0.04	15.90 ± 0.04	0.020	0.08	0.12
cs233	9 26 57.95	29 17 18.5	15.46 ± 0.03	16.02 ± 0.03	0.019	0.06	0.10
cs3076	9 27 01.75	29 12 37.6	16.31 ± 0.05	16.94 ± 0.04	0.019	0.07	0.12
cs234	9 27 06.02	29 45 04.2	15.64 ± 0.06	16.19 ± 0.06	0.023	0.02	0.04
cs235	9 27 08.07	29 24 08.6	14.51 ± 0.04	15.10 ± 0.03	0.021	0.03	0.05
cs237	9 27 28.45	29 46 41.1	16.12 ± 0.04	16.77 ± 0.04	0.023	0.13	0.19
cs238	9 27 34.64	29 26 28.2	15.80 ± 0.04	16.36 ± 0.04	0.019	0.06	0.11
cs239 <sup>c</sup>	9 27 36.11	28 47 55.1	14.03 ± 0.05	14.53 ± 0.04	0.020	0.01	0.02
cs240	9 27 40.20	29 33 01.0	15.67 ± 0.03	16.18 ± 0.03	0.019	0.01	0.03
cs241	9 28 08.90	29 37 22.6	15.37 ± 0.03	16.02 ± 0.03	0.018	0.04	0.06
cs242	9 28 17.85	29 42 21.8	14.11 ± 0.04	14.65 ± 0.04	0.019	0.02	0.04

Table 1—Continued

ID	RA <sub>J2000</sub>	Dec <sub>J2000</sub>	<i>R</i>	<i>V</i>	<i>E(B-V)</i> <sup>a</sup>	<i>k<sub>R</sub></i> <sup>b</sup>	<i>k<sub>V</sub></i> <sup>b</sup>
cs243	9 28 31.85	29 31 21.5	16.03 ± 0.05	16.68 ± 0.06	0.018	0.10	0.15
cs244	9 28 40.86	29 46 07.5	16.01 ± 0.05	16.66 ± 0.04	0.020	0.10	0.15
cs245	9 28 45.63	28 52 35.7	15.28 ± 0.04	15.88 ± 0.04	0.021	0.06	0.10
cs246 <sup>c</sup>	9 29 03.36	29 28 16.7	15.92 ± 0.04	16.44 ± 0.07	0.018	0.02	0.04
cs247	9 30 09.15	28 53 51.5	15.57 ± 0.04	16.25 ± 0.04	0.021	0.05	0.08
cs248	9 30 16.95	29 32 23.9	12.60 ± 0.04	13.11 ± 0.04	0.017	0.00	0.01
cs249	9 30 29.35	29 16 03.7	16.30 ± 0.10	17.02 ± 0.11	0.018	0.21	0.30
cs3078	9 30 42.61	29 38 40.0	16.21 ± 0.05	16.81 ± 0.05	0.018	0.08	0.12
cs250	9 31 09.63	29 30 33.5	15.74 ± 0.04	16.20 ± 0.05	0.018	0.02	0.03
cs251	9 31 38.74	29 08 57.6	15.26 ± 0.03	15.85 ± 0.03	0.017	0.08	0.12
cs3079	9 32 08.32	29 14 58.8	16.13 ± 0.04	16.80 ± 0.03	0.016	0.18	0.27
cs252	9 32 22.98	29 00 25.0	15.16 ± 0.05	15.77 ± 0.04	0.017	0.05	0.08
cs253	9 33 05.30	29 10 15.4	15.55 ± 0.06	16.20 ± 0.06	0.016	0.17	0.25
cs255	9 34 22.37	29 13 45.7	16.34 ± 0.04	16.91 ± 0.05	0.017	0.12	0.19
cs256	9 35 19.91	28 51 32.6	15.84 ± 0.05	16.51 ± 0.06	0.019	0.17	0.25
cs257	9 35 46.41	29 33 16.2	15.07 ± 0.03	15.66 ± 0.03	0.018	0.05	0.09
cs258	9 36 07.55	29 06 45.1	14.36 ± 0.04	14.78 ± 0.04	0.018	0.00	0.00
cs259	9 36 15.07	28 47 19.7	16.19 ± 0.05	16.69 ± 0.04	0.019	0.02	0.04
cs260	9 36 18.92	28 46 53.2	15.48 ± 0.05	16.12 ± 0.04	0.019	0.07	0.10
cs261	9 36 32.76	29 32 21.9	16.00 ± 0.10	16.63 ± 0.07	0.019	0.14	0.20
cs262	9 36 38.91	29 18 21.9	15.68 ± 0.03	16.27 ± 0.04	0.020	0.12	0.18
cs263	9 37 07.26	28 53 02.3	15.59 ± 0.06	16.11 ± 0.04	0.020	0.03	0.05
cs264	9 37 08.17	28 57 40.3	15.94 ± 0.05	16.56 ± 0.03	0.020	0.06	0.10
cs265	9 37 13.32	29 17 38.8	16.12 ± 0.05	16.69 ± 0.05	0.020	0.11	0.17
cs266	9 37 24.25	29 00 23.1	15.83 ± 0.14	16.44 ± 0.17	0.020	0.13	0.20
cs268	9 37 32.13	29 05 12.1	15.95 ± 0.06	16.56 ± 0.07	0.020	0.14	0.20
cs269	9 37 39.23	28 59 54.0	15.94 ± 0.04	16.54 ± 0.03	0.020	0.06	0.09
cs271	9 38 02.90	29 13 31.2	15.66 ± 0.05	16.23 ± 0.04	0.020	0.08	0.13
cs273	9 39 34.43	29 43 21.4	15.82 ± 0.04	16.38 ± 0.04	0.019	0.06	0.10
cs3082	9 39 41.73	29 01 48.9	16.24 ± 0.03	16.92 ± 0.05	0.017	0.18	0.26
cs274	9 39 49.45	28 54 36.7	15.20 ± 0.04	15.80 ± 0.04	0.019	0.05	0.09
cs275	9 39 55.83	29 03 48.8	16.33 ± 0.03	16.93 ± 0.03	0.018	0.14	0.21
cs277	9 40 31.82	28 58 09.4	14.90 ± 0.04	15.30 ± 0.04	0.019	0.01	0.00
cs278	9 40 46.10	29 41 20.5	15.28 ± 0.04	15.97 ± 0.03	0.023	0.11	0.16
cs279	9 40 50.61	29 17 29.8	15.96 ± 0.05	16.47 ± 0.05	0.019	0.03	0.05
cs282	9 42 27.33	28 57 10.3	14.06 ± 0.06	14.66 ± 0.05	0.017	0.03	0.06

Table 1—Continued

ID	RA <sub>J2000</sub>	Dec <sub>J2000</sub>	<i>R</i>	<i>V</i>	<i>E(B-V)</i> <sup>a</sup>	<i>k<sub>R</sub></i> <sup>b</sup>	<i>k<sub>V</sub></i> <sup>b</sup>
cs283	9 42 47.13	29 05 01.1	15.75 ± 0.08	16.41 ± 0.08	0.018	0.17	0.24
cs284	9 42 51.67	29 00 00.4	16.02 ± 0.05	16.42 ± 0.03	0.018	0.01	0.00
cs285	9 42 55.16	28 58 50.5	13.02 ± 0.04	13.55 ± 0.03	0.018	0.02	0.04
cs286	9 43 00.61	28 49 17.8	15.56 ± 0.03	16.23 ± 0.03	0.017	0.07	0.11
cs287	9 43 12.00	28 55 21.8	15.94 ± 0.03	16.43 ± 0.04	0.017	0.01	0.02
cs288	9 43 33.98	29 16 35.5	15.78 ± 0.05	16.39 ± 0.08	0.019	0.12	0.19
cs289	9 43 36.96	29 09 36.4	16.30 ± 0.05	16.97 ± 0.04	0.018	0.15	0.21
cs290	9 43 49.84	28 57 06.7	16.28 ± 0.03	16.78 ± 0.05	0.017	0.05	0.06
cs291	9 43 55.50	29 06 57.3	15.58 ± 0.11	15.99 ± 0.05	0.018	0.01	0.01
cs3086	9 44 00.32	28 52 26.8	16.25 ± 0.14	16.75 ± 0.10	0.018	0.05	0.06
cs293	9 44 03.26	29 36 34.2	14.07 ± 0.04	14.56 ± 0.03	0.016	0.01	0.02
cs294	9 44 04.83	29 09 36.3	16.24 ± 0.04	16.80 ± 0.04	0.018	0.10	0.16
cs295	9 44 14.07	29 12 15.5	15.39 ± 0.04	16.02 ± 0.03	0.018	0.14	0.20
cs297	9 44 47.63	29 20 31.6	16.21 ± 0.03	16.70 ± 0.03	0.017	0.01	0.03
cs298	9 45 00.34	29 27 08.1	13.30 ± 0.04	13.90 ± 0.03	0.018	0.04	0.06
cs299	9 45 04.73	29 09 15.0	16.27 ± 0.07	16.87 ± 0.03	0.017	0.14	0.21
cs300	9 45 23.08	29 23 22.0	15.77 ± 0.03	16.29 ± 0.03	0.019	0.02	0.04
cs302	9 45 47.69	29 34 54.7	15.93 ± 0.06	16.59 ± 0.05	0.018	0.15	0.21
cs303	9 46 37.75	29 43 13.5	15.85 ± 0.08	16.51 ± 0.06	0.020	0.15	0.21
cs3090	9 46 42.23	29 20 13.7	16.32 ± 0.05	16.96 ± 0.05	0.022	0.15	0.21
cs3092	9 46 57.73	29 41 45.6	16.38 ± 0.06	17.02 ± 0.06	0.020	0.14	0.20
cs304	9 47 00.91	29 38 24.5	15.99 ± 0.05	16.47 ± 0.05	0.020	0.05	0.05
cs305	9 47 04.76	29 25 25.4	15.74 ± 0.03	16.36 ± 0.04	0.020	0.11	0.17
cs306	9 47 10.17	29 03 12.7	15.93 ± 0.06	16.62 ± 0.09	0.019	0.15	0.20
cs307	9 47 38.11	29 01 49.7	15.93 ± 0.10	16.43 ± 0.15	0.019	0.03	0.05
cs308	9 48 23.43	28 49 19.8	15.75 ± 0.05	16.40 ± 0.04	0.018	0.10	0.14
cs309	9 48 24.38	28 54 24.6	16.21 ± 0.04	16.78 ± 0.05	0.017	0.09	0.15
cs3095	9 48 31.11	29 14 58.6	16.06 ± 0.10	16.67 ± 0.11	0.016	0.13	0.19
cs311	9 48 39.83	29 07 32.6	15.73 ± 0.03	16.33 ± 0.04	0.015	0.12	0.18
cs314	9 48 52.56	28 53 38.6	14.99 ± 0.04	15.54 ± 0.03	0.018	0.04	0.07
cs315	9 48 53.15	29 20 32.1	16.14 ± 0.04	16.67 ± 0.03	0.016	0.06	0.09
cs316	9 48 54.59	28 54 42.2	15.79 ± 0.05	16.43 ± 0.03	0.017	0.06	0.09
cs3096	9 49 15.10	28 55 43.4	16.30 ± 0.04	17.00 ± 0.03	0.017	0.07	0.11
cs317	9 49 16.47	29 15 48.9	15.02 ± 0.04	15.59 ± 0.03	0.017	0.04	0.08
cs319	9 50 16.64	28 53 13.3	16.27 ± 0.04	16.72 ± 0.06	0.019	0.04	0.04
cs321	9 50 34.34	28 51 23.2	16.15 ± 0.04	16.80 ± 0.05	0.020	0.14	0.20

Table 1—Continued

ID	RA <sub>J2000</sub>	Dec <sub>J2000</sub>	<i>R</i>	<i>V</i>	<i>E(B-V)</i> <sup>a</sup>	<i>k<sub>R</sub></i> <sup>b</sup>	<i>k<sub>V</sub></i> <sup>b</sup>
cs322	9 50 40.17	28 47 57.6	16.20 ± 0.06	16.85 ± 0.07	0.020	0.14	0.21
cs323	9 50 53.31	28 48 15.4	15.91 ± 0.04	16.55 ± 0.05	0.021	0.14	0.20
cs324	9 50 55.55	28 51 16.7	16.15 ± 0.05	16.82 ± 0.04	0.019	0.16	0.22
cs325	9 50 57.85	29 44 36.9	16.29 ± 0.05	16.83 ± 0.05	0.016	0.05	0.09
cs326	9 52 08.18	29 14 09.8	11.84 ± 0.07	12.33 ± 0.07	0.020	0.00	0.01
cs327	9 52 57.42	29 18 40.6	16.11 ± 0.09	16.42 ± 0.10	0.019	0.00	0.00
cs328	9 53 29.88	29 10 37.7	16.22 ± 0.04	16.58 ± 0.04	0.020	0.01	-0.01
cs331	9 54 01.98	28 49 51.5	16.15 ± 0.07	16.76 ± 0.06	0.018	0.12	0.17
cs333	9 54 39.76	29 42 59.6	15.84 ± 0.06	16.34 ± 0.04	0.017	0.01	0.02
cs334	9 54 48.61	29 01 59.0	15.89 ± 0.04	16.39 ± 0.04	0.019	0.04	0.05
cs335	9 54 53.58	28 54 54.8	15.93 ± 0.07	16.50 ± 0.05	0.019	0.07	0.12
cs329 <sup>c</sup>	9 56 32.74	29 12 23.5	16.36 ± 0.08	16.74 ± 0.04	0.018	0.00	0.00
cs337	9 57 28.62	29 40 36.4	16.29 ± 0.04	16.81 ± 0.03	0.017	0.07	0.09
cs338	9 58 01.69	28 51 35.5	16.20 ± 0.08	16.88 ± 0.04	0.019	0.19	0.27
cs339	9 58 38.07	28 52 16.0	15.07 ± 0.03	15.63 ± 0.03	0.018	0.02	0.04
cs3103	9 58 40.15	28 52 39.3	13.40 ± 0.04	14.05 ± 0.04	0.019	0.03	0.05
cs340	9 58 45.57	28 48 46.5	16.23 ± 0.04	16.79 ± 0.07	0.018	0.07	0.12
cs341	9 58 57.60	28 46 23.8	14.87 ± 0.04	15.55 ± 0.03	0.017	0.10	0.15
cs342	9 59 00.43	29 00 57.7	16.39 ± 0.07	17.09 ± 0.03	0.019	0.17	0.23
cs343	9 59 10.81	29 03 08.2	16.19 ± 0.04	16.88 ± 0.05	0.019	0.16	0.22
cs3104	9 59 57.15	29 17 19.8	14.52 ± 0.03	15.09 ± 0.03	0.017	0.02	0.04
cs344	10 00 14.76	29 06 54.0	16.05 ± 0.06	16.51 ± 0.05	0.018	0.04	0.03
cs346	10 01 02.82	28 53 12.8	16.32 ± 0.04	16.97 ± 0.03	0.024	0.13	0.19
cs347	10 01 17.51	28 51 11.2	15.28 ± 0.04	15.93 ± 0.03	0.024	0.11	0.16
cs349	10 02 17.17	28 54 19.4	16.25 ± 0.05	16.90 ± 0.08	0.023	0.17	0.24
cs350	10 02 17.49	29 35 24.7	16.07 ± 0.04	16.56 ± 0.03	0.021	0.05	0.07
cs352	10 02 46.77	29 30 32.4	16.22 ± 0.09	16.94 ± 0.03	0.020	0.21	0.29
cs354	10 02 54.81	29 00 57.9	16.24 ± 0.09	16.76 ± 0.12	0.021	0.04	0.06
cs356	10 03 04.19	29 00 22.9	16.31 ± 0.03	16.92 ± 0.03	0.021	0.09	0.15
cs358	10 03 13.18	29 21 12.6	16.31 ± 0.03	16.84 ± 0.04	0.026	0.06	0.08
cs359	10 03 38.96	29 01 19.0	15.42 ± 0.06	16.07 ± 0.04	0.021	0.12	0.18
cs361	10 03 43.28	29 13 33.3	16.24 ± 0.04	16.88 ± 0.04	0.025	0.11	0.16
cs362	10 03 44.95	28 59 48.9	15.86 ± 0.06	16.41 ± 0.04	0.021	0.07	0.11
cs363	10 03 46.97	29 14 03.2	16.28 ± 0.04	16.80 ± 0.06	0.025	0.04	0.07
cs364	10 03 58.74	29 28 11.9	15.05 ± 0.03	15.64 ± 0.03	0.019	0.05	0.09
cs365	10 04 21.14	29 43 26.6	15.49 ± 0.04	16.16 ± 0.04	0.021	0.07	0.11

Table 1—Continued

ID	RA <sub>J2000</sub>	Dec <sub>J2000</sub>	<i>R</i>	<i>V</i>	<i>E(B-V)</i> <sup>a</sup>	<i>k<sub>R</sub></i> <sup>b</sup>	<i>k<sub>V</sub></i> <sup>b</sup>
cs367	10 04 48.68	29 12 42.5	15.98 ± 0.06	16.62 ± 0.08	0.021	0.12	0.17
cs368	10 04 49.18	29 15 15.4	15.70 ± 0.05	16.34 ± 0.07	0.020	0.12	0.17
cs369	10 05 02.69	29 07 11.0	16.09 ± 0.04	16.76 ± 0.04	0.021	0.16	0.22
cs370	10 05 21.47	28 58 06.7	15.02 ± 0.05	15.66 ± 0.04	0.021	0.06	0.10
cs371	10 05 26.73	29 04 12.5	15.65 ± 0.05	16.30 ± 0.06	0.020	0.12	0.18
cs372	10 05 36.75	29 16 59.6	15.47 ± 0.14	16.07 ± 0.12	0.019	0.10	0.15
cs3107	10 05 37.17	29 16 55.0	15.67 ± 0.08	16.37 ± 0.06	0.019	0.15	0.20
cs373	10 05 42.76	29 05 01.0	15.80 ± 0.05	16.47 ± 0.06	0.020	0.18	0.26
cs374	10 05 55.01	29 08 21.0	15.14 ± 0.04	15.62 ± 0.04	0.020	0.02	0.03
cs376	10 06 03.53	29 26 09.4	15.68 ± 0.04	16.23 ± 0.04	0.022	0.04	0.07
cs377	10 06 06.99	29 07 55.1	15.46 ± 0.04	16.04 ± 0.03	0.020	0.04	0.08
cs3108	10 06 18.14	28 56 40.5	13.78 ± 0.04	14.20 ± 0.06	0.020	0.00	0.00
cs379	10 06 40.66	29 01 45.4	15.64 ± 0.05	16.29 ± 0.04	0.020	0.12	0.18
cs381	10 06 57.20	29 26 41.3	15.56 ± 0.05	16.15 ± 0.05	0.022	0.10	0.15
cs384	10 07 31.63	29 08 05.3	16.19 ± 0.04	16.62 ± 0.03	0.019	0.01	0.01
cs386	10 07 44.83	29 23 45.9	16.14 ± 0.05	16.62 ± 0.06	0.021	0.05	0.05
cs387	10 07 46.66	29 20 15.9	15.17 ± 0.04	15.64 ± 0.04	0.019	0.02	0.03
cs388	10 07 54.19	29 27 37.5	14.61 ± 0.04	15.05 ± 0.04	0.023	0.01	0.01
cs390 <sup>c</sup>	10 08 07.65	29 32 30.5	15.10 ± 0.14	15.47 ± 0.17	0.022	0.00	0.00
cs391	10 08 45.31	29 22 22.8	16.32 ± 0.04	16.96 ± 0.04	0.021	0.12	0.17
cs392	10 08 49.08	29 05 01.9	15.84 ± 0.05	16.42 ± 0.05	0.024	0.05	0.08
cs393	10 08 49.46	29 05 07.4	15.89 ± 0.05	16.47 ± 0.04	0.024	0.05	0.08
cs394	10 09 03.16	29 19 02.0	16.03 ± 0.04	16.65 ± 0.04	0.023	0.11	0.17
cs396	10 09 08.00	29 16 52.4	15.67 ± 0.03	16.31 ± 0.03	0.024	0.12	0.18
cs397	10 09 16.63	29 40 31.6	16.19 ± 0.05	16.82 ± 0.06	0.023	0.11	0.17
cs398	10 09 26.26	29 36 55.0	16.02 ± 0.06	16.66 ± 0.06	0.024	0.12	0.18
cs400	10 09 32.23	29 26 53.3	16.25 ± 0.03	16.77 ± 0.03	0.026	0.06	0.07
cs401	10 10 26.38	28 58 45.4	16.03 ± 0.05	16.66 ± 0.04	0.035	0.04	0.07
cs3114	10 10 42.57	28 50 11.6	15.79 ± 0.04	16.32 ± 0.03	0.037	0.02	0.04
cs389	10 10 45.59	29 10 11.4	16.36 ± 0.04	16.93 ± 0.05	0.021	0.10	0.17
cs404	10 11 33.45	28 58 42.0	15.82 ± 0.05	16.27 ± 0.03	0.036	0.01	0.01
cs406	10 12 15.35	29 34 01.6	15.66 ± 0.03	16.24 ± 0.04	0.031	0.04	0.08
cs407	10 12 41.62	29 18 32.6	14.39 ± 0.03	14.97 ± 0.03	0.028	0.04	0.08
cs408	10 12 45.09	29 03 07.8	15.35 ± 0.07	15.91 ± 0.05	0.025	0.04	0.08
cs409	10 12 51.63	29 37 31.9	16.31 ± 0.06	16.94 ± 0.04	0.027	0.15	0.22
cs410	10 13 04.90	29 33 53.3	15.26 ± 0.04	15.87 ± 0.04	0.028	0.05	0.09

Table 1—Continued

ID	RA <sub>J2000</sub>	Dec <sub>J2000</sub>	<i>R</i>	<i>V</i>	<i>E(B-V)</i> <sup>a</sup>	<i>k<sub>R</sub></i> <sup>b</sup>	<i>k<sub>V</sub></i> <sup>b</sup>
cs411	10 13 19.90	28 59 25.2	15.36 ± 0.09	15.94 ± 0.15	0.026	0.04	0.08
cs412	10 13 48.08	29 32 47.8	15.40 ± 0.07	15.82 ± 0.04	0.027	0.01	0.01
cs413	10 13 58.95	29 39 00.8	15.80 ± 0.05	16.43 ± 0.04	0.027	0.06	0.10
cs414	10 14 02.76	29 38 25.6	15.85 ± 0.07	16.27 ± 0.09	0.027	0.01	0.01
cs415	10 14 11.85	29 05 47.8	16.30 ± 0.07	16.73 ± 0.06	0.037	0.02	0.01
cs3117	10 14 33.61	29 19 06.9	15.14 ± 0.03	15.65 ± 0.03	0.031	0.01	0.02
cs417	10 15 10.90	28 50 53.5	14.81 ± 0.05	15.23 ± 0.03	0.039	0.01	0.00
cs418	10 15 11.17	29 27 46.3	15.31 ± 0.05	15.90 ± 0.04	0.029	0.04	0.07
cs419	10 15 40.76	29 38 16.5	16.27 ± 0.03	16.85 ± 0.06	0.027	0.09	0.15
cs420	10 16 08.76	29 34 09.2	15.16 ± 0.03	15.76 ± 0.03	0.030	0.05	0.09
cs421	10 16 34.19	29 19 14.0	15.58 ± 0.04	16.23 ± 0.05	0.031	0.10	0.14
cs422	10 16 41.48	29 34 03.3	16.31 ± 0.02	16.92 ± 0.03	0.032	0.11	0.16
cs423	10 16 50.80	29 13 52.4	15.18 ± 0.04	15.81 ± 0.04	0.029	0.06	0.09
cs424	10 17 06.00	29 36 45.4	15.21 ± 0.05	15.84 ± 0.04	0.030	0.09	0.14
cs425	10 17 08.14	29 13 41.2	15.39 ± 0.06	15.99 ± 0.06	0.029	0.05	0.08
cs426	10 17 12.78	29 38 21.4	16.06 ± 0.10	16.65 ± 0.10	0.030	0.07	0.12
cs3118	10 17 18.24	29 14 34.1	14.79 ± 0.06	15.25 ± 0.06	0.029	0.02	0.02
cs429	10 17 56.27	29 23 11.4	16.31 ± 0.04	16.91 ± 0.04	0.027	0.10	0.16
cs430	10 18 39.26	29 07 13.3	15.81 ± 0.06	16.38 ± 0.07	0.030	0.08	0.13
cs431	10 18 47.57	29 41 14.4	15.07 ± 0.05	15.69 ± 0.06	0.027	0.09	0.14
cs432	10 19 19.25	29 41 16.3	15.98 ± 0.19	16.60 ± 0.22	0.030	0.15	0.24
cs433	10 19 58.90	29 24 00.9	15.91 ± 0.06	16.48 ± 0.05	0.029	0.07	0.12
cs434	10 20 20.00	29 24 41.9	15.89 ± 0.10	16.44 ± 0.10	0.028	0.06	0.09
cs3122	10 20 21.07	29 24 45.7	16.34 ± 0.05	16.93 ± 0.05	0.028	0.08	0.13
cs435	10 20 34.91	29 14 10.7	15.53 ± 0.05	16.08 ± 0.04	0.030	0.03	0.07
cs436	10 20 43.97	29 41 55.7	16.26 ± 0.04	16.89 ± 0.04	0.028	0.11	0.17
cs439	10 21 26.45	28 59 24.3	15.89 ± 0.03	16.50 ± 0.06	0.025	0.08	0.12
cs440	10 22 27.25	28 56 22.8	15.49 ± 0.04	16.14 ± 0.03	0.026	0.11	0.17
cs441	10 22 40.89	29 20 46.7	16.04 ± 0.03	16.67 ± 0.03	0.028	0.06	0.10
cs444	10 24 10.02	28 49 13.6	15.75 ± 0.04	16.33 ± 0.05	0.026	0.07	0.12
cs443	10 26 43.55	28 47 26.9	16.33 ± 0.06	16.70 ± 0.14	0.026	0.01	-0.01
cs445	10 27 12.78	28 35 35.0	16.32 ± 0.12	16.71 ± 0.04	0.026	0.01	0.00
cs449	10 28 10.56	29 25 27.9	16.30 ± 0.06	16.85 ± 0.04	0.025	0.07	0.12
cs450	10 28 17.91	29 28 45.4	14.98 ± 0.08	15.61 ± 0.13	0.026	0.07	0.11
cs451	10 28 18.48	29 32 16.8	16.26 ± 0.03	16.76 ± 0.04	0.025	0.03	0.04
cs452	10 28 35.22	29 09 09.6	15.94 ± 0.04	16.28 ± 0.07	0.023	0.01	-0.03

Table 1—Continued

ID	RA <sub>J2000</sub>	Dec <sub>J2000</sub>	<i>R</i>	<i>V</i>	<i>E(B-V)</i> <sup>a</sup>	<i>k<sub>R</sub></i> <sup>b</sup>	<i>k<sub>V</sub></i> <sup>b</sup>
cs453	10 28 58.65	29 07 34.7	16.05 ± 0.04	16.67 ± 0.03	0.024	0.11	0.16
cs454	10 29 01.22	29 38 05.2	15.06 ± 0.03	15.51 ± 0.03	0.027	0.01	0.01
cs455	10 29 19.93	29 29 30.9	11.35 ± 0.04	11.83 ± 0.04	0.024	0.00	0.01
cs456	10 29 26.22	28 46 54.0	15.49 ± 0.05	16.11 ± 0.04	0.025	0.09	0.14
cs461	10 31 06.76	28 47 47.1	12.97 ± 0.07	13.54 ± 0.06	0.027	0.01	0.01
cs462	10 31 34.30	28 47 00.8	15.86 ± 0.05	16.27 ± 0.04	0.026	0.02	0.00
cs463	10 32 33.84	29 34 52.7	16.16 ± 0.04	16.62 ± 0.03	0.023	0.03	0.03
cs464	10 33 15.44	29 22 23.7	15.94 ± 0.05	16.46 ± 0.05	0.026	0.05	0.07
cs465	10 33 39.62	28 59 02.7	15.07 ± 0.04	15.47 ± 0.04	0.024	0.01	0.00
cs466	10 34 14.14	28 49 03.9	15.17 ± 0.04	15.74 ± 0.03	0.021	0.04	0.08
cs470	10 35 17.60	29 26 50.8	15.72 ± 0.03	16.21 ± 0.03	0.022	0.01	0.02
cs471	10 35 34.20	29 30 57.5	16.15 ± 0.04	16.68 ± 0.03	0.023	0.04	0.07
cs472	10 35 43.33	29 35 30.7	14.94 ± 0.05	15.46 ± 0.03	0.022	0.01	0.02
cs473	10 35 53.91	28 53 18.2	15.93 ± 0.03	16.40 ± 0.03	0.029	0.04	0.04
cs474	10 36 02.60	28 53 33.3	16.05 ± 0.04	16.56 ± 0.03	0.028	0.05	0.06
cs476	10 36 29.04	28 51 29.8	15.39 ± 0.04	16.05 ± 0.03	0.026	0.11	0.16
cs478	10 36 41.49	28 57 44.1	16.30 ± 0.03	16.94 ± 0.03	0.023	0.05	0.08
cs479	10 37 00.72	28 49 55.6	14.52 ± 0.03	15.03 ± 0.03	0.021	0.02	0.04
cs480	10 37 03.01	28 50 57.7	15.90 ± 0.04	16.52 ± 0.06	0.021	0.13	0.19
cs482	10 37 10.40	29 18 43.7	16.23 ± 0.04	16.66 ± 0.04	0.023	0.02	0.01
cs483	10 37 10.50	29 00 58.1	15.65 ± 0.04	16.33 ± 0.04	0.021	0.19	0.28
cs484	10 37 15.88	29 34 54.5	16.18 ± 0.03	16.60 ± 0.04	0.026	0.02	0.01
cs485	10 38 05.91	29 16 08.6	16.02 ± 0.04	16.44 ± 0.04	0.022	0.02	0.01
cs486	10 38 23.19	28 57 28.5	15.91 ± 0.06	16.55 ± 0.10	0.017	0.11	0.16
cs487	10 38 31.88	28 50 00.0	15.61 ± 0.04	16.24 ± 0.03	0.016	0.10	0.15
cs488	10 38 40.77	29 12 07.6	16.02 ± 0.04	16.62 ± 0.03	0.019	0.04	0.07
cs490	10 38 47.59	29 06 50.3	15.45 ± 0.04	15.90 ± 0.04	0.018	0.01	0.01
cs491	10 38 56.04	28 48 44.7	15.71 ± 0.07	16.24 ± 0.08	0.017	0.05	0.08
cs492	10 39 17.81	29 29 28.6	15.97 ± 0.05	16.66 ± 0.05	0.023	0.11	0.16
cs493	10 39 21.59	28 55 39.5	16.24 ± 0.04	16.61 ± 0.03	0.019	0.01	-0.01
cs494	10 39 27.54	29 39 27.9	16.32 ± 0.04	17.01 ± 0.06	0.025	0.19	0.28
cs495	10 40 04.86	29 19 22.1	16.15 ± 0.06	16.80 ± 0.08	0.025	0.13	0.18
cs3129	10 40 07.24	29 20 05.2	16.36 ± 0.04	17.00 ± 0.04	0.026	0.12	0.18
cs496	10 40 12.62	29 14 32.5	15.96 ± 0.04	16.60 ± 0.07	0.025	0.08	0.13
cs497	10 40 17.07	29 03 16.7	16.31 ± 0.06	16.96 ± 0.04	0.026	0.13	0.18
cs498	10 40 24.33	29 00 16.7	16.24 ± 0.13	16.99 ± 0.25	0.025	0.14	0.19

Table 1—Continued

ID	RA <sub>J2000</sub>	Dec <sub>J2000</sub>	<i>R</i>	<i>V</i>	<i>E(B-V)</i> <sup>a</sup>	<i>k<sub>R</sub></i> <sup>b</sup>	<i>k<sub>V</sub></i> <sup>b</sup>
cs499	10 40 29.09	28 53 10.0	14.70 ± 0.04	15.23 ± 0.04	0.026	0.03	0.05
cs3130	10 41 22.93	29 33 00.3	16.35 ± 0.02	17.04 ± 0.03	0.027	0.18	0.24
cs500	10 41 32.83	29 43 21.4	15.74 ± 0.04	16.36 ± 0.04	0.026	0.04	0.07
cs502	10 41 47.53	28 52 46.9	15.58 ± 0.04	16.18 ± 0.06	0.025	0.09	0.14
cs3131	10 42 04.16	29 33 23.6	15.62 ± 0.03	16.10 ± 0.03	0.031	0.01	0.03
cs504	10 42 10.15	28 57 20.5	16.14 ± 0.05	16.74 ± 0.03	0.027	0.05	0.09
cs505	10 42 37.55	28 59 41.5	15.22 ± 0.04	15.85 ± 0.03	0.027	0.08	0.13
cs506	10 43 00.41	29 06 05.8	15.01 ± 0.04	15.48 ± 0.03	0.026	0.01	0.02
cs507	10 43 13.77	29 15 44.5	15.87 ± 0.05	16.26 ± 0.07	0.033	0.01	0.00
cs508	10 43 27.27	29 10 04.4	15.06 ± 0.05	15.54 ± 0.05	0.026	0.01	0.02
cs509	10 43 45.10	29 42 06.7	15.75 ± 0.04	16.40 ± 0.05	0.032	0.06	0.10
cs511	10 45 06.32	29 12 31.4	16.05 ± 0.05	16.61 ± 0.05	0.024	0.02	0.04
cs512	10 45 15.34	29 27 13.0	15.44 ± 0.03	15.94 ± 0.03	0.029	0.02	0.04
cs513	10 45 20.11	29 29 09.6	15.92 ± 0.05	16.51 ± 0.03	0.031	0.03	0.06
cs514	10 45 24.33	29 13 07.6	13.95 ± 0.04	14.49 ± 0.04	0.025	0.02	0.04
cs515	10 45 44.14	29 17 32.5	15.88 ± 0.06	16.51 ± 0.05	0.023	0.15	0.22
cs516	10 45 51.98	29 04 55.4	16.28 ± 0.06	16.87 ± 0.04	0.020	0.08	0.13
cs517	10 45 57.94	28 56 07.7	15.30 ± 0.05	15.86 ± 0.05	0.021	0.03	0.06
cs518 <sup>c</sup>	10 46 11.47	29 02 14.7	15.96 ± 0.05	16.43 ± 0.05	0.019	0.01	0.02
cs519	10 46 17.36	29 21 34.3	15.13 ± 0.05	15.40 ± 0.05	0.022	0.00	-0.05
cs521	10 46 24.63	28 56 39.9	15.86 ± 0.05	16.38 ± 0.05	0.021	0.04	0.06
cs522	10 46 58.08	29 17 55.5	15.74 ± 0.05	16.31 ± 0.05	0.021	0.04	0.08
cs524	10 47 13.93	29 19 17.4	15.44 ± 0.04	16.00 ± 0.04	0.021	0.04	0.08
cs525	10 47 35.72	29 26 42.3	16.18 ± 0.05	16.83 ± 0.05	0.021	0.14	0.20
cs526	10 48 35.77	29 42 16.8	15.90 ± 0.06	16.21 ± 0.08	0.021	0.00	-0.03
cs528	10 49 17.73	29 33 38.2	15.92 ± 0.06	16.43 ± 0.06	0.020	0.02	0.03
cs529	10 49 22.28	29 17 20.0	15.93 ± 0.03	16.57 ± 0.03	0.020	0.14	0.20
cs530	10 49 26.68	29 22 55.7	15.49 ± 0.03	16.10 ± 0.03	0.021	0.05	0.09
cs531	10 49 40.44	29 21 52.3	15.58 ± 0.04	16.21 ± 0.03	0.020	0.10	0.15
cs532	10 49 45.98	29 01 19.7	15.54 ± 0.04	16.06 ± 0.05	0.016	0.02	0.04
cs523	10 49 54.86	29 04 32.0	16.30 ± 0.05	16.74 ± 0.04	0.022	0.02	0.01
cs533	10 50 16.77	29 29 09.3	16.03 ± 0.04	16.59 ± 0.03	0.020	0.04	0.08
cs534 <sup>c</sup>	10 50 19.27	29 22 47.8	16.19 ± 0.04	16.52 ± 0.11	0.017	0.00	-0.02
cs536	10 50 53.53	29 42 56.9	16.15 ± 0.02	16.74 ± 0.07	0.024	0.12	0.18
cs538	10 51 16.40	28 56 42.6	16.18 ± 0.04	16.80 ± 0.04	0.015	0.14	0.20
cs540	10 52 59.47	28 49 19.1	16.15 ± 0.04	16.79 ± 0.06	0.016	0.15	0.22

Table 1—Continued

ID	RA <sub>J2000</sub>	Dec <sub>J2000</sub>	<i>R</i>	<i>V</i>	<i>E(B-V)</i> <sup>a</sup>	<i>k<sub>R</sub></i> <sup>b</sup>	<i>k<sub>V</sub></i> <sup>b</sup>
cs541	10 53 09.41	28 47 56.7	16.14 ± 0.06	16.77 ± 0.09	0.015	0.14	0.21
cs542	10 53 22.76	29 19 38.0	16.23 ± 0.06	16.67 ± 0.08	0.017	0.01	0.01
cs544	10 54 00.04	29 25 37.6	15.10 ± 0.03	15.63 ± 0.04	0.021	0.03	0.06
cs545	10 54 19.40	29 42 04.3	14.63 ± 0.03	15.10 ± 0.03	0.020	0.01	0.02
cs547	10 55 00.72	29 32 35.9	14.15 ± 0.04	14.72 ± 0.05	0.026	0.04	0.08
cs548	10 55 09.48	29 30 01.2	15.81 ± 0.04	16.37 ± 0.04	0.026	0.06	0.11
cs549	10 55 13.17	29 29 24.3	16.12 ± 0.06	16.79 ± 0.04	0.025	0.10	0.14
cs551	10 56 09.33	29 40 13.5	15.36 ± 0.06	15.92 ± 0.03	0.019	0.04	0.08
cs552	10 56 31.48	29 32 50.2	15.13 ± 0.05	15.69 ± 0.04	0.020	0.03	0.06
cs553	10 56 51.33	29 32 50.4	16.25 ± 0.05	16.80 ± 0.04	0.021	0.08	0.13
cs554	10 57 00.49	29 37 19.0	16.09 ± 0.05	16.67 ± 0.04	0.020	0.03	0.06
cs555	10 57 49.71	29 40 45.4	16.27 ± 0.04	16.79 ± 0.04	0.022	0.03	0.05
cs556	10 57 51.41	29 39 08.2	14.74 ± 0.05	15.35 ± 0.05	0.021	0.06	0.10
cs557	10 58 15.27	29 34 06.3	16.07 ± 0.05	16.70 ± 0.05	0.021	0.08	0.13
cs558	10 58 20.43	29 29 28.7	15.68 ± 0.03	16.29 ± 0.04	0.023	0.08	0.13
cs559	10 58 21.67	29 38 39.8	14.84 ± 0.04	15.45 ± 0.04	0.021	0.06	0.10
cs560	10 58 44.73	29 30 40.2	15.41 ± 0.12	16.02 ± 0.13	0.023	0.08	0.12
cs563	11 00 12.43	29 37 16.0	15.42 ± 0.05	16.03 ± 0.04	0.026	0.05	0.09
cs566	11 00 29.47	29 36 22.4	15.87 ± 0.04	16.50 ± 0.03	0.028	0.08	0.13
cs567	11 00 31.97	29 41 45.1	14.24 ± 0.05	14.74 ± 0.05	0.027	0.01	0.03
cs569	11 00 42.57	29 36 01.5	16.18 ± 0.06	16.73 ± 0.05	0.030	0.03	0.05
cs570 <sup>c</sup>	11 00 44.48	29 06 44.8	15.86 ± 0.12	16.11 ± 0.09	0.030	0.00	-0.02
cs571	11 01 05.10	29 43 48.6	14.91 ± 0.04	15.49 ± 0.04	0.030	0.03	0.06
cs572	11 01 32.89	29 38 08.0	15.18 ± 0.05	15.77 ± 0.04	0.033	0.03	0.06
cs573	11 01 38.86	28 50 38.8	15.49 ± 0.04	15.91 ± 0.03	0.039	0.01	0.01
cs574	11 01 40.55	29 43 20.8	15.79 ± 0.04	16.38 ± 0.03	0.033	0.04	0.07
cs575	11 01 51.04	29 08 02.8	16.15 ± 0.04	16.44 ± 0.06	0.034	0.01	-0.06
cs576	11 01 54.31	29 14 59.2	16.05 ± 0.03	16.66 ± 0.06	0.029	0.07	0.12
cs578	11 02 14.03	29 13 20.5	15.71 ± 0.05	16.33 ± 0.08	0.032	0.07	0.12
cs579	11 02 15.69	29 07 24.9	15.27 ± 0.05	15.84 ± 0.05	0.034	0.09	0.14
cs580	11 02 21.51	29 39 32.3	14.84 ± 0.04	15.44 ± 0.05	0.034	0.03	0.06
cs581	11 02 28.57	29 34 37.3	14.78 ± 0.04	15.31 ± 0.04	0.031	0.02	0.04
cs582	11 02 28.88	29 17 29.6	15.90 ± 0.04	16.52 ± 0.03	0.028	0.08	0.12
cs583	11 02 29.62	29 07 50.9	16.14 ± 0.05	16.72 ± 0.05	0.034	0.06	0.11
cs584	11 02 36.80	29 15 05.8	15.70 ± 0.05	16.32 ± 0.07	0.030	0.08	0.12
cs585	11 02 38.40	29 15 25.1	14.90 ± 0.03	15.52 ± 0.03	0.030	0.07	0.12

Table 1—Continued

ID	RA <sub>J2000</sub>	Dec <sub>J2000</sub>	<i>R</i>	<i>V</i>	<i>E(B-V)</i> <sup>a</sup>	<i>k<sub>R</sub></i> <sup>b</sup>	<i>k<sub>V</sub></i> <sup>b</sup>
cs587	11 02 51.54	29 02 00.2	15.70 ± 0.04	16.33 ± 0.04	0.030	0.08	0.13
cs588	11 02 52.84	29 16 33.1	15.88 ± 0.04	16.52 ± 0.03	0.027	0.08	0.13
cs589	11 03 05.10	28 55 03.0	16.05 ± 0.04	16.73 ± 0.04	0.028	0.10	0.15
cs590	11 03 06.44	28 48 51.7	16.27 ± 0.08	16.96 ± 0.10	0.027	0.19	0.27
cs591	11 03 07.25	29 15 04.2	15.97 ± 0.04	16.52 ± 0.06	0.026	0.05	0.09
cs592	11 03 19.32	29 25 23.7	16.16 ± 0.03	16.61 ± 0.03	0.025	0.01	0.02
cs3139	11 03 30.59	29 08 56.7	16.26 ± 0.03	16.82 ± 0.03	0.028	0.03	0.05
cs593	11 03 43.19	29 14 31.7	15.13 ± 0.04	15.75 ± 0.04	0.023	0.07	0.12
cs595	11 03 45.33	29 30 19.3	16.08 ± 0.04	16.64 ± 0.05	0.025	0.06	0.10
cs596	11 03 45.60	29 29 58.6	15.75 ± 0.05	16.35 ± 0.09	0.025	0.07	0.12
cs597	11 03 55.82	28 46 11.4	16.18 ± 0.05	16.59 ± 0.04	0.020	0.02	0.01
cs598 <sup>c</sup>	11 03 58.61	29 36 04.5	16.09 ± 0.04	16.39 ± 0.11	0.030	0.00	-0.03
cs599	11 04 22.24	28 59 22.9	15.71 ± 0.11	16.30 ± 0.12	0.028	0.03	0.06
cs600	11 04 29.16	29 04 26.9	14.31 ± 0.03	14.86 ± 0.03	0.027	0.03	0.05
cs601	11 04 35.71	29 31 09.5	13.87 ± 0.04	14.44 ± 0.03	0.026	0.03	0.05
cs602	11 04 36.73	29 13 20.2	15.63 ± 0.06	16.07 ± 0.06	0.023	0.02	0.02
cs604	11 05 36.37	29 08 20.8	16.22 ± 0.05	16.87 ± 0.06	0.027	0.09	0.14
cs605	11 05 40.94	29 08 48.7	14.79 ± 0.06	15.40 ± 0.07	0.027	0.04	0.06
cs606	11 05 53.79	28 47 59.8	14.28 ± 0.05	14.94 ± 0.04	0.027	0.05	0.07
cs608 <sup>c</sup>	11 05 56.19	29 34 37.2	16.13 ± 0.05	16.50 ± 0.05	0.023	0.01	-0.01
cs610	11 06 21.59	29 15 53.5	15.71 ± 0.03	16.26 ± 0.03	0.024	0.08	0.12
cs611	11 06 22.00	29 15 02.9	16.21 ± 0.03	16.82 ± 0.03	0.024	0.12	0.18
cs612	11 06 43.69	29 19 26.9	15.47 ± 0.03	16.07 ± 0.03	0.025	0.03	0.06
cs613	11 07 02.39	29 06 25.0	15.78 ± 0.07	16.17 ± 0.11	0.023	0.01	0.00
cs614	11 07 02.69	28 54 40.5	15.64 ± 0.03	16.25 ± 0.04	0.034	0.07	0.12
cs615	11 07 12.80	28 46 55.5	14.78 ± 0.04	15.21 ± 0.03	0.031	0.01	0.01
cs618	11 08 14.09	28 51 43.6	16.21 ± 0.06	16.76 ± 0.04	0.029	0.03	0.06
cs619	11 08 16.00	28 50 38.2	15.54 ± 0.04	16.17 ± 0.03	0.029	0.04	0.07
cs607	11 08 35.99	28 35 11.1	16.38 ± 0.04	16.78 ± 0.04	0.027	0.01	0.00
cs621	11 08 42.10	28 57 01.9	15.09 ± 0.04	15.68 ± 0.03	0.029	0.03	0.06
cs622	11 08 43.48	29 13 25.6	14.82 ± 0.05	15.36 ± 0.06	0.026	0.05	0.08
cs623	11 08 47.55	29 07 56.2	15.75 ± 0.06	16.35 ± 0.03	0.026	0.08	0.13
cs609	11 08 52.34	28 28 08.1	16.30 ± 0.04	16.75 ± 0.04	0.025	0.01	0.01
cs624	11 08 52.37	29 09 26.0	15.68 ± 0.05	16.29 ± 0.04	0.025	0.08	0.13
cs625	11 09 05.40	29 07 54.6	16.24 ± 0.04	16.82 ± 0.04	0.026	0.03	0.06
cs626	11 09 05.63	29 12 17.5	16.19 ± 0.03	16.81 ± 0.04	0.024	0.09	0.14

Table 1—Continued

ID	RA <sub>J2000</sub>	Dec <sub>J2000</sub>	<i>R</i>	<i>V</i>	<i>E(B-V)</i> <sup>a</sup>	<i>k<sub>R</sub></i> <sup>b</sup>	<i>k<sub>V</sub></i> <sup>b</sup>
cs627	11 09 14.26	29 33 18.6	15.38 ± 0.03	15.96 ± 0.03	0.028	0.03	0.06
cs630	11 09 25.87	29 34 08.8	13.55 ± 0.04	14.09 ± 0.04	0.028	0.02	0.05
cs631	11 09 26.68	29 14 15.2	15.93 ± 0.04	16.51 ± 0.03	0.024	0.04	0.08
cs634	11 09 41.71	28 54 53.1	14.46 ± 0.04	15.05 ± 0.04	0.021	0.03	0.06
cs635	11 09 42.45	29 11 56.8	16.10 ± 0.06	16.68 ± 0.08	0.023	0.07	0.12
cs636	11 09 50.09	28 43 46.5	16.21 ± 0.04	16.77 ± 0.04	0.019	0.03	0.06
cs637	11 09 50.30	28 58 15.8	14.85 ± 0.04	15.42 ± 0.03	0.022	0.03	0.06
cs638	11 10 14.70	29 26 23.7	16.03 ± 0.05	16.46 ± 0.04	0.032	0.01	0.01
cs639	11 10 17.08	28 47 24.7	16.06 ± 0.05	16.64 ± 0.06	0.022	0.04	0.07
cs640	11 10 17.29	29 02 39.7	15.32 ± 0.05	15.79 ± 0.05	0.025	0.01	0.02
cs641	11 10 29.72	29 26 28.1	15.28 ± 0.03	15.77 ± 0.03	0.034	0.01	0.02
cs642	11 10 31.73	28 47 25.5	15.94 ± 0.05	16.47 ± 0.03	0.023	0.02	0.05
cs643	11 10 37.55	28 43 56.9	14.27 ± 0.04	14.89 ± 0.04	0.020	0.04	0.06
cs644	11 10 38.52	28 46 03.1	12.59 ± 0.05	13.22 ± 0.05	0.021	0.04	0.07
cs646	11 10 49.30	29 39 29.0	15.80 ± 0.05	16.43 ± 0.09	0.020	0.04	0.07
cs648	11 10 52.06	29 34 06.5	14.56 ± 0.04	15.15 ± 0.04	0.022	0.04	0.06
cs649	11 10 55.96	29 19 39.0	15.52 ± 0.05	16.04 ± 0.05	0.032	0.02	0.03
cs651	11 10 59.51	28 44 41.7	15.04 ± 0.04	15.63 ± 0.04	0.017	0.03	0.06
cs652	11 10 59.94	29 20 10.8	14.45 ± 0.03	15.12 ± 0.03	0.030	0.04	0.07
cs3144 <sup>c</sup>	11 11 13.02	28 45 58.1	15.70 ± 0.22	15.94 ± 0.25	0.017	0.00	-0.04
cs653	11 11 15.38	28 56 58.3	15.56 ± 0.04	16.23 ± 0.04	0.019	0.05	0.07
cs654	11 11 20.16	29 01 14.6	15.85 ± 0.04	16.35 ± 0.05	0.017	0.01	0.03
cs655	11 11 24.25	28 43 49.3	14.30 ± 0.04	14.89 ± 0.04	0.018	0.03	0.06
cs656	11 11 34.24	28 45 16.9	15.58 ± 0.05	16.16 ± 0.04	0.018	0.03	0.06
cs657	11 11 34.85	28 48 33.9	15.95 ± 0.04	16.48 ± 0.04	0.017	0.02	0.04
cs658	11 11 35.41	28 44 42.1	14.98 ± 0.04	15.48 ± 0.04	0.018	0.01	0.03
cs659	11 11 39.09	28 49 12.1	15.84 ± 0.04	16.41 ± 0.03	0.017	0.03	0.06
cs660	11 11 48.86	29 40 21.1	14.62 ± 0.05	15.15 ± 0.04	0.017	0.03	0.06
cs661	11 11 58.85	29 28 41.6	15.76 ± 0.05	16.25 ± 0.05	0.018	0.01	0.03
cs662	11 11 59.70	29 25 39.6	15.95 ± 0.05	16.36 ± 0.04	0.018	0.01	0.00
cs665	11 12 10.55	29 27 47.2	15.63 ± 0.08	16.31 ± 0.07	0.016	0.11	0.16
cs666	11 12 37.90	29 15 38.8	16.10 ± 0.04	16.67 ± 0.04	0.016	0.10	0.15
cs667	11 12 47.26	29 39 58.6	15.44 ± 0.05	16.05 ± 0.04	0.016	0.05	0.08
cs668	11 12 53.28	29 25 39.1	15.96 ± 0.05	16.59 ± 0.06	0.016	0.13	0.19
cs669	11 12 53.96	28 48 42.6	15.53 ± 0.09	16.15 ± 0.06	0.016	0.12	0.18
cs670	11 12 57.82	29 30 29.5	16.13 ± 0.04	16.68 ± 0.05	0.017	0.04	0.08

Table 1—Continued

ID	RA <sub>J2000</sub>	Dec <sub>J2000</sub>	<i>R</i>	<i>V</i>	<i>E(B-V)</i> <sup>a</sup>	<i>k<sub>R</sub></i> <sup>b</sup>	<i>k<sub>V</sub></i> <sup>b</sup>
cs671	11 13 01.79	28 45 01.5	15.04 ± 0.05	15.57 ± 0.04	0.015	0.02	0.04
cs672	11 13 09.49	28 47 34.0	15.91 ± 0.06	16.42 ± 0.06	0.015	0.02	0.03
cs674	11 13 26.67	28 57 09.8	15.12 ± 0.05	15.68 ± 0.05	0.015	0.03	0.06
cs675	11 13 30.40	29 40 05.7	16.07 ± 0.05	16.71 ± 0.04	0.019	0.06	0.09
cs676	11 13 55.57	29 21 14.3	16.28 ± 0.04	16.84 ± 0.04	0.013	0.05	0.09
cs677	11 13 59.47	29 28 49.0	14.87 ± 0.08	15.42 ± 0.05	0.017	0.03	0.07
cs678	11 14 11.11	29 15 16.1	15.72 ± 0.03	16.31 ± 0.03	0.014	0.05	0.08
cs679	11 14 19.95	29 26 40.3	16.18 ± 0.03	16.79 ± 0.03	0.016	0.07	0.12
cs680	11 14 29.35	29 15 15.7	16.02 ± 0.03	16.63 ± 0.03	0.015	0.05	0.09
cs681	11 14 34.12	29 32 42.5	14.53 ± 0.04	15.15 ± 0.04	0.016	0.05	0.09
cs682	11 14 34.30	28 55 10.9	15.72 ± 0.03	16.20 ± 0.03	0.015	0.02	0.03
cs683	11 14 38.93	29 05 26.1	15.60 ± 0.05	16.24 ± 0.05	0.016	0.06	0.09
cs684	11 14 40.84	29 30 34.1	16.00 ± 0.04	16.59 ± 0.04	0.016	0.05	0.08
cs685	11 14 44.00	29 13 11.3	15.35 ± 0.03	15.91 ± 0.04	0.015	0.04	0.07
cs686	11 15 01.76	29 09 19.8	14.99 ± 0.04	15.60 ± 0.04	0.015	0.05	0.08
cs687	11 15 10.19	29 31 49.0	13.78 ± 0.04	14.40 ± 0.04	0.019	0.06	0.10
cs688	11 15 13.22	29 16 17.3	15.00 ± 0.03	15.52 ± 0.03	0.016	0.04	0.06
cs689	11 15 18.41	29 31 39.4	14.31 ± 0.04	14.92 ± 0.04	0.019	0.05	0.09
cs690	11 15 21.53	28 43 49.2	15.87 ± 0.04	16.52 ± 0.04	0.017	0.09	0.14
cs691	11 15 24.18	29 08 53.9	15.93 ± 0.04	16.48 ± 0.04	0.016	0.04	0.07
cs692	11 15 25.59	29 27 41.5	15.64 ± 0.03	16.26 ± 0.03	0.017	0.05	0.09
cs693	11 15 25.78	29 33 45.9	15.68 ± 0.04	16.32 ± 0.04	0.019	0.06	0.09
cs694	11 15 30.23	29 21 36.8	15.34 ± 0.04	15.94 ± 0.03	0.017	0.05	0.09
cs695	11 15 31.84	29 27 42.9	15.96 ± 0.04	16.54 ± 0.04	0.017	0.04	0.08
cs696	11 15 32.57	29 31 39.1	15.57 ± 0.04	16.06 ± 0.04	0.018	0.02	0.03
cs697	11 15 36.78	29 01 48.2	15.41 ± 0.04	16.01 ± 0.05	0.017	0.05	0.08
cs698	11 15 43.23	29 26 37.4	15.50 ± 0.03	16.08 ± 0.03	0.016	0.03	0.05
cs699	11 15 45.87	29 22 23.9	15.39 ± 0.07	16.00 ± 0.05	0.016	0.05	0.09
cs700	11 15 51.07	29 04 41.9	14.61 ± 0.04	15.22 ± 0.04	0.018	0.05	0.09
cs702	11 15 52.23	29 15 10.8	15.85 ± 0.03	16.41 ± 0.03	0.017	0.04	0.07
cs703	11 15 55.54	29 18 20.8	16.14 ± 0.05	16.72 ± 0.05	0.017	0.04	0.08
cs704	11 16 03.22	28 47 22.5	14.49 ± 0.03	15.02 ± 0.03	0.017	0.02	0.04
cs705	11 16 09.42	29 05 13.2	15.48 ± 0.04	16.03 ± 0.04	0.018	0.03	0.06
cs3149	11 16 10.79	29 26 32.0	14.47 ± 0.03	14.99 ± 0.03	0.015	0.02	0.04
cs706	11 16 11.30	29 10 23.1	16.16 ± 0.03	16.73 ± 0.03	0.017	0.04	0.07
cs707	11 16 13.60	29 23 06.4	13.62 ± 0.04	14.23 ± 0.03	0.016	0.03	0.06

Table 1—Continued

ID	RA <sub>J2000</sub>	Dec <sub>J2000</sub>	<i>R</i>	<i>V</i>	<i>E(B-V)</i> <sup>a</sup>	<i>k<sub>R</sub></i> <sup>b</sup>	<i>k<sub>V</sub></i> <sup>b</sup>
cs708	11 16 13.90	29 15 29.6	16.09 ± 0.04	16.67 ± 0.03	0.016	0.04	0.08
cs709	11 16 17.44	29 13 34.6	13.91 ± 0.09	14.52 ± 0.07	0.016	0.05	0.08
cs710	11 16 21.99	29 26 22.5	15.40 ± 0.03	15.95 ± 0.03	0.016	0.02	0.05
cs711	11 16 22.79	29 15 08.1	13.66 ± 0.05	14.26 ± 0.04	0.016	0.05	0.08
cs712	11 16 25.72	29 16 12.4	15.65 ± 0.04	16.28 ± 0.03	0.016	0.06	0.09
cs713	11 16 25.84	29 08 46.6	16.22 ± 0.03	16.81 ± 0.02	0.018	0.04	0.08
cs3151	11 16 27.53	29 11 31.7	14.88 ± 0.03	15.43 ± 0.04	0.018	0.03	0.06
cs714	11 16 27.85	29 11 13.3	15.26 ± 0.03	15.72 ± 0.03	0.018	0.02	0.03
cs715	11 16 27.99	29 22 16.7	16.10 ± 0.04	16.67 ± 0.03	0.016	0.04	0.07
cs716	11 16 28.08	29 19 35.0	14.09 ± 0.04	14.56 ± 0.04	0.016	0.02	0.03
cs717	11 16 28.49	29 17 09.4	14.57 ± 0.04	15.18 ± 0.04	0.016	0.05	0.09
cs718	11 16 30.84	29 13 43.6	15.02 ± 0.03	15.62 ± 0.03	0.017	0.05	0.09
cs719	11 16 32.36	29 16 33.6	14.87 ± 0.09	15.49 ± 0.09	0.016	0.05	0.09
cs720	11 16 32.37	28 46 35.2	15.49 ± 0.03	15.96 ± 0.02	0.018	0.01	0.02
cs721	11 16 33.38	29 18 44.7	15.12 ± 0.04	15.70 ± 0.03	0.016	0.04	0.08
cs722	11 16 33.90	28 46 06.9	15.05 ± 0.04	15.42 ± 0.03	0.018	0.00	0.00
cs723	11 16 34.65	29 15 17.1	14.31 ± 0.05	14.90 ± 0.04	0.017	0.05	0.08
cs724	11 16 35.06	29 14 59.1	14.52 ± 0.05	15.10 ± 0.04	0.017	0.05	0.08
cs725	11 16 38.62	29 18 47.0	15.89 ± 0.04	16.50 ± 0.03	0.016	0.06	0.09
cs726	11 16 43.20	29 19 44.6	15.87 ± 0.04	16.34 ± 0.03	0.017	0.02	0.03
cs3154	11 16 48.75	29 39 21.6	16.27 ± 0.02	16.89 ± 0.03	0.017	0.07	0.11
cs727	11 16 57.02	29 16 03.2	15.79 ± 0.04	16.39 ± 0.03	0.018	0.05	0.08
cs728	11 17 00.41	29 08 25.8	14.41 ± 0.03	15.01 ± 0.03	0.019	0.05	0.08
cs729	11 17 01.23	29 13 01.3	16.02 ± 0.03	16.59 ± 0.03	0.019	0.04	0.07
cs730	11 17 01.88	29 05 56.7	14.72 ± 0.03	15.33 ± 0.03	0.019	0.05	0.09
cs731	11 17 06.24	29 31 53.7	15.76 ± 0.02	16.36 ± 0.03	0.019	0.03	0.06
cs732	11 17 10.71	29 15 14.7	15.70 ± 0.04	16.31 ± 0.03	0.018	0.05	0.09
cs733	11 17 14.40	29 31 14.4	15.55 ± 0.02	16.14 ± 0.03	0.019	0.08	0.13
cs734	11 17 16.29	29 20 09.4	15.59 ± 0.04	16.03 ± 0.03	0.018	0.01	0.01
cs735	11 17 16.64	29 28 14.5	16.08 ± 0.03	16.68 ± 0.03	0.018	0.05	0.08
cs737	11 17 18.66	29 36 10.5	15.48 ± 0.02	16.19 ± 0.03	0.018	0.08	0.12
cs738	11 17 20.85	29 28 11.2	15.89 ± 0.03	16.55 ± 0.03	0.018	0.06	0.10
cs739	11 17 29.04	28 46 44.0	14.87 ± 0.03	15.46 ± 0.03	0.019	0.04	0.08
cs740	11 17 33.14	29 22 00.6	15.14 ± 0.04	15.75 ± 0.05	0.017	0.05	0.09
cs741	11 17 36.73	28 55 31.3	15.58 ± 0.04	16.19 ± 0.03	0.018	0.05	0.09
cs742	11 17 37.22	29 29 44.6	14.89 ± 0.03	15.47 ± 0.03	0.019	0.04	0.07

Table 1—Continued

ID	RA <sub>J2000</sub>	Dec <sub>J2000</sub>	<i>R</i>	<i>V</i>	<i>E(B-V)</i> <sup>a</sup>	<i>k<sub>R</sub></i> <sup>b</sup>	<i>k<sub>V</sub></i> <sup>b</sup>
cs743	11 17 44.31	29 36 25.5	15.40 ± 0.02	15.98 ± 0.04	0.018	0.04	0.08
cs744	11 17 49.28	28 53 04.8	15.91 ± 0.03	16.52 ± 0.03	0.018	0.05	0.08
cs745	11 17 52.68	29 18 16.8	14.53 ± 0.03	15.06 ± 0.03	0.017	0.02	0.03
cs746	11 17 52.73	29 25 13.3	15.77 ± 0.04	16.34 ± 0.03	0.019	0.04	0.08
cs747	11 17 54.63	29 27 04.3	16.14 ± 0.04	16.75 ± 0.04	0.021	0.05	0.09
cs748	11 18 09.37	28 50 48.2	16.18 ± 0.03	16.86 ± 0.03	0.018	0.19	0.28
cs749	11 18 09.45	28 53 56.7	15.07 ± 0.03	15.67 ± 0.03	0.018	0.05	0.08
cs750	11 18 13.30	28 54 58.2	15.38 ± 0.04	15.97 ± 0.03	0.018	0.07	0.11
cs751	11 18 20.02	29 22 46.9	16.26 ± 0.04	16.75 ± 0.04	0.017	0.02	0.03
cs752	11 18 29.27	29 39 44.1	16.31 ± 0.05	16.94 ± 0.05	0.016	0.15	0.21
cs753	11 18 33.00	29 07 59.4	16.27 ± 0.08	16.79 ± 0.07	0.018	0.04	0.06
cs755	11 18 41.84	29 22 38.2	16.02 ± 0.03	16.60 ± 0.03	0.017	0.05	0.08
cs756	11 18 49.16	28 55 28.9	15.54 ± 0.04	16.15 ± 0.04	0.017	0.05	0.09
cs757	11 18 54.52	29 10 35.1	15.73 ± 0.07	16.29 ± 0.06	0.018	0.05	0.09
cs758	11 18 59.35	28 58 55.7	15.91 ± 0.06	16.50 ± 0.05	0.017	0.05	0.08
cs759	11 19 10.26	29 00 00.2	15.75 ± 0.10	16.36 ± 0.16	0.017	0.07	0.11
cs760	11 19 23.46	29 16 02.4	16.21 ± 0.03	16.57 ± 0.03	0.017	0.01	-0.02
cs761	11 19 27.21	29 22 21.6	15.30 ± 0.03	15.90 ± 0.03	0.016	0.06	0.10
cs3164	11 19 28.28	28 45 48.2	15.96 ± 0.03	16.52 ± 0.04	0.017	0.05	0.09
cs762	11 19 32.70	29 01 43.1	15.61 ± 0.08	16.25 ± 0.06	0.017	0.07	0.11
cs763	11 19 33.03	29 09 58.5	15.67 ± 0.08	16.32 ± 0.07	0.017	0.07	0.12
cs764	11 19 34.59	29 10 59.6	13.96 ± 0.09	14.60 ± 0.05	0.017	0.08	0.12
cs765	11 19 35.86	29 09 01.6	15.11 ± 0.07	15.73 ± 0.06	0.017	0.07	0.11
cs766	11 19 49.29	29 10 29.0	15.99 ± 0.09	16.48 ± 0.05	0.017	0.02	0.04
cs767	11 19 51.87	29 04 09.3	15.39 ± 0.08	15.99 ± 0.08	0.017	0.06	0.10
cs3168	11 19 52.67	29 14 34.5	16.18 ± 0.03	16.77 ± 0.03	0.017	0.06	0.10
cs736	11 19 57.79	28 30 14.9	16.28 ± 0.03	16.80 ± 0.04	0.019	0.02	0.05
cs768	11 20 03.13	28 59 36.7	15.30 ± 0.10	15.93 ± 0.18	0.017	0.08	0.13
cs771	11 20 25.19	29 27 46.5	15.87 ± 0.03	16.40 ± 0.03	0.016	0.04	0.07
cs772	11 20 30.46	29 12 03.1	15.23 ± 0.08	15.85 ± 0.08	0.017	0.08	0.13
cs774	11 20 37.83	29 12 07.0	15.74 ± 0.15	16.35 ± 0.13	0.017	0.08	0.13
cs775	11 20 39.18	29 41 22.2	15.61 ± 0.03	16.19 ± 0.03	0.016	0.08	0.13
cs776	11 20 44.35	29 28 48.6	15.88 ± 0.05	16.34 ± 0.04	0.016	0.02	0.02
cs777	11 20 45.73	28 50 25.6	14.87 ± 0.04	15.45 ± 0.04	0.018	0.04	0.08
cs778	11 20 49.30	29 05 00.1	15.61 ± 0.05	16.06 ± 0.03	0.018	0.02	0.02
cs780	11 20 54.25	29 04 22.1	15.62 ± 0.04	16.00 ± 0.03	0.018	0.01	0.00

Table 1—Continued

ID	RA <sub>J2000</sub>	Dec <sub>J2000</sub>	<i>R</i>	<i>V</i>	<i>E(B-V)</i> <sup>a</sup>	<i>k<sub>R</sub></i> <sup>b</sup>	<i>k<sub>V</sub></i> <sup>b</sup>
cs781	11 20 57.00	29 37 57.2	15.81 ± 0.03	16.43 ± 0.03	0.016	0.10	0.15
cs782	11 20 59.66	29 15 23.2	15.81 ± 0.06	16.37 ± 0.09	0.018	0.04	0.09
cs783	11 21 02.56	29 09 39.5	15.14 ± 0.05	15.68 ± 0.03	0.018	0.02	0.05
cs784	11 21 03.41	29 38 13.8	15.79 ± 0.04	16.17 ± 0.04	0.017	0.01	0.00
cs785	11 21 05.43	28 45 39.1	15.67 ± 0.05	16.29 ± 0.05	0.018	0.07	0.11
cs787	11 21 18.87	28 59 52.6	15.88 ± 0.05	16.46 ± 0.04	0.019	0.07	0.12
cs788	11 21 48.58	29 26 44.1	15.07 ± 0.06	15.42 ± 0.06	0.019	0.01	-0.02
cs789	11 22 52.59	29 37 38.5	16.10 ± 0.06	16.67 ± 0.04	0.018	0.07	0.12
cs790	11 22 54.85	29 31 31.7	16.32 ± 0.04	16.90 ± 0.04	0.019	0.12	0.20
cs791	11 22 55.91	28 54 19.6	16.00 ± 0.05	16.63 ± 0.03	0.020	0.09	0.13
cs793	11 23 11.45	29 35 54.0	14.10 ± 0.04	14.75 ± 0.04	0.019	0.06	0.10
cs794	11 23 32.80	29 13 48.4	15.51 ± 0.06	16.01 ± 0.07	0.020	0.03	0.05
cs795	11 24 04.86	29 19 00.6	15.56 ± 0.03	16.21 ± 0.03	0.020	0.15	0.21
cs796	11 24 21.38	29 20 21.2	16.08 ± 0.03	16.56 ± 0.04	0.020	0.04	0.04
cs797	11 24 48.61	28 45 07.4	14.64 ± 0.04	15.17 ± 0.04	0.021	0.03	0.06
cs798	11 25 53.09	29 06 12.1	15.70 ± 0.03	16.21 ± 0.03	0.022	0.02	0.04
cs799	11 26 26.04	29 42 36.8	16.15 ± 0.04	16.75 ± 0.04	0.021	0.12	0.18
cs800	11 26 26.69	29 23 49.5	15.16 ± 0.05	15.56 ± 0.04	0.023	0.01	0.00
cs801	11 27 08.60	29 07 31.6	14.99 ± 0.05	15.60 ± 0.04	0.024	0.09	0.14
cs803	11 28 00.58	29 30 40.2	12.07 ± 0.04	12.58 ± 0.03	0.022	0.01	0.01
cs804	11 28 04.16	29 30 38.2	15.97 ± 0.06	16.41 ± 0.06	0.022	0.00	0.00
cs805	11 28 05.01	28 49 22.7	16.16 ± 0.03	16.77 ± 0.03	0.024	0.09	0.14
cs806	11 28 33.72	28 45 24.4	16.30 ± 0.05	17.01 ± 0.13	0.024	0.20	0.28
cs807	11 29 01.33	28 49 14.2	15.09 ± 0.04	15.65 ± 0.03	0.025	0.02	0.04
cs808	11 29 28.02	28 45 25.6	16.21 ± 0.11	16.81 ± 0.09	0.024	0.08	0.13
cs809	11 29 46.23	29 23 45.6	16.29 ± 0.05	16.76 ± 0.10	0.022	0.04	0.04
cs802 <sup>c</sup>	11 30 33.69	28 36 58.4	16.33 ± 0.05	16.78 ± 0.10	0.024	0.01	0.01
cs810	11 31 00.56	29 40 18.6	14.90 ± 0.04	15.43 ± 0.04	0.022	0.03	0.06
cs811	11 31 04.20	29 18 06.5	14.02 ± 0.04	14.64 ± 0.03	0.022	0.04	0.06
cs813	11 32 06.07	29 20 12.7	16.15 ± 0.03	16.78 ± 0.03	0.023	0.14	0.21
cs3175	11 32 23.86	28 56 07.0	16.34 ± 0.05	16.96 ± 0.04	0.024	0.12	0.18
cs815	11 32 47.65	28 56 50.0	16.41 ± 0.10	17.10 ± 0.08	0.024	0.20	0.28
cs816	11 32 52.97	28 57 36.1	16.07 ± 0.04	16.76 ± 0.04	0.024	0.19	0.28
cs817	11 33 03.31	28 47 01.7	16.19 ± 0.05	16.82 ± 0.03	0.024	0.12	0.18
cs819	11 33 17.95	29 20 15.6	15.62 ± 0.04	16.11 ± 0.03	0.024	0.03	0.04
cs820	11 33 26.95	28 56 22.7	14.39 ± 0.04	15.00 ± 0.04	0.024	0.04	0.06

Table 1—Continued

ID	RA <sub>J2000</sub>	Dec <sub>J2000</sub>	<i>R</i>	<i>V</i>	<i>E(B-V)</i> <sup>a</sup>	<i>k<sub>R</sub></i> <sup>b</sup>	<i>k<sub>V</sub></i> <sup>b</sup>
cs821	11 33 40.75	29 29 06.8	15.95 ± 0.05	16.62 ± 0.04	0.023	0.11	0.16
cs822	11 33 41.82	29 29 28.7	15.94 ± 0.05	16.65 ± 0.04	0.023	0.13	0.18
cs812	11 33 46.95	29 09 22.1	16.35 ± 0.03	16.74 ± 0.03	0.022	0.01	0.00
cs824	11 33 57.55	28 59 14.0	15.73 ± 0.04	16.17 ± 0.03	0.024	0.01	0.01
cs826	11 34 21.06	28 56 20.2	16.05 ± 0.05	16.60 ± 0.03	0.024	0.07	0.11
cs828	11 35 17.05	29 33 12.9	16.39 ± 0.03	17.02 ± 0.03	0.022	0.15	0.23
cs830	11 36 04.93	29 41 56.4	16.09 ± 0.06	16.59 ± 0.05	0.023	0.03	0.05
cs831	11 36 32.25	28 59 20.5	16.15 ± 0.07	16.84 ± 0.08	0.023	0.18	0.25
cs832	11 36 35.94	29 32 39.9	15.76 ± 0.06	16.40 ± 0.05	0.022	0.10	0.15
cs3176	11 36 48.27	29 37 55.9	16.25 ± 0.06	16.92 ± 0.09	0.023	0.18	0.27
cs833	11 37 09.59	28 46 21.8	16.20 ± 0.05	16.86 ± 0.05	0.022	0.17	0.24
cs827	11 37 49.54	29 17 14.4	16.28 ± 0.03	16.72 ± 0.05	0.022	0.01	0.01
cs3177	11 38 06.32	29 34 46.3	16.26 ± 0.07	16.90 ± 0.06	0.022	0.16	0.24
cs834	11 38 10.67	29 32 38.4	15.56 ± 0.05	16.24 ± 0.04	0.022	0.18	0.26
cs835	11 38 40.20	29 17 14.3	15.64 ± 0.05	16.27 ± 0.15	0.024	0.15	0.22
cs3178	11 38 40.99	29 17 18.1	16.30 ± 0.05	16.92 ± 0.05	0.024	0.14	0.22
cs836	11 39 21.36	29 06 13.2	16.28 ± 0.04	16.73 ± 0.05	0.024	0.04	0.04
cs3180	11 39 36.13	28 56 10.8	16.19 ± 0.05	16.86 ± 0.04	0.022	0.19	0.28
cs837	11 40 39.19	28 51 49.5	14.17 ± 0.04	14.56 ± 0.04	0.022	0.01	0.00
cs3183	11 40 39.62	29 32 26.0	16.30 ± 0.05	16.87 ± 0.05	0.021	0.07	0.12
cs838	11 41 33.49	28 47 00.5	16.17 ± 0.08	16.80 ± 0.08	0.024	0.08	0.13
cs3185	11 41 46.21	28 56 36.1	15.96 ± 0.09	16.50 ± 0.28	0.023	0.07	0.09
cs839	11 42 14.11	28 50 29.4	15.73 ± 0.04	16.30 ± 0.04	0.025	0.09	0.15
cs3187	11 42 54.38	28 54 48.7	16.04 ± 0.06	16.63 ± 0.06	0.022	0.10	0.15
cs840	11 44 05.43	29 30 53.1	16.09 ± 0.05	16.74 ± 0.04	0.024	0.13	0.18
cs841	11 44 12.18	28 57 02.4	15.83 ± 0.03	16.37 ± 0.03	0.021	0.04	0.08
cs842	11 44 32.97	29 20 55.7	15.30 ± 0.04	15.87 ± 0.04	0.023	0.06	0.11
cs3186	11 44 40.27	28 35 38.6	16.33 ± 0.05	16.78 ± 0.03	0.025	0.04	0.04
cs3189	11 45 01.18	29 39 02.8	16.32 ± 0.05	16.86 ± 0.04	0.025	0.06	0.10
cs843	11 45 18.15	29 38 55.3	15.63 ± 0.05	16.26 ± 0.04	0.025	0.12	0.17
cs844	11 45 39.73	29 34 39.6	15.92 ± 0.04	16.48 ± 0.04	0.023	0.07	0.12
cs845	11 45 46.75	29 28 17.4	15.39 ± 0.04	15.98 ± 0.03	0.022	0.03	0.06
cs846	11 45 58.41	29 19 57.7	14.79 ± 0.03	15.37 ± 0.03	0.023	0.02	0.04
cs847	11 45 59.68	29 27 57.6	15.80 ± 0.04	16.34 ± 0.03	0.023	0.06	0.10
cs848	11 46 02.12	29 35 19.4	16.13 ± 0.04	16.55 ± 0.04	0.022	0.01	0.01
cs3190	11 46 17.95	28 53 58.3	16.30 ± 0.04	17.04 ± 0.04	0.024	0.23	0.32

Table 1—Continued

ID	RA <sub>J2000</sub>	Dec <sub>J2000</sub>	<i>R</i>	<i>V</i>	<i>E(B-V)</i> <sup>a</sup>	<i>k<sub>R</sub></i> <sup>b</sup>	<i>k<sub>V</sub></i> <sup>b</sup>
cs3192	11 46 25.65	29 35 46.6	16.28 ± 0.06	16.98 ± 0.05	0.021	0.21	0.30
cs850	11 47 07.90	29 34 39.1	13.45 ± 0.04	14.08 ± 0.04	0.022	0.03	0.05
cs851	11 47 08.11	29 37 27.3	15.68 ± 0.04	16.07 ± 0.03	0.022	0.01	0.00
cs852	11 47 38.76	29 23 03.5	15.82 ± 0.04	16.42 ± 0.04	0.022	0.06	0.10
cs3195	11 47 39.23	29 10 22.4	16.20 ± 0.05	16.83 ± 0.04	0.023	0.16	0.23
cs853	11 47 41.89	29 22 39.2	16.21 ± 0.04	16.82 ± 0.04	0.022	0.06	0.10
cs3196	11 47 51.53	29 01 28.8	16.32 ± 0.06	16.93 ± 0.05	0.023	0.06	0.10
cs854	11 48 00.68	29 07 20.7	16.04 ± 0.04	16.63 ± 0.06	0.023	0.04	0.08
cs855	11 48 10.67	29 16 42.9	16.07 ± 0.05	16.66 ± 0.03	0.023	0.05	0.09
cs856	11 48 17.63	29 21 01.9	15.81 ± 0.06	16.27 ± 0.04	0.023	0.02	0.02
cs857	11 48 26.90	29 06 29.6	15.15 ± 0.04	15.79 ± 0.03	0.023	0.06	0.10
cs858	11 48 30.89	29 06 14.8	15.90 ± 0.04	16.51 ± 0.03	0.023	0.05	0.09
cs859	11 48 31.03	29 05 51.8	16.15 ± 0.09	16.76 ± 0.06	0.023	0.06	0.09
cs860	11 48 45.94	29 38 28.7	14.17 ± 0.04	14.85 ± 0.03	0.023	0.04	0.06
cs861	11 48 55.22	29 01 08.8	16.10 ± 0.04	16.74 ± 0.03	0.023	0.11	0.17
cs862	11 48 56.46	29 10 39.9	16.30 ± 0.04	16.86 ± 0.04	0.022	0.07	0.11
cs863	11 49 19.63	29 37 00.0	16.09 ± 0.04	16.70 ± 0.04	0.020	0.07	0.12
cs864	11 49 37.39	29 35 04.2	15.97 ± 0.04	16.58 ± 0.04	0.021	0.05	0.08
cs865	11 49 49.42	29 13 00.6	15.59 ± 0.04	16.17 ± 0.04	0.021	0.04	0.08
cs867	11 49 52.29	29 25 38.8	14.37 ± 0.05	14.91 ± 0.05	0.021	0.04	0.07
cs868	11 49 56.12	28 58 56.5	14.91 ± 0.04	15.54 ± 0.04	0.023	0.05	0.08
cs869	11 49 56.39	29 17 01.8	15.02 ± 0.05	15.58 ± 0.08	0.022	0.04	0.08
cs870	11 50 11.43	29 16 03.9	15.91 ± 0.03	16.38 ± 0.03	0.021	0.01	0.02
cs871	11 50 21.22	29 00 25.7	15.92 ± 0.10	16.32 ± 0.09	0.023	0.01	0.00
cs872	11 50 47.74	29 09 17.1	16.16 ± 0.05	16.78 ± 0.04	0.023	0.05	0.08
cs873	11 50 56.25	29 02 07.6	15.94 ± 0.05	16.59 ± 0.04	0.022	0.09	0.13
cs874	11 51 01.72	29 01 48.0	15.03 ± 0.04	15.52 ± 0.04	0.022	0.01	0.03
cs875	11 51 05.48	29 17 19.5	16.11 ± 0.03	16.62 ± 0.03	0.021	0.03	0.04
cs876	11 51 18.84	28 48 14.1	15.88 ± 0.04	16.55 ± 0.05	0.024	0.18	0.26
cs878	11 51 31.82	29 14 49.5	16.02 ± 0.05	16.62 ± 0.04	0.023	0.06	0.10
cs879	11 51 44.67	29 16 40.5	15.28 ± 0.05	15.93 ± 0.04	0.023	0.06	0.09
cs880	11 52 13.72	29 04 32.8	16.03 ± 0.05	16.47 ± 0.03	0.024	0.01	0.01
cs882	11 52 47.34	29 19 43.6	13.30 ± 0.10	13.90 ± 0.11	0.022	0.03	0.06
cs883	11 52 58.06	29 02 14.2	16.22 ± 0.04	16.83 ± 0.03	0.024	0.12	0.18
cs884	11 53 43.84	29 15 10.9	15.08 ± 0.03	15.60 ± 0.03	0.025	0.03	0.05
cs885	11 54 04.14	29 33 46.9	16.03 ± 0.09	16.61 ± 0.10	0.022	0.04	0.07

Table 1—Continued

ID	RA <sub>J2000</sub>	Dec <sub>J2000</sub>	<i>R</i>	<i>V</i>	<i>E(B-V)</i> <sup>a</sup>	<i>k<sub>R</sub></i> <sup>b</sup>	<i>k<sub>V</sub></i> <sup>b</sup>
cs886	11 54 37.95	28 58 39.6	16.03 ± 0.04	16.50 ± 0.04	0.026	0.01	0.02
cs887	11 54 48.15	29 35 52.3	15.58 ± 0.05	16.16 ± 0.04	0.019	0.04	0.07
cs888	11 54 55.82	29 20 33.9	15.84 ± 0.03	16.26 ± 0.03	0.023	0.01	0.00
cs889	11 55 15.21	29 15 49.0	15.94 ± 0.03	16.42 ± 0.03	0.023	0.02	0.04
cs890	11 55 36.65	29 21 04.3	15.57 ± 0.03	16.13 ± 0.03	0.023	0.04	0.07
cs891	11 56 10.84	28 46 09.3	15.46 ± 0.04	16.10 ± 0.03	0.021	0.09	0.13
cs892	11 56 40.60	29 21 01.9	16.07 ± 0.04	16.55 ± 0.04	0.019	0.05	0.06
cs893	11 56 41.48	28 50 08.8	15.79 ± 0.03	16.36 ± 0.03	0.021	0.06	0.11
cs894	11 56 45.92	28 51 40.4	15.64 ± 0.03	16.16 ± 0.03	0.021	0.04	0.06
cs895	11 56 50.75	29 41 01.1	16.23 ± 0.05	16.78 ± 0.05	0.018	0.05	0.09
cs896	11 57 35.70	29 14 13.5	16.02 ± 0.04	16.45 ± 0.06	0.020	0.01	0.01
cs3210	11 57 39.94	29 08 12.7	16.26 ± 0.04	16.85 ± 0.07	0.021	0.13	0.22
cs897	11 57 51.68	29 02 22.6	13.80 ± 0.12	14.26 ± 0.12	0.020	0.01	0.01
cs3212	11 58 38.43	29 40 04.5	16.24 ± 0.05	16.68 ± 0.04	0.020	0.03	0.02
cs898	11 58 51.42	28 59 06.2	15.54 ± 0.12	16.04 ± 0.14	0.023	0.02	0.04
cs899	11 58 53.84	29 33 27.5	16.15 ± 0.05	16.60 ± 0.04	0.023	0.03	0.02
cs3213 <sup>c</sup>	11 58 59.09	29 11 36.2	16.00 ± 0.10	16.40 ± 0.06	0.021	0.00	0.00
cs900	11 59 44.67	29 29 37.9	16.04 ± 0.05	16.69 ± 0.04	0.021	0.12	0.18
cs901	11 59 48.66	29 38 26.6	14.90 ± 0.04	15.38 ± 0.04	0.022	0.01	0.02
cs902	11 59 48.87	29 09 29.4	15.93 ± 0.06	16.54 ± 0.04	0.022	0.09	0.14
cs904	12 00 24.95	28 54 57.1	16.07 ± 0.04	16.72 ± 0.03	0.020	0.09	0.14
cs905	12 00 28.91	29 09 14.0	15.77 ± 0.04	16.41 ± 0.03	0.023	0.10	0.15
cs906	12 00 31.92	29 00 17.4	15.16 ± 0.04	15.81 ± 0.04	0.020	0.10	0.15
cs907	12 00 32.52	28 59 07.0	16.33 ± 0.06	16.95 ± 0.04	0.020	0.09	0.14
cs908	12 00 35.63	29 11 45.8	15.45 ± 0.04	16.08 ± 0.03	0.022	0.10	0.15
cs910	12 00 53.90	28 52 39.7	15.84 ± 0.05	16.26 ± 0.05	0.020	0.02	0.01
cs911	12 00 59.58	29 03 04.5	16.11 ± 0.06	16.59 ± 0.03	0.021	0.04	0.04
cs912	12 01 05.91	28 59 43.2	15.74 ± 0.05	16.20 ± 0.03	0.020	0.00	0.01
cs913	12 01 09.97	29 17 20.9	15.71 ± 0.04	16.32 ± 0.04	0.021	0.09	0.14
cs914	12 01 32.58	28 56 07.0	15.05 ± 0.04	15.58 ± 0.03	0.019	0.03	0.06
cs915	12 01 44.21	29 25 44.0	16.19 ± 0.06	16.68 ± 0.05	0.020	0.03	0.04
cs916	12 01 45.07	29 42 36.6	15.72 ± 0.03	16.35 ± 0.04	0.022	0.08	0.13
cs918	12 02 05.32	28 51 27.5	16.17 ± 0.05	16.59 ± 0.06	0.018	0.01	0.01
cs919	12 02 22.60	29 39 04.6	16.25 ± 0.04	16.85 ± 0.07	0.020	0.08	0.12
cs920	12 02 24.49	29 22 34.2	16.01 ± 0.03	16.38 ± 0.04	0.018	0.01	0.00
cs921	12 02 25.36	29 28 14.0	14.61 ± 0.04	15.00 ± 0.03	0.019	0.00	0.00

Table 1—Continued

ID	RA <sub>J2000</sub>	Dec <sub>J2000</sub>	<i>R</i>	<i>V</i>	<i>E(B-V)</i> <sup>a</sup>	<i>k<sub>R</sub></i> <sup>b</sup>	<i>k<sub>V</sub></i> <sup>b</sup>
cs922	12 02 29.46	29 35 17.9	16.13 ± 0.06	16.75 ± 0.06	0.019	0.09	0.14
cs924	12 02 29.49	29 02 05.7	15.86 ± 0.11	16.50 ± 0.10	0.018	0.10	0.15
cs923	12 02 29.51	29 00 48.5	15.22 ± 0.05	15.87 ± 0.04	0.019	0.11	0.16
cs925	12 02 32.49	29 28 35.6	16.21 ± 0.03	16.61 ± 0.06	0.019	0.02	0.00
cs926	12 02 45.29	28 51 57.2	15.63 ± 0.04	16.12 ± 0.05	0.021	0.01	0.03
cs927	12 02 45.64	29 00 03.7	15.65 ± 0.05	16.24 ± 0.04	0.019	0.08	0.13
cs928	12 02 46.10	29 22 58.5	16.11 ± 0.04	16.71 ± 0.04	0.016	0.09	0.15
cs929	12 02 53.50	29 04 13.9	16.15 ± 0.04	16.82 ± 0.04	0.018	0.11	0.16
cs930	12 03 19.72	29 14 28.5	16.02 ± 0.05	16.55 ± 0.05	0.019	0.04	0.07
cs931	12 03 21.38	29 25 10.0	14.08 ± 0.03	14.48 ± 0.03	0.018	0.00	0.00
cs932	12 03 34.30	29 41 52.1	16.19 ± 0.06	16.74 ± 0.06	0.017	0.04	0.08
cs934	12 03 40.78	29 37 35.4	16.02 ± 0.05	16.49 ± 0.04	0.016	0.02	0.03
cs935	12 03 42.78	29 38 19.2	15.95 ± 0.05	16.46 ± 0.04	0.016	0.02	0.03
cs936	12 03 48.50	29 37 45.6	16.07 ± 0.05	16.65 ± 0.04	0.016	0.11	0.17
cs937	12 03 49.67	29 42 56.8	14.72 ± 0.04	15.16 ± 0.04	0.016	0.00	0.01
cs939	12 04 30.00	28 55 34.5	15.50 ± 0.05	16.27 ± 0.04	0.023	0.15	0.20
cs940	12 04 35.48	29 39 48.1	16.29 ± 0.06	16.95 ± 0.08	0.015	0.19	0.28
cs941	12 05 02.18	28 52 18.2	15.78 ± 0.07	16.21 ± 0.06	0.024	0.01	0.01
cs942	12 05 02.99	29 02 52.2	16.16 ± 0.04	16.74 ± 0.03	0.023	0.07	0.12
cs3219 <sup>c</sup>	12 05 05.24	28 57 55.2	16.29 ± 0.18	16.51 ± 0.11	0.017	0.00	-0.03
cs943	12 05 12.78	28 46 55.2	14.00 ± 0.05	14.48 ± 0.11	0.024	0.01	0.01
cs944	12 05 29.95	29 11 45.2	15.36 ± 0.04	15.86 ± 0.04	0.021	0.01	0.03
cs945	12 06 12.47	29 42 50.3	15.20 ± 0.04	15.81 ± 0.04	0.018	0.08	0.12
cs946	12 06 13.12	29 40 39.2	16.16 ± 0.05	16.76 ± 0.05	0.018	0.07	0.12
cs947	12 06 45.64	29 28 11.5	15.86 ± 0.05	16.49 ± 0.03	0.020	0.09	0.13
cs948	12 07 25.59	29 08 48.4	15.32 ± 0.04	15.90 ± 0.04	0.020	0.03	0.05
cs949	12 07 44.77	29 12 53.0	15.83 ± 0.03	16.47 ± 0.05	0.020	0.09	0.13
cs3222 <sup>c</sup>	12 08 24.57	29 10 05.6	16.30 ± 0.09	16.62 ± 0.04	0.019	0.00	-0.01
cs3226	12 08 35.66	29 32 29.7	16.37 ± 0.04	17.09 ± 0.04	0.019	0.22	0.31
cs951	12 08 40.95	29 10 45.2	15.20 ± 0.05	15.83 ± 0.05	0.019	0.07	0.11
cs952	12 08 41.27	29 41 03.9	15.41 ± 0.05	16.10 ± 0.04	0.021	0.20	0.29
cs953	12 08 43.26	28 44 38.0	16.02 ± 0.08	16.72 ± 0.11	0.019	0.20	0.28
cs954	12 08 47.29	29 18 17.6	12.70 ± 0.04	13.27 ± 0.04	0.020	0.01	0.03
cs955	12 08 50.92	29 22 52.6	14.65 ± 0.04	15.29 ± 0.04	0.020	0.07	0.11
cs957	12 09 01.39	29 15 01.5	13.43 ± 0.05	13.99 ± 0.04	0.020	0.01	0.03
cs958	12 09 02.53	28 44 21.6	16.31 ± 0.06	16.88 ± 0.04	0.020	0.07	0.12

Table 1—Continued

ID	RA <sub>J2000</sub>	Dec <sub>J2000</sub>	<i>R</i>	<i>V</i>	<i>E(B-V)</i> <sup>a</sup>	<i>k<sub>R</sub></i> <sup>b</sup>	<i>k<sub>V</sub></i> <sup>b</sup>
cs959	12 09 09.57	29 16 25.0	15.35 ± 0.04	15.76 ± 0.05	0.021	0.00	0.00
cs960	12 09 10.08	29 10 36.8	12.63 ± 0.04	13.10 ± 0.03	0.021	0.01	0.01
cs961	12 09 30.35	28 53 14.4	15.31 ± 0.05	15.75 ± 0.05	0.019	0.02	0.02
cs962	12 09 32.32	29 30 10.9	15.53 ± 0.02	16.13 ± 0.02	0.021	0.06	0.10
cs963	12 09 42.52	29 23 10.9	15.83 ± 0.04	16.47 ± 0.04	0.021	0.11	0.16
cs964	12 09 56.36	29 18 08.5	15.46 ± 0.04	16.10 ± 0.04	0.019	0.09	0.14
cs966	12 10 36.17	29 00 02.0	15.83 ± 0.05	16.37 ± 0.03	0.019	0.06	0.09
cs967	12 11 14.61	29 22 41.5	16.00 ± 0.03	16.64 ± 0.03	0.020	0.13	0.19
cs968	12 11 24.37	28 56 39.0	15.91 ± 0.04	16.46 ± 0.04	0.018	0.06	0.09
cs969	12 11 31.86	29 05 22.0	13.30 ± 0.06	13.94 ± 0.05	0.017	0.04	0.06
cs970	12 11 44.46	29 02 31.8	15.90 ± 0.06	16.40 ± 0.06	0.019	0.04	0.05
cs971	12 11 53.47	29 19 00.5	16.00 ± 0.05	16.70 ± 0.05	0.019	0.20	0.28
cs972	12 11 56.80	29 30 33.9	15.74 ± 0.06	16.31 ± 0.05	0.022	0.08	0.14
cs973	12 12 03.64	29 25 02.7	15.52 ± 0.03	15.89 ± 0.03	0.019	0.00	0.00
cs974	12 12 18.80	29 10 46.0	11.73 ± 0.06	12.34 ± 0.05	0.019	0.02	0.03
cs975	12 12 20.97	29 12 31.0	12.95 ± 0.07	13.34 ± 0.06	0.020	0.00	0.00
cs976	12 12 22.50	29 30 28.7	15.96 ± 0.05	16.62 ± 0.04	0.020	0.14	0.20
cs3234	12 12 22.87	29 29 47.3	16.26 ± 0.08	16.94 ± 0.07	0.020	0.15	0.21
cs977	12 12 24.37	28 49 01.9	13.67 ± 0.04	14.22 ± 0.03	0.020	0.01	0.02
cs978	12 12 26.91	29 08 57.2	13.07 ± 0.07	13.64 ± 0.05	0.020	0.01	0.03
cs979	12 12 31.16	29 10 05.8	12.77 ± 0.06	13.45 ± 0.04	0.020	0.03	0.04
cs980	12 12 42.29	29 24 29.3	15.73 ± 0.04	16.36 ± 0.04	0.020	0.13	0.18
cs3235	12 13 03.87	29 30 20.9	16.23 ± 0.05	16.89 ± 0.04	0.020	0.13	0.18
cs981	12 13 04.77	29 33 36.1	16.10 ± 0.05	16.62 ± 0.04	0.021	0.05	0.07
cs982	12 13 05.42	29 33 12.6	16.31 ± 0.10	16.95 ± 0.09	0.021	0.16	0.24
cs983	12 13 13.91	28 50 10.4	14.01 ± 0.05	14.49 ± 0.04	0.021	0.01	0.01
cs984	12 13 22.02	29 13 01.1	16.36 ± 0.05	17.02 ± 0.05	0.022	0.18	0.27
cs985	12 13 28.25	29 15 25.2	15.75 ± 0.06	16.41 ± 0.05	0.021	0.18	0.27
cs986	12 13 32.00	29 28 54.7	14.99 ± 0.05	15.44 ± 0.04	0.020	0.01	0.01
cs987	12 13 33.01	28 51 46.1	15.37 ± 0.05	15.91 ± 0.07	0.021	0.05	0.09
cs988	12 13 33.20	29 16 05.3	16.03 ± 0.05	16.74 ± 0.05	0.021	0.21	0.30
cs989	12 13 45.39	29 41 03.2	16.12 ± 0.05	16.77 ± 0.05	0.020	0.14	0.19
cs990	12 13 47.42	29 30 01.8	16.11 ± 0.02	16.74 ± 0.03	0.021	0.08	0.13
cs3240	12 13 49.74	29 36 43.5	16.24 ± 0.04	16.77 ± 0.04	0.021	0.04	0.06
cs991	12 14 04.44	29 42 50.8	15.97 ± 0.03	16.61 ± 0.04	0.021	0.13	0.19
cs3242	12 14 06.01	28 56 39.8	16.34 ± 0.05	17.01 ± 0.06	0.020	0.18	0.26

Table 1—Continued

ID	RA <sub>J2000</sub>	Dec <sub>J2000</sub>	<i>R</i>	<i>V</i>	<i>E(B-V)</i> <sup>a</sup>	<i>k<sub>R</sub></i> <sup>b</sup>	<i>k<sub>V</sub></i> <sup>b</sup>
cs992	12 14 10.68	28 55 31.6	16.28 ± 0.05	16.94 ± 0.03	0.019	0.18	0.27
cs3243	12 14 17.85	29 31 43.5	16.21 ± 0.08	16.27 ± 0.07	0.021	-0.01	-0.13
cs994	12 14 18.27	29 31 46.4	15.33 ± 0.06	15.90 ± 0.06	0.021	0.05	0.10
cs995	12 14 22.58	29 08 19.9	16.13 ± 0.05	16.66 ± 0.08	0.021	0.06	0.08
cs996	12 14 34.48	28 43 51.1	16.22 ± 0.05	16.79 ± 0.04	0.019	0.07	0.12
cs3244	12 14 40.32	29 17 19.5	15.91 ± 0.04	16.54 ± 0.05	0.019	0.09	0.13
cs997	12 14 45.42	29 18 53.7	15.86 ± 0.05	16.49 ± 0.05	0.019	0.09	0.13
cs998	12 15 03.52	29 06 02.1	15.97 ± 0.04	16.61 ± 0.05	0.020	0.13	0.19
cs1001	12 15 16.15	29 15 08.2	15.97 ± 0.04	16.62 ± 0.04	0.020	0.17	0.25
cs1002	12 15 23.76	29 10 45.7	15.67 ± 0.04	16.21 ± 0.03	0.021	0.02	0.04
cs1003	12 15 33.80	28 59 04.6	15.90 ± 0.04	16.45 ± 0.05	0.020	0.06	0.10
cs1004	12 15 36.62	28 59 25.9	15.22 ± 0.05	15.65 ± 0.04	0.020	0.01	0.01
cs1005	12 15 39.60	29 25 14.3	16.20 ± 0.04	16.83 ± 0.07	0.021	0.09	0.14
cs1006	12 16 14.12	28 45 45.1	14.13 ± 0.06	14.72 ± 0.03	0.025	0.03	0.05
cs3245 <sup>c</sup>	12 16 43.17	28 43 56.2	15.10 ± 0.04	15.49 ± 0.04	0.026	0.00	0.00
cs1007	12 16 44.50	28 45 11.4	16.05 ± 0.05	16.72 ± 0.06	0.026	0.17	0.24
cs1008 <sup>c</sup>	12 16 51.40	29 03 17.3	16.17 ± 0.14	16.60 ± 0.07	0.023	0.00	0.00
cs3246	12 17 29.60	29 12 21.8	16.25 ± 0.05	16.86 ± 0.07	0.023	0.12	0.18
cs1011	12 17 56.73	29 07 15.9	15.72 ± 0.04	16.19 ± 0.04	0.024	0.02	0.02
cs3248	12 18 02.83	29 24 39.0	16.34 ± 0.04	16.98 ± 0.08	0.023	0.12	0.18
cs1012	12 18 12.21	29 15 05.6	15.80 ± 0.07	16.16 ± 0.17	0.024	0.00	-0.01
cs1013	12 18 19.36	29 15 13.4	14.68 ± 0.05	15.08 ± 0.05	0.024	0.01	0.00
cs1014	12 18 23.32	28 58 09.9	15.97 ± 0.04	16.48 ± 0.05	0.023	0.04	0.06
cs1015	12 18 35.92	28 48 13.1	15.71 ± 0.04	16.34 ± 0.03	0.023	0.09	0.14
cs1016	12 18 41.58	28 49 24.3	16.29 ± 0.05	16.95 ± 0.04	0.022	0.10	0.15
cs1017	12 18 44.48	29 22 47.6	15.90 ± 0.05	16.32 ± 0.06	0.024	0.01	0.01
cs3251	12 19 03.14	29 21 07.3	16.17 ± 0.05	16.77 ± 0.05	0.023	0.06	0.10
cs1018	12 19 32.75	28 56 33.0	15.04 ± 0.04	15.71 ± 0.03	0.024	0.11	0.16
cs1020	12 19 41.28	28 49 32.6	14.17 ± 0.05	14.77 ± 0.04	0.023	0.03	0.05
cs1019	12 19 41.30	28 47 09.8	14.65 ± 0.04	15.23 ± 0.03	0.022	0.03	0.05
cs1021	12 19 41.58	28 43 30.4	14.11 ± 0.04	14.72 ± 0.03	0.020	0.03	0.05
cs1022	12 19 43.91	28 51 46.7	14.21 ± 0.04	14.74 ± 0.03	0.025	0.02	0.04
cs1023	12 19 44.13	29 34 50.3	15.57 ± 0.05	16.13 ± 0.05	0.023	0.05	0.10
cs1025	12 20 04.55	28 53 50.1	15.08 ± 0.04	15.64 ± 0.04	0.025	0.02	0.04
cs1027	12 20 13.45	29 04 09.2	15.84 ± 0.04	16.36 ± 0.04	0.024	0.03	0.05
cs1029	12 20 20.80	29 18 39.4	11.70 ± 0.05	12.28 ± 0.06	0.026	0.01	0.01

Table 1—Continued

ID	RA <sub>J2000</sub>	Dec <sub>J2000</sub>	<i>R</i>	<i>V</i>	<i>E(B-V)</i> <sup>a</sup>	<i>k<sub>R</sub></i> <sup>b</sup>	<i>k<sub>V</sub></i> <sup>b</sup>
cs1030	12 20 32.20	29 38 18.8	15.43 ± 0.04	16.06 ± 0.04	0.023	0.08	0.12
cs3254	12 20 35.78	29 17 59.8	16.19 ± 0.04	16.82 ± 0.04	0.025	0.11	0.16
cs1032	12 20 59.50	29 07 29.5	15.75 ± 0.04	16.45 ± 0.04	0.021	0.20	0.28
cs1033	12 21 00.97	29 31 23.4	15.81 ± 0.05	16.43 ± 0.04	0.022	0.06	0.10
cs1034	12 21 15.20	29 19 32.3	16.15 ± 0.05	16.55 ± 0.07	0.024	0.01	0.00
cs1036 <sup>c</sup>	12 21 20.11	29 42 55.5	14.89 ± 0.04	15.43 ± 0.04	0.024	0.00	0.01
cs1038	12 22 14.90	28 48 46.3	14.96 ± 0.04	15.59 ± 0.04	0.026	0.07	0.12
cs1039	12 22 19.50	28 49 53.5	14.55 ± 0.04	15.12 ± 0.04	0.028	0.05	0.10
cs1040	12 22 21.86	29 34 52.1	15.69 ± 0.03	16.14 ± 0.03	0.022	0.01	0.01
cs1042	12 22 38.91	29 26 18.0	14.29 ± 0.05	14.73 ± 0.04	0.023	0.01	0.01
cs1045	12 23 16.65	28 57 42.3	15.19 ± 0.04	15.80 ± 0.04	0.025	0.06	0.11
cs3256	12 23 25.02	29 08 42.3	16.35 ± 0.03	16.81 ± 0.03	0.024	0.04	0.04
cs1037 <sup>c</sup>	12 24 22.82	28 40 29.2	16.29 ± 0.04	16.70 ± 0.06	0.023	0.01	0.00
cs1048	12 25 12.29	29 39 22.7	16.29 ± 0.05	16.96 ± 0.04	0.020	0.10	0.15
cs1049	12 25 20.22	29 28 03.8	15.73 ± 0.04	16.31 ± 0.04	0.021	0.06	0.10
cs1050	12 25 23.48	28 47 04.4	15.73 ± 0.06	16.41 ± 0.04	0.021	0.18	0.25
cs1051	12 25 25.48	28 56 37.4	15.29 ± 0.05	15.78 ± 0.03	0.024	0.03	0.04
cs3261	12 25 27.16	28 57 32.0	16.32 ± 0.04	16.99 ± 0.04	0.024	0.09	0.13
cs1052	12 25 28.12	29 09 49.0	15.13 ± 0.07	15.74 ± 0.05	0.025	0.03	0.06
cs1053	12 25 28.90	28 55 37.8	16.16 ± 0.05	16.54 ± 0.03	0.024	0.02	0.00
cs1054	12 25 47.68	29 39 47.2	15.40 ± 0.04	16.01 ± 0.05	0.021	0.03	0.06
cs1055	12 26 30.77	28 50 48.6	16.19 ± 0.06	16.48 ± 0.05	0.022	0.00	-0.03
cs1057	12 26 39.49	29 33 45.0	16.08 ± 0.03	16.51 ± 0.03	0.020	0.02	0.02
cs1058	12 27 08.69	28 57 23.0	16.03 ± 0.04	16.59 ± 0.03	0.022	0.02	0.04
cs1059	12 27 29.74	29 13 55.6	16.24 ± 0.03	16.68 ± 0.05	0.025	0.02	0.02
cs1060	12 27 58.78	28 49 44.5	15.17 ± 0.04	15.76 ± 0.03	0.020	0.05	0.09
cs3264	12 28 53.89	28 50 21.5	16.29 ± 0.04	16.86 ± 0.03	0.019	0.04	0.08
cs1061	12 28 56.41	28 52 09.5	15.99 ± 0.07	16.48 ± 0.07	0.020	0.04	0.05
cs1062	12 28 59.32	28 51 42.1	14.62 ± 0.04	15.16 ± 0.03	0.019	0.02	0.04
cs1063	12 29 18.20	29 00 06.0	15.16 ± 0.09	15.75 ± 0.08	0.021	0.05	0.09
cs1064	12 29 41.36	29 05 42.8	15.73 ± 0.06	16.41 ± 0.05	0.021	0.17	0.23
cs1065	12 29 43.03	29 05 14.7	15.66 ± 0.06	16.17 ± 0.04	0.021	0.06	0.07
cs1066	12 30 02.60	28 45 30.4	15.64 ± 0.04	16.30 ± 0.03	0.017	0.08	0.13
cs3268	12 30 11.82	29 34 18.5	16.27 ± 0.06	16.79 ± 0.08	0.020	0.07	0.09
cs1067	12 30 26.86	28 59 14.2	15.77 ± 0.08	16.41 ± 0.07	0.018	0.07	0.12
cs3272	12 30 53.30	29 03 46.1	16.27 ± 0.04	16.97 ± 0.04	0.018	0.09	0.14

Table 1—Continued

ID	RA <sub>J2000</sub>	Dec <sub>J2000</sub>	<i>R</i>	<i>V</i>	<i>E(B-V)</i> <sup>a</sup>	<i>k<sub>R</sub></i> <sup>b</sup>	<i>k<sub>V</sub></i> <sup>b</sup>
cs1068	12 30 54.14	28 56 20.3	16.18 ± 0.05	16.79 ± 0.03	0.017	0.07	0.11
cs1069	12 30 56.71	28 51 45.3	14.57 ± 0.04	15.24 ± 0.03	0.017	0.08	0.12
cs1070	12 31 00.21	28 58 15.0	15.07 ± 0.04	15.73 ± 0.03	0.017	0.08	0.12
cs1072	12 31 04.40	28 51 09.7	14.47 ± 0.04	15.11 ± 0.03	0.017	0.08	0.12
cs3273	12 31 04.52	28 51 14.5	14.63 ± 0.05	15.28 ± 0.03	0.017	0.08	0.13
cs3274	12 31 08.00	28 50 29.0	16.30 ± 0.04	16.93 ± 0.03	0.017	0.07	0.12
cs1073	12 31 10.10	28 52 04.3	15.97 ± 0.05	16.59 ± 0.04	0.017	0.07	0.12
cs1074	12 31 17.21	28 53 30.5	15.99 ± 0.05	16.64 ± 0.03	0.017	0.08	0.12
cs1075	12 31 22.42	29 03 53.7	15.83 ± 0.04	16.47 ± 0.04	0.017	0.07	0.11
cs1076	12 31 22.91	29 08 11.4	12.95 ± 0.05	13.52 ± 0.03	0.017	0.02	0.03
cs1077	12 31 24.06	28 51 18.6	14.01 ± 0.05	14.65 ± 0.03	0.017	0.07	0.12
cs1079	12 31 55.69	28 49 12.7	15.26 ± 0.05	15.86 ± 0.08	0.016	0.06	0.10
cs1080	12 32 20.21	29 16 59.9	15.84 ± 0.05	16.46 ± 0.05	0.016	0.10	0.15
cs1081	12 32 21.79	29 24 41.0	16.16 ± 0.05	16.57 ± 0.08	0.018	0.01	0.00
cs1082	12 32 38.48	28 46 29.8	15.32 ± 0.06	15.81 ± 0.05	0.016	0.02	0.04
cs1083	12 32 41.76	28 44 22.7	16.01 ± 0.05	16.69 ± 0.03	0.016	0.07	0.11
cs1084	12 32 42.98	29 42 43.9	13.52 ± 0.03	13.96 ± 0.04	0.020	0.01	0.01
cs1085	12 32 43.11	28 55 29.2	16.05 ± 0.06	16.60 ± 0.04	0.015	0.07	0.12
cs3278	12 32 43.57	29 22 53.0	14.54 ± 0.05	15.05 ± 0.04	0.019	0.03	0.05
cs1086	12 32 49.66	28 57 31.5	15.28 ± 0.06	15.61 ± 0.04	0.016	0.00	-0.02
cs1087	12 32 50.34	29 35 22.2	15.75 ± 0.04	16.41 ± 0.03	0.019	0.08	0.12
cs1088	12 33 28.98	29 02 06.4	15.31 ± 0.04	15.96 ± 0.05	0.017	0.08	0.12
cs1090	12 33 47.83	29 42 16.2	16.03 ± 0.04	16.63 ± 0.03	0.018	0.10	0.15
cs1078 <sup>c</sup>	12 33 53.88	28 54 36.3	16.27 ± 0.05	16.67 ± 0.05	0.017	0.00	0.00
cs1091	12 34 00.43	29 04 44.8	15.19 ± 0.04	15.70 ± 0.05	0.019	0.03	0.05
cs1093	12 34 21.79	29 39 20.3	15.54 ± 0.05	16.03 ± 0.05	0.016	0.02	0.03
cs1095	12 34 45.07	29 14 10.2	15.85 ± 0.04	16.36 ± 0.05	0.021	0.03	0.05
cs3281	12 35 08.76	29 10 51.6	16.23 ± 0.01	16.84 ± 0.01	0.018	0.07	0.11
cs1096	12 35 09.42	28 44 17.6	15.62 ± 0.03	16.20 ± 0.03	0.019	0.10	0.15
cs1097	12 35 17.03	28 49 01.1	15.51 ± 0.04	16.18 ± 0.03	0.017	0.14	0.20
cs3282	12 35 18.60	29 06 15.0	16.07 ± 0.04	16.67 ± 0.03	0.018	0.06	0.10
cs1099	12 35 23.99	29 29 30.7	14.15 ± 0.03	14.55 ± 0.03	0.017	0.00	0.00
cs1100	12 35 40.90	29 10 54.0	16.18 ± 0.03	16.79 ± 0.03	0.019	0.07	0.11
cs1101	12 35 46.82	28 57 50.2	15.98 ± 0.03	16.59 ± 0.03	0.017	0.06	0.09
cs1102	12 35 48.76	29 11 37.9	14.52 ± 0.03	15.10 ± 0.04	0.018	0.06	0.10
cs3284	12 35 49.79	29 11 19.2	15.72 ± 0.04	16.31 ± 0.03	0.018	0.06	0.10

Table 1—Continued

ID	RA <sub>J2000</sub>	Dec <sub>J2000</sub>	<i>R</i>	<i>V</i>	<i>E(B-V)</i> <sup>a</sup>	<i>k<sub>R</sub></i> <sup>b</sup>	<i>k<sub>V</sub></i> <sup>b</sup>
cs1089 <sup>c</sup>	12 35 58.85	28 39 38.6	16.32 ± 0.12	16.59 ± 0.12	0.017	0.00	-0.04
cs1103	12 36 14.71	29 40 54.1	15.23 ± 0.03	15.73 ± 0.04	0.016	0.02	0.04
cs1104	12 36 19.66	29 03 17.5	15.81 ± 0.03	16.42 ± 0.03	0.014	0.12	0.17
cs1106	12 37 00.91	29 39 39.9	15.57 ± 0.03	16.08 ± 0.03	0.014	0.02	0.04
cs1108	12 37 17.69	28 58 41.2	14.93 ± 0.05	15.46 ± 0.07	0.014	0.04	0.07
cs1109	12 37 39.79	29 12 47.0	15.85 ± 0.07	16.55 ± 0.05	0.013	0.10	0.14
cs3283	12 38 07.85	28 39 37.8	16.29 ± 0.03	16.74 ± 0.02	0.017	0.03	0.03
cs1110	12 38 13.30	28 56 13.2	13.74 ± 0.04	14.22 ± 0.03	0.016	0.01	0.02
cs1105	12 39 12.50	28 34 41.6	16.37 ± 0.05	16.71 ± 0.05	0.015	0.01	-0.03
cs1113	12 39 14.58	29 42 58.8	15.54 ± 0.04	16.11 ± 0.04	0.014	0.05	0.09
cs1114	12 39 18.58	28 54 15.4	13.85 ± 0.04	14.45 ± 0.05	0.015	0.03	0.05
cs1116	12 39 49.47	29 11 01.5	15.53 ± 0.04	16.14 ± 0.04	0.013	0.07	0.12
cs1117	12 40 30.09	28 59 23.3	15.63 ± 0.08	16.22 ± 0.04	0.014	0.06	0.09
cs1118	12 40 30.65	29 11 26.0	15.04 ± 0.04	15.66 ± 0.03	0.013	0.04	0.07
cs1119	12 40 56.19	29 27 56.0	13.80 ± 0.04	14.28 ± 0.04	0.013	0.01	0.02
cs1120	12 41 08.79	29 32 16.6	14.67 ± 0.04	15.24 ± 0.06	0.013	0.02	0.04
cs1121	12 41 09.48	29 32 18.8	16.05 ± 0.06	16.52 ± 0.09	0.013	0.01	0.02
cs3285	12 41 12.38	29 03 53.9	16.26 ± 0.05	16.93 ± 0.05	0.014	0.18	0.26
cs3286	12 41 13.09	28 53 09.6	16.22 ± 0.05	16.82 ± 0.03	0.013	0.07	0.11
cs3287	12 41 27.98	28 47 28.5	15.04 ± 0.05	15.59 ± 0.04	0.014	0.03	0.06
cs1122	12 41 30.62	29 32 09.5	16.21 ± 0.04	16.78 ± 0.04	0.014	0.02	0.04
cs1123	12 41 35.07	28 50 36.8	15.93 ± 0.06	16.55 ± 0.04	0.015	0.07	0.12
cs1115	12 41 47.89	28 38 21.0	16.34 ± 0.06	16.74 ± 0.04	0.015	0.01	0.00
cs1126	12 43 11.67	29 38 52.9	16.13 ± 0.09	16.78 ± 0.07	0.016	0.13	0.18
cs1127	12 43 28.71	29 27 59.6	14.24 ± 0.04	14.80 ± 0.04	0.014	0.03	0.05
cs1128	12 43 32.68	29 28 21.5	15.94 ± 0.04	16.62 ± 0.04	0.014	0.19	0.27
cs1129	12 43 55.17	29 37 49.4	15.94 ± 0.08	16.59 ± 0.06	0.014	0.14	0.19
cs1130	12 44 03.48	28 54 03.2	14.00 ± 0.04	14.58 ± 0.02	0.013	0.03	0.05
cs3288	12 44 08.79	29 32 03.1	16.13 ± 0.03	16.77 ± 0.04	0.014	0.12	0.18
cs3289	12 44 28.05	29 42 30.6	16.22 ± 0.03	16.88 ± 0.04	0.015	0.14	0.20
cs1132	12 44 30.64	29 14 02.2	16.14 ± 0.08	16.69 ± 0.06	0.014	0.08	0.11
cs1133	12 44 36.71	28 45 58.6	15.04 ± 0.04	15.61 ± 0.03	0.013	0.03	0.06
cs1134	12 44 53.72	28 44 11.1	15.91 ± 0.04	16.54 ± 0.03	0.012	0.08	0.13
cs1135	12 44 54.69	29 40 06.3	15.85 ± 0.07	16.46 ± 0.05	0.015	0.06	0.10
cs1136	12 45 07.45	28 45 17.8	16.02 ± 0.04	16.63 ± 0.02	0.011	0.06	0.10
cs1137	12 45 08.07	29 34 19.2	16.23 ± 0.04	16.61 ± 0.05	0.016	0.01	0.00

Table 1—Continued

ID	RA <sub>J2000</sub>	Dec <sub>J2000</sub>	<i>R</i>	<i>V</i>	<i>E(B-V)</i> <sup>a</sup>	<i>k<sub>R</sub></i> <sup>b</sup>	<i>k<sub>V</sub></i> <sup>b</sup>
cs1138	12 45 35.33	28 45 42.9	15.04 ± 0.04	15.57 ± 0.03	0.012	0.02	0.04
cs1139	12 45 37.64	29 18 24.3	15.82 ± 0.05	16.51 ± 0.04	0.014	0.14	0.20
cs1140	12 45 42.89	29 19 54.3	15.98 ± 0.11	16.46 ± 0.05	0.014	0.03	0.04
cs1141	12 45 43.46	29 25 58.8	14.53 ± 0.05	14.95 ± 0.04	0.015	0.01	0.01
cs1142	12 46 01.04	28 48 46.6	15.87 ± 0.03	16.34 ± 0.03	0.011	0.01	0.02
cs1143	12 46 09.11	28 57 30.4	16.16 ± 0.04	16.59 ± 0.06	0.013	0.01	0.01
cs1144	12 46 46.35	29 23 19.4	16.09 ± 0.07	16.44 ± 0.05	0.012	0.01	-0.01
cs1145	12 47 11.12	29 11 18.2	15.96 ± 0.04	16.38 ± 0.05	0.015	0.01	0.01
cs1146	12 47 12.99	29 27 31.6	16.04 ± 0.03	16.42 ± 0.03	0.011	0.01	0.00
cs1147	12 48 05.96	29 26 35.3	15.45 ± 0.07	15.80 ± 0.14	0.010	0.00	-0.01
cs1148	12 48 14.05	28 51 02.3	16.27 ± 0.04	16.81 ± 0.03	0.013	0.07	0.11
cs1149	12 48 18.17	28 57 04.2	14.97 ± 0.03	15.60 ± 0.03	0.013	0.07	0.11
cs1150	12 48 34.91	28 50 49.5	15.99 ± 0.04	16.30 ± 0.03	0.012	0.00	-0.02
cs1151	12 48 42.12	29 27 53.3	15.48 ± 0.04	16.06 ± 0.03	0.013	0.08	0.13
cs1152	12 48 42.68	29 14 20.4	15.94 ± 0.06	16.27 ± 0.09	0.017	0.00	-0.01
cs1153	12 48 49.50	29 25 27.1	15.91 ± 0.04	16.44 ± 0.03	0.014	0.02	0.04
cs1154	12 48 51.20	28 58 04.7	15.75 ± 0.03	16.39 ± 0.03	0.014	0.05	0.07
cs3297	12 49 04.09	28 53 08.9	16.22 ± 0.04	16.78 ± 0.04	0.012	0.05	0.10
cs1155 <sup>c</sup>	12 49 23.81	29 19 16.0	16.16 ± 0.08	16.52 ± 0.05	0.013	0.00	0.00
cs1156	12 49 25.19	28 56 21.9	15.19 ± 0.04	15.76 ± 0.03	0.012	0.05	0.09
cs3294	12 49 31.51	29 12 13.7	16.32 ± 0.04	16.71 ± 0.04	0.011	0.01	0.00
cs1157	12 49 38.86	29 19 42.4	15.42 ± 0.04	16.07 ± 0.03	0.013	0.11	0.16
cs1159	12 50 00.59	28 48 59.4	15.61 ± 0.04	16.27 ± 0.04	0.011	0.08	0.12
cs1160	12 50 43.21	28 59 00.5	15.71 ± 0.04	16.45 ± 0.04	0.011	0.10	0.14
cs1161	12 51 01.80	28 55 40.0	13.90 ± 0.04	14.44 ± 0.03	0.011	0.02	0.04
cs3296	12 51 04.18	28 55 06.2	16.34 ± 0.04	16.73 ± 0.05	0.017	0.01	0.00
cs1162	12 51 08.90	28 47 17.2	13.19 ± 0.04	13.81 ± 0.04	0.009	0.02	0.04
cs1163	12 51 25.66	29 41 35.4	15.85 ± 0.04	16.33 ± 0.04	0.015	0.04	0.05
cs1164	12 52 14.96	29 25 43.0	15.15 ± 0.04	15.59 ± 0.03	0.012	0.02	0.02
cs1165	12 52 25.26	28 58 23.6	15.67 ± 0.07	16.29 ± 0.05	0.010	0.07	0.11
cs1166	12 52 41.88	28 57 34.1	15.93 ± 0.07	16.37 ± 0.09	0.010	0.01	0.01
cs1167	12 52 53.10	29 13 28.0	16.24 ± 0.05	16.80 ± 0.04	0.012	0.08	0.13
cs3299	12 52 57.99	28 28 42.6	16.30 ± 0.10	16.67 ± 0.09	0.009	0.01	0.00
cs1168	12 53 05.89	29 23 43.0	15.28 ± 0.04	15.82 ± 0.03	0.011	0.04	0.08
cs1170	12 53 48.66	29 35 18.5	14.11 ± 0.04	14.63 ± 0.04	0.011	0.03	0.05
cs1171	12 53 49.23	28 56 32.8	15.82 ± 0.05	16.36 ± 0.05	0.009	0.02	0.04

Table 1—Continued

ID	RA <sub>J2000</sub>	Dec <sub>J2000</sub>	<i>R</i>	<i>V</i>	<i>E(B-V)</i> <sup>a</sup>	<i>k<sub>R</sub></i> <sup>b</sup>	<i>k<sub>V</sub></i> <sup>b</sup>
cs1172	12 53 51.54	28 58 45.7	14.68 ± 0.04	15.21 ± 0.03	0.010	0.02	0.04
cs3300	12 53 54.12	29 21 44.3	16.23 ± 0.05	16.79 ± 0.03	0.011	0.05	0.09
cs1173	12 54 02.53	29 36 13.1	13.28 ± 0.03	13.93 ± 0.03	0.011	0.03	0.05
cs1174	12 54 06.39	29 14 33.0	16.02 ± 0.07	16.53 ± 0.04	0.010	0.01	0.03
cs1175	12 54 26.56	29 30 26.6	15.95 ± 0.03	16.56 ± 0.03	0.010	0.06	0.10
cs1176	12 54 38.43	29 09 37.5	15.72 ± 0.06	16.34 ± 0.05	0.011	0.07	0.11
cs1177	12 54 40.73	28 56 17.9	11.41 ± 0.04	11.92 ± 0.03	0.011	0.01	0.01
cs1180	12 54 55.43	29 00 44.8	15.69 ± 0.06	16.25 ± 0.04	0.011	0.02	0.04
cs1183	12 55 10.93	29 34 41.6	14.40 ± 0.04	14.98 ± 0.04	0.009	0.03	0.05
cs1184	12 55 34.92	29 00 02.6	15.30 ± 0.06	15.91 ± 0.04	0.013	0.07	0.11
cs1185	12 56 01.76	29 15 11.8	15.17 ± 0.04	15.66 ± 0.04	0.010	0.03	0.04
cs1186	12 56 20.30	29 18 00.5	15.01 ± 0.04	15.53 ± 0.05	0.010	0.02	0.04
cs1188	12 56 35.96	28 56 51.2	15.93 ± 0.03	16.43 ± 0.03	0.009	0.03	0.04
cs1190	12 56 50.60	28 55 46.9	14.19 ± 0.03	14.69 ± 0.04	0.009	0.01	0.03
cs1191	12 56 51.23	29 22 41.3	14.89 ± 0.03	15.39 ± 0.03	0.010	0.01	0.03
cs1192	12 56 55.50	28 57 22.3	15.47 ± 0.04	16.13 ± 0.04	0.009	0.09	0.14
cs1193	12 57 00.15	28 54 13.2	15.52 ± 0.05	16.14 ± 0.08	0.009	0.08	0.13
cs1194	12 57 01.60	29 03 45.1	14.01 ± 0.04	14.59 ± 0.07	0.010	0.03	0.05
cs3304	12 57 05.28	28 58 52.9	15.24 ± 0.06	15.90 ± 0.05	0.009	0.09	0.14
cs1195	12 57 11.39	29 02 41.6	13.57 ± 0.12	14.15 ± 0.10	0.010	0.03	0.05
cs1197	12 57 42.41	29 34 32.1	16.17 ± 0.05	16.70 ± 0.05	0.010	0.06	0.10
cs1198	12 57 44.15	29 01 13.2	15.71 ± 0.06	16.14 ± 0.04	0.011	0.01	0.01
cs1199	12 57 47.06	29 08 57.9	14.69 ± 0.03	15.24 ± 0.04	0.011	0.02	0.04
cs1200	12 57 49.96	29 39 15.4	14.38 ± 0.06	14.76 ± 0.05	0.011	0.00	0.00
cs1201	12 58 05.66	29 01 02.3	16.15 ± 0.03	16.59 ± 0.07	0.011	0.01	0.01
cs1203	12 58 13.34	28 56 53.1	13.89 ± 0.03	14.44 ± 0.03	0.011	0.02	0.04
cs3306	12 58 18.25	29 07 43.2	14.22 ± 0.04	14.72 ± 0.03	0.011	0.01	0.03
cs3307	12 58 18.28	29 07 30.3	15.27 ± 0.13	15.70 ± 0.16	0.011	0.02	0.01
cs1204	12 58 26.91	29 36 44.5	14.65 ± 0.03	15.17 ± 0.03	0.012	0.01	0.03
cs1205	12 58 27.85	28 58 26.6	15.01 ± 0.04	15.56 ± 0.05	0.011	0.02	0.04
cs1206	12 58 30.27	28 51 31.9	14.96 ± 0.04	15.53 ± 0.03	0.011	0.03	0.05
cs1208	12 58 43.20	28 54 36.3	14.86 ± 0.04	15.30 ± 0.04	0.011	0.01	0.01
cs1209	12 58 48.01	28 50 36.4	16.00 ± 0.03	16.58 ± 0.04	0.011	0.08	0.13
cs1210	12 59 00.29	29 11 01.7	15.90 ± 0.03	16.44 ± 0.06	0.010	0.05	0.09
cs1189	12 59 04.37	29 19 22.3	16.29 ± 0.04	16.73 ± 0.04	0.010	0.03	0.03
cs1212	12 59 26.24	29 08 45.8	16.00 ± 0.07	16.40 ± 0.06	0.011	0.02	0.00

Table 1—Continued

ID	RA <sub>J2000</sub>	Dec <sub>J2000</sub>	<i>R</i>	<i>V</i>	<i>E(B-V)</i> <sup>a</sup>	<i>k<sub>R</sub></i> <sup>b</sup>	<i>k<sub>V</sub></i> <sup>b</sup>
cs3308	12 59 37.63	29 28 19.8	15.86 ± 0.03	16.41 ± 0.03	0.013	0.08	0.13
cs1214	12 59 39.17	28 53 44.3	13.38 ± 0.04	14.00 ± 0.03	0.010	0.03	0.05
cs1216	12 59 39.83	28 55 35.3	13.76 ± 0.07	14.36 ± 0.07	0.010	0.03	0.04
cs3309	13 00 06.60	29 27 45.0	14.73 ± 0.05	15.31 ± 0.06	0.012	0.02	0.04
cs1218	13 00 13.34	29 37 13.3	15.57 ± 0.09	16.21 ± 0.07	0.011	0.11	0.16
cs1219	13 00 14.04	28 49 41.7	13.98 ± 0.06	14.58 ± 0.04	0.010	0.03	0.05
cs3310	13 00 21.18	29 20 12.7	15.06 ± 0.04	15.62 ± 0.04	0.011	0.05	0.09
cs1221	13 00 25.66	28 52 04.0	14.10 ± 0.05	14.68 ± 0.04	0.010	0.03	0.04
cs1202 <sup>c</sup>	13 00 31.25	28 45 55.3	16.29 ± 0.07	16.72 ± 0.02	0.011	0.01	0.01
cs1223	13 00 39.65	29 01 10.0	13.49 ± 0.05	14.04 ± 0.06	0.009	0.02	0.04
cs1224	13 00 47.64	29 12 02.8	16.23 ± 0.05	16.81 ± 0.04	0.010	0.03	0.06
cs1226	13 00 58.62	29 37 35.6	15.84 ± 0.06	16.36 ± 0.05	0.010	0.04	0.07
cs1230	13 01 15.44	29 22 12.7	15.96 ± 0.11	16.60 ± 0.08	0.013	0.11	0.17
cs1231	13 01 15.74	28 52 20.2	15.91 ± 0.05	16.49 ± 0.04	0.010	0.03	0.05
cs1232	13 01 19.57	29 11 00.2	16.23 ± 0.09	16.64 ± 0.05	0.011	0.02	0.01
cs1233	13 01 22.05	29 20 23.7	16.28 ± 0.04	16.93 ± 0.03	0.012	0.12	0.17
cs1234	13 01 23.15	29 00 36.1	16.24 ± 0.08	16.94 ± 0.06	0.010	0.14	0.20
cs3315	13 01 24.53	29 18 30.6	12.75 ± 0.05	13.33 ± 0.04	0.011	0.03	0.04
cs3316	13 01 25.27	29 18 48.3	14.03 ± 0.03	14.62 ± 0.03	0.011	0.03	0.05
cs1236	13 01 33.62	29 07 50.0	13.18 ± 0.07	13.84 ± 0.08	0.011	0.04	0.06
cs3317	13 01 39.59	29 20 13.9	16.27 ± 0.05	16.83 ± 0.04	0.011	0.07	0.12
cs1240	13 01 43.42	29 02 40.6	13.47 ± 0.05	14.05 ± 0.03	0.011	0.03	0.04
cs1241	13 01 44.00	28 59 58.3	14.71 ± 0.04	15.29 ± 0.03	0.010	0.02	0.04
cs1244	13 01 55.84	29 19 21.9	15.37 ± 0.05	15.93 ± 0.04	0.011	0.02	0.04
cs1245	13 02 04.18	29 15 12.9	13.35 ± 0.05	13.95 ± 0.04	0.010	0.03	0.05
cs3319	13 02 04.44	28 53 40.1	14.69 ± 0.04	15.29 ± 0.03	0.010	0.03	0.06
cs3320	13 02 19.43	28 57 09.2	15.40 ± 0.04	16.01 ± 0.03	0.011	0.04	0.07
cs1248	13 02 29.53	29 12 34.4	16.20 ± 0.04	16.63 ± 0.03	0.011	0.03	0.03
cs1249	13 02 35.54	28 44 42.8	16.07 ± 0.05	16.64 ± 0.05	0.008	0.02	0.04
cs1252	13 03 23.13	28 51 51.5	15.45 ± 0.05	16.04 ± 0.04	0.010	0.03	0.04
cs1253	13 03 29.02	28 59 17.6	16.02 ± 0.05	16.59 ± 0.03	0.010	0.08	0.13
cs1254	13 03 42.22	28 54 19.6	15.15 ± 0.05	15.73 ± 0.04	0.010	0.02	0.04
cs1237	13 04 05.16	29 06 48.0	16.38 ± 0.04	16.69 ± 0.04	0.011	0.01	-0.04
cs1239	13 04 07.02	28 54 37.4	16.25 ± 0.04	16.76 ± 0.03	0.012	0.01	0.03
cs1255	13 04 10.20	29 00 55.3	15.45 ± 0.10	16.03 ± 0.08	0.011	0.03	0.04
cs1256	13 04 17.91	29 01 46.2	14.41 ± 0.03	14.97 ± 0.04	0.011	0.02	0.04

Table 1—Continued

ID	RA <sub>J2000</sub>	Dec <sub>J2000</sub>	<i>R</i>	<i>V</i>	<i>E(B-V)</i> <sup>a</sup>	<i>k<sub>R</sub></i> <sup>b</sup>	<i>k<sub>V</sub></i> <sup>b</sup>
cs1257	13 04 22.69	28 48 38.3	14.89 ± 0.05	15.21 ± 0.04	0.010	0.00	-0.02
cs1258	13 04 23.35	29 22 59.8	15.94 ± 0.03	16.57 ± 0.02	0.011	0.11	0.16
cs1260	13 04 38.97	29 13 28.3	15.67 ± 0.15	16.35 ± 0.05	0.011	0.04	0.05
cs3323	13 04 58.39	29 07 19.7	12.40 ± 0.04	13.01 ± 0.04	0.010	0.03	0.04
cs1262	13 05 02.56	28 44 19.6	15.09 ± 0.03	15.62 ± 0.04	0.011	0.02	0.04
cs1250	13 05 12.67	28 49 19.8	16.27 ± 0.03	16.74 ± 0.03	0.012	0.04	0.04
cs1264	13 05 23.63	29 30 38.0	15.70 ± 0.04	16.25 ± 0.03	0.008	0.02	0.04
cs1265	13 05 25.25	29 17 47.5	13.97 ± 0.04	14.54 ± 0.03	0.009	0.02	0.04
cs1266	13 05 32.83	29 00 41.4	15.06 ± 0.06	15.58 ± 0.03	0.009	0.01	0.03
cs1268	13 05 45.38	28 52 17.0	16.05 ± 0.04	16.30 ± 0.07	0.010	0.00	-0.04
cs1269	13 05 53.05	29 35 58.0	16.20 ± 0.04	16.66 ± 0.04	0.010	0.02	0.03
cs1270	13 05 58.88	29 01 26.1	15.35 ± 0.03	15.85 ± 0.04	0.007	0.01	0.03
cs3325	13 05 59.60	29 16 43.6	13.98 ± 0.03	14.53 ± 0.03	0.009	0.02	0.04
cs3326	13 06 14.90	29 03 52.5	15.99 ± 0.04	16.39 ± 0.06	0.008	0.01	0.00
cs3327	13 06 17.25	29 03 47.9	12.93 ± 0.10	13.44 ± 0.18	0.008	0.01	0.03
cs1274	13 06 21.47	29 10 11.9	15.14 ± 0.02	15.68 ± 0.02	0.010	0.02	0.04
cs1275	13 06 22.17	29 39 27.2	15.07 ± 0.06	15.48 ± 0.04	0.011	0.01	0.00
cs1276	13 06 32.99	29 21 57.1	15.85 ± 0.05	16.20 ± 0.05	0.011	0.00	-0.01
cs1277	13 06 33.17	29 11 02.4	15.31 ± 0.03	15.85 ± 0.03	0.009	0.02	0.05
cs1278	13 06 37.85	28 50 59.4	14.36 ± 0.03	14.66 ± 0.03	0.010	0.00	-0.02
cs3328	13 06 41.92	28 54 24.3	16.05 ± 0.03	16.61 ± 0.03	0.010	0.02	0.05
cs1279	13 06 45.00	29 22 17.7	16.04 ± 0.03	16.57 ± 0.03	0.011	0.02	0.04
cs1280	13 06 46.91	29 07 50.4	15.91 ± 0.06	16.38 ± 0.03	0.008	0.01	0.02
cs1259	13 07 02.11	28 42 20.3	16.33 ± 0.04	16.69 ± 0.04	0.011	0.00	0.00
cs1285	13 07 39.98	28 49 43.5	16.23 ± 0.06	16.71 ± 0.03	0.008	0.01	0.02
cs1288	13 08 13.21	28 50 51.7	15.29 ± 0.05	15.83 ± 0.06	0.008	0.04	0.08
cs1289	13 08 14.92	28 44 07.0	15.65 ± 0.03	16.20 ± 0.04	0.008	0.03	0.06
cs1290	13 08 21.61	29 13 41.7	15.70 ± 0.03	16.22 ± 0.04	0.009	0.02	0.04
cs1291	13 08 27.81	29 24 20.2	15.72 ± 0.03	16.35 ± 0.02	0.010	0.15	0.22
cs1292	13 08 46.43	28 52 48.3	16.19 ± 0.08	16.54 ± 0.12	0.009	0.01	-0.02
cs1293	13 08 50.75	28 53 10.6	15.77 ± 0.03	16.26 ± 0.03	0.009	0.04	0.05
cs1295	13 08 54.86	29 32 39.7	15.90 ± 0.04	16.39 ± 0.03	0.009	0.01	0.02
cs1294	13 08 55.07	29 02 26.5	14.73 ± 0.11	15.20 ± 0.05	0.010	0.01	0.02
cs1296	13 09 08.94	28 53 32.9	15.09 ± 0.02	15.62 ± 0.03	0.009	0.02	0.04
cs3331	13 09 16.15	29 22 02.8	14.48 ± 0.05	14.93 ± 0.04	0.009	0.01	0.01
cs1299	13 09 30.60	28 59 09.2	14.81 ± 0.05	15.41 ± 0.05	0.009	0.03	0.04

Table 1—Continued

ID	RA <sub>J2000</sub>	Dec <sub>J2000</sub>	<i>R</i>	<i>V</i>	<i>E(B-V)</i> <sup>a</sup>	<i>k<sub>R</sub></i> <sup>b</sup>	<i>k<sub>V</sub></i> <sup>b</sup>
cs1300	13 09 34.35	29 17 32.8	16.18 ± 0.03	16.88 ± 0.06	0.010	0.19	0.26
cs1301	13 09 40.58	29 13 22.9	16.09 ± 0.03	16.78 ± 0.04	0.010	0.13	0.18
cs1302	13 09 47.40	28 54 23.9	12.89 ± 0.06	13.38 ± 0.06	0.009	0.01	0.02
cs1303	13 09 51.70	28 54 01.4	15.48 ± 0.04	15.99 ± 0.03	0.009	0.02	0.03
cs1287	13 10 26.75	28 43 57.2	16.31 ± 0.03	16.65 ± 0.04	0.007	0.00	-0.01
cs3332	13 10 47.72	29 42 34.8	14.21 ± 0.03	14.65 ± 0.04	0.010	0.01	0.01
cs3333	13 11 01.56	29 38 12.0	12.57 ± 0.04	13.15 ± 0.04	0.011	0.03	0.05
cs1305	13 11 01.71	29 34 42.2	13.57 ± 0.03	14.16 ± 0.04	0.011	0.03	0.05
cs1306	13 12 59.69	29 36 02.4	15.87 ± 0.04	16.46 ± 0.03	0.009	0.07	0.12
cs1307	13 13 06.16	29 39 56.8	15.04 ± 0.07	15.71 ± 0.04	0.009	0.11	0.16
cs1308	13 13 35.26	29 07 34.9	15.65 ± 0.06	16.30 ± 0.06	0.010	0.03	0.05
cs1309	13 13 52.01	29 18 50.6	16.03 ± 0.05	16.69 ± 0.04	0.011	0.10	0.15
cs1310	13 14 01.44	29 24 25.0	14.97 ± 0.03	15.47 ± 0.03	0.011	0.01	0.03
cs1311	13 14 35.89	29 03 24.1	15.43 ± 0.05	16.22 ± 0.04	0.011	0.24	0.31
cs1312	13 14 39.66	28 44 36.9	16.03 ± 0.03	16.56 ± 0.04	0.015	0.07	0.10
cs1315	13 15 01.88	29 10 48.8	14.82 ± 0.03	15.38 ± 0.02	0.012	0.03	0.06
cs1316	13 15 06.44	29 36 59.0	15.72 ± 0.06	16.33 ± 0.05	0.011	0.10	0.16
cs1317	13 15 09.36	29 38 09.6	14.91 ± 0.04	15.43 ± 0.03	0.011	0.01	0.03
cs1318	13 15 19.28	29 05 39.1	16.14 ± 0.05	16.72 ± 0.03	0.012	0.08	0.13
cs1319	13 15 24.01	28 52 05.1	15.88 ± 0.04	16.43 ± 0.03	0.014	0.06	0.11
cs1320	13 15 27.28	29 04 27.2	14.49 ± 0.03	15.07 ± 0.03	0.012	0.04	0.06
cs1321	13 15 34.89	29 40 33.3	13.01 ± 0.04	13.57 ± 0.04	0.012	0.02	0.04
cs1324	13 15 39.33	29 36 38.8	15.64 ± 0.04	16.10 ± 0.03	0.010	0.01	0.01
cs1325	13 15 41.13	29 19 47.3	15.53 ± 0.05	16.17 ± 0.07	0.011	0.12	0.18
cs1326	13 15 58.61	29 16 49.1	15.73 ± 0.03	16.34 ± 0.07	0.013	0.10	0.16
cs1328	13 16 37.62	28 55 26.2	15.83 ± 0.04	16.43 ± 0.03	0.015	0.08	0.12
cs1329	13 16 55.36	29 12 09.9	15.91 ± 0.04	16.34 ± 0.06	0.015	0.03	0.02
cs1330	13 17 01.69	28 52 19.3	16.14 ± 0.03	16.74 ± 0.04	0.015	0.06	0.10
cs1332	13 17 22.01	28 53 45.9	14.58 ± 0.05	15.23 ± 0.03	0.015	0.08	0.12
cs3340	13 17 32.45	28 59 12.3	15.31 ± 0.04	15.91 ± 0.04	0.014	0.06	0.11
cs1322	13 17 59.20	29 23 43.7	16.28 ± 0.13	16.66 ± 0.06	0.011	0.01	0.00
cs1335	13 18 02.14	28 53 53.6	16.03 ± 0.03	16.41 ± 0.04	0.016	0.01	0.00
cs1336	13 18 09.19	29 27 02.9	15.33 ± 0.03	15.90 ± 0.02	0.012	0.07	0.11
cs1337	13 18 12.25	28 45 05.5	15.15 ± 0.03	15.53 ± 0.04	0.016	0.01	0.00
cs3338	13 18 25.34	29 07 08.8	16.23 ± 0.03	16.34 ± 0.03	0.011	-0.01	-0.09
cs1338	13 18 31.23	29 02 44.2	15.74 ± 0.03	16.36 ± 0.06	0.014	0.08	0.12

Table 1—Continued

ID	RA <sub>J2000</sub>	Dec <sub>J2000</sub>	<i>R</i>	<i>V</i>	<i>E(B-V)</i> <sup>a</sup>	<i>k<sub>R</sub></i> <sup>b</sup>	<i>k<sub>V</sub></i> <sup>b</sup>
cs1340	13 18 42.18	28 44 32.0	$15.24 \pm 0.03$	$15.80 \pm 0.04$	0.017	0.03	0.05
cs1343	13 18 57.35	29 38 47.3	$15.22 \pm 0.04$	$15.86 \pm 0.04$	0.013	0.09	0.14
cs1344	13 19 04.04	29 38 35.8	$14.89 \pm 0.06$	$15.49 \pm 0.05$	0.013	0.08	0.12
cs3339	13 19 21.41	28 43 38.3	$16.31 \pm 0.13$	$16.73 \pm 0.13$	0.015	0.03	0.01
cs1346	13 19 56.24	29 26 53.4	$15.40 \pm 0.04$	$15.96 \pm 0.02$	0.015	0.03	0.06
cs1347	13 19 58.86	29 25 38.6	$14.63 \pm 0.03$	$15.11 \pm 0.02$	0.015	0.01	0.02
cs1348	13 20 33.13	29 22 53.1	$15.93 \pm 0.03$	$16.51 \pm 0.07$	0.014	0.12	0.18
cs1349	13 20 40.42	29 37 00.8	$15.67 \pm 0.03$	$16.05 \pm 0.02$	0.016	0.01	0.00
cs1350	13 20 47.11	29 36 00.0	$15.42 \pm 0.05$	$16.02 \pm 0.04$	0.016	0.05	0.09
cs1351	13 20 54.16	29 21 52.5	$16.21 \pm 0.03$	$16.86 \pm 0.04$	0.014	0.16	0.23
cs1352	13 20 59.85	28 58 10.2	$15.76 \pm 0.04$	$16.15 \pm 0.03$	0.016	0.01	0.00
cs1353	13 21 05.78	29 21 54.9	$15.31 \pm 0.04$	$15.96 \pm 0.03$	0.014	0.08	0.12
cs1354	13 21 26.55	29 18 58.5	$16.32 \pm 0.03$	$16.95 \pm 0.03$	0.015	0.17	0.25
cs1355	13 21 37.81	28 52 34.6	$15.79 \pm 0.03$	$16.39 \pm 0.03$	0.015	0.08	0.13
cs1356	13 21 56.60	28 50 39.3	$14.10 \pm 0.02$	$14.67 \pm 0.04$	0.016	0.03	0.06
cs1357	13 21 57.85	29 36 19.8	$16.08 \pm 0.04$	$16.60 \pm 0.03$	0.014	0.04	0.06
cs1358	13 22 11.36	28 58 53.0	$15.84 \pm 0.02$	$16.48 \pm 0.03$	0.017	0.12	0.17
cs1359	13 22 12.73	29 39 30.3	$15.98 \pm 0.04$	$16.48 \pm 0.04$	0.014	0.03	0.05
cs1362	13 22 44.07	29 24 35.2	$16.09 \pm 0.02$	$16.68 \pm 0.06$	0.016	0.10	0.15
cs1363	13 22 54.74	29 39 32.5	$15.68 \pm 0.05$	$16.14 \pm 0.04$	0.017	0.03	0.03
cs1364	13 23 02.99	29 22 29.1	$15.94 \pm 0.05$	$16.53 \pm 0.10$	0.015	0.11	0.17
cs1365	13 23 09.20	29 35 02.1	$15.41 \pm 0.04$	$16.05 \pm 0.04$	0.017	0.09	0.14
cs1366	13 24 42.55	29 02 58.7	$15.27 \pm 0.02$	$15.74 \pm 0.02$	0.014	0.01	0.02
cs3343	13 24 53.80	28 46 16.8	$15.98 \pm 0.04$	$16.54 \pm 0.03$	0.011	0.05	0.09
cs1367	13 25 13.83	29 24 51.1	$15.42 \pm 0.02$	$15.90 \pm 0.02$	0.011	0.01	0.02
cs1368	13 25 20.08	29 29 39.7	$15.96 \pm 0.07$	$16.32 \pm 0.04$	0.011	0.00	0.00
cs1369	13 25 39.96	28 53 39.6	$15.96 \pm 0.04$	$16.60 \pm 0.05$	0.014	0.08	0.12
cs3346	13 26 24.65	29 30 36.7	$15.88 \pm 0.04$	$16.39 \pm 0.03$	0.013	0.06	0.08
cs1370	13 27 26.07	29 02 38.0	$16.15 \pm 0.04$	$16.86 \pm 0.05$	0.010	0.20	0.28
cs1371	13 28 22.13	29 24 00.8	$15.95 \pm 0.03$	$16.49 \pm 0.03$	0.009	0.08	0.12
cs1372	13 28 48.14	28 51 24.9	$15.91 \pm 0.03$	$16.43 \pm 0.03$	0.013	0.02	0.05
cs1373	13 29 11.03	29 27 42.2	$15.27 \pm 0.03$	$15.84 \pm 0.02$	0.011	0.07	0.11
cs1374	13 29 40.38	29 40 58.1	$15.23 \pm 0.04$	$15.86 \pm 0.05$	0.014	0.06	0.09
cs1375	13 29 49.18	28 52 08.4	$16.22 \pm 0.05$	$16.67 \pm 0.03$	0.013	0.03	0.03
cs1376	13 29 49.78	29 34 46.9	$15.85 \pm 0.03$	$16.25 \pm 0.03$	0.011	0.01	0.00

<sup>a</sup>Values from Schlegel et al. (1998).<sup>b</sup>Values interpolated from Poggianti (1997) types E, Sa, and Sc and Frei & Gunn (1994)type Im for the Kron Cousins *R* and Johnson *V* filters.<sup>c</sup>LSB galaxy with central surface brightness  $\mu_V(0)_0 > 21.2$  and/or  $\mu_R(0)_0 > 20.8$  mag arcsec<sup>-2</sup>.